Electronic Supplementary Material (ESI) for Inorganic Chemistry Frontiers.

Electronic Supplementary Information

Dimeric iodine(I) and silver(I) cages from tripodal *N*-donor ligands via the [N–Ag–N]$^+$ to [N–I–N]$^+$ cation exchange reaction

Essi Taipale,[a] Jas S. Ward,*[a] Giorgia Fiorini,[a] Daniel L. Stares,[b] Christoph A. Schalley,[b] and Kari Rissanen*[a]

a. University of Jyvaskyla, Department of Chemistry, P. O. BOX 35, Survontie 9B, 40014 Jyväskylä, Finland. E-mail: kari.t.rissanen@jyu.fi

b. Institut für Chemie und Biochemie, Organische Chemie, Freie Universität Berlin, Arnimallee 20, 14195 Berlin, Germany.

Contents

Experimental

General Details

All reagents and solvents obtained from commercial suppliers were used without further purification. The syntheses of all prepared compounds are described below. Compound **1** was prepared according to literature procedures and compounds **2** - **6** were prepared with slight modifications of the first synthesis.[1] All used solvents were acquired dry from commercial suppliers. For NMR assignments, ^{1}H and ^{15}N NMR spectra were recorded using Bruker Avance III 500 MHz spectrometer, whereas ^{19}F NMR was recorded using Bruker 300 Avance instrument, all at 303 K. Chemical shifts are reported on the δ scale in ppm using the residual solvent signal as internal standard (CD_3CN; δH 1.94, DMSO-d_6; δH 2.50). For ^{1}H NMR spectroscopy, each resonance was assigned according to the following conventions: chemical shift (δ) measured in ppm, observed multiplicity, number of hydrogens, and observed coupling constant (J Hz). Multiplicities are denoted as s (singlet), d (doublet), t (triplet), q (quartet) m (multiplet), and br (broad). Spectral windows of 4 ppm (^{1}H) and 600 ppm (^{15}N) were used in the ^{1}H-^{15}N HMBC spectroscopy, with 2048 points in the direct dimension and 512 increments used in the indirect dimension, and subsequent peak shape analysis was performed.

Abbreviations:

CID = collision-induced dissociation
DMF = dimethylformamide
DMSO = dimethylsulfoxide
HMBC = heteronuclear multiple bond correlation
HRMS = high resolution mass spectrometry
IM-MS = ion mobility mass spectrometry
MeCN = acetonitrile
MeOH = methanol
NMR = nuclear magnetic resonance
SY = survivor yield
TBME = methyl tert-butyl ether
THF = tetrahydrofuran

Synthesis and Characterisation: Ligands

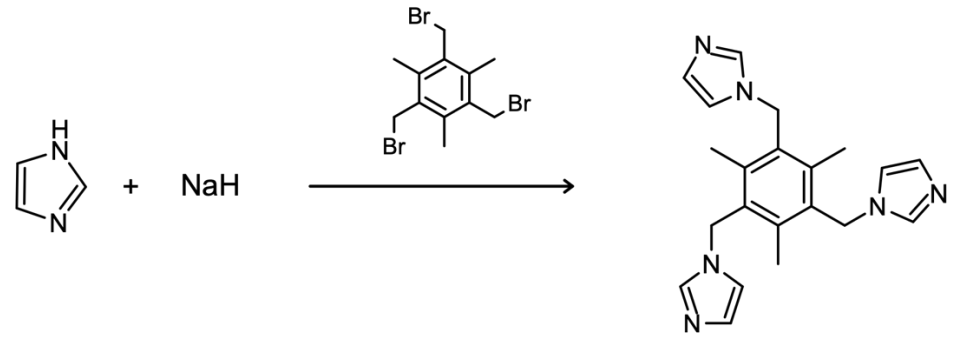

1

Scheme S1. Synthesis of compound **1**.

Synthesis of compound 1 (1,1',1''-((2,4,6-trimethylbenzene-1,3,5-triyl)tris(methylene))tris(1*H*-imidazole)).[1] To a solution of imidazole (5.926 mmol, 403.4 mg) in dry DMF (6 mL) under argon, 6.121 mmol NaH (146.9 mg) was added. After stirring for 30 minutes at ambient temperature, 1,3,5-tris(bromomethyl)-2,4,6-trimethylbenzene (1.975 mmol, 788.0 mg) in dry DMF (6 mL) was added dropwise over 2 hours. The mixture was stirred for 20 hours, the solvent was removed under reduced pressure and the residue was washed with water after which a white solid was obtained (334.9 mg, 47%). ^{1}H NMR (500 MHz, CD_3CN) δ 7.32 (s, 3H), 6.90 (s, 3H), 6.82 (s, 3H), 5.27 (s, 6H), 2.28 (s, 9H).

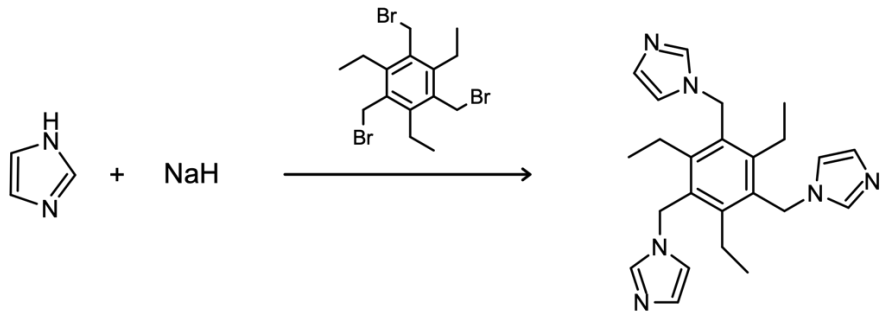

2

Scheme S2. Synthesis of compound **2**.

Synthesis of compound 2 (1,1',1''-((2,4,6-triethylbenzene-1,3,5-triyl)tris(methylene))tris(1*H*-imidazole)).[1] All the glassware was oven-dried overnight to remove any moisture. Imidazole (7.453 mmol, 507.4 mg) and 1,3,5-tris(bromomethyl)-2,4,6-triethylbenzene (2.4841 mmol, 1095.6 mg) were weighed in air. A flask with imidazole was evacuated, flushed with argon three times, and left under vacuum. The flask was introduced into a glove box where 7.700 mmol NaH (184.8 mg) was weighed and added to the flask. The flask was connected to a Schlenk line, put under argon, and dry DMF (6 mL) was added. After stirring at ambient temperature for 30 minutes, 1,3,5-tris(bromomethyl)-2,4,6-triethylbenzene in DMF (6 mL) and THF (6 mL) was added dropwise over 1 hour. The mixture was stirred for 20 hours, the solvent was removed under reduced pressure and the residue was washed with water after which a white solid was obtained (859.6 mg, 86%). ^{1}H NMR (500 MHz, CD_3CN) δ 7.30 (s, 3H), 6.90 (s, 3H), 6.81 (s, 3H), 5.26 (s, 6H), 2.66 (q, *J* = 7.54 Hz, 6H), 0.91 (t, *J* = 7.54 Hz, 9H).

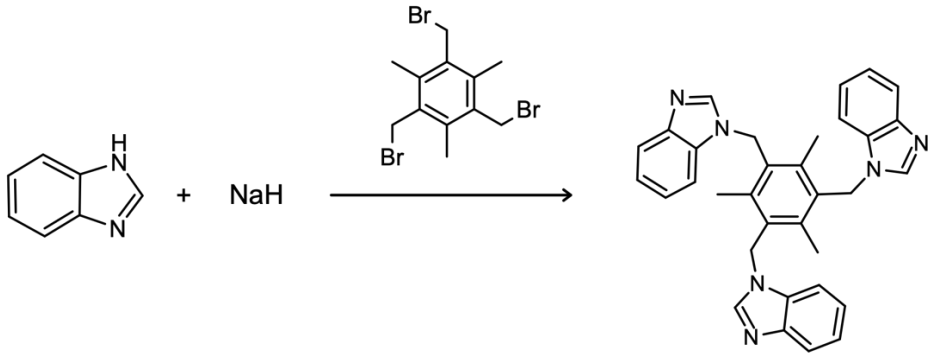

3

Scheme S3. Synthesis of compound **3**.

Synthesis of compound 3 (1,1',1''-((2,4,6-trimethylbenzene-1,3,5-triyl)tris(methylene))tris(1*H*-benzo[*d*]imidazole)).[1] All the glassware was oven-dried overnight to remove any moisture. 1*H*-benzo[*d*]imidazole (5.880 mmol, 694.7 mg) and 1,3,5-tris(bromomethyl)-2,4,6-trimethylbenzene (1.959 mmol, 781.4 mg) were weighed in air. A flask with 1*H*-benzo[*d*]imidazole was evacuated, flushed with argon three times, and left under vacuum. The flask was introduced into a glove box where 6.071 mmol NaH (145.7 mg) was weighed and added to the flask. The flask was connected to a Schlenk line, put under argon and dry DMF (6 mL) was added. After stirring at ambient temperature for 30 minutes, 1,3,5-tris(bromomethyl)-2,4,6-triethylbenzene in DMF (6 mL) was added dropwise over 2 hours. The mixture was stirred for 20 hours, the solvent was removed under reduced pressure and the residue was washed with water after which a white solid was obtained (630.6 mg, 63%). ^{1}H NMR (500 MHz, CD_3CN) δ 7.88 (s, 3H), 7.66 (br, 3H), 7.54 (br, 3H) 7.22 (t, 6H), 5.52 (s, 6H) 2.24 (s, 9H).

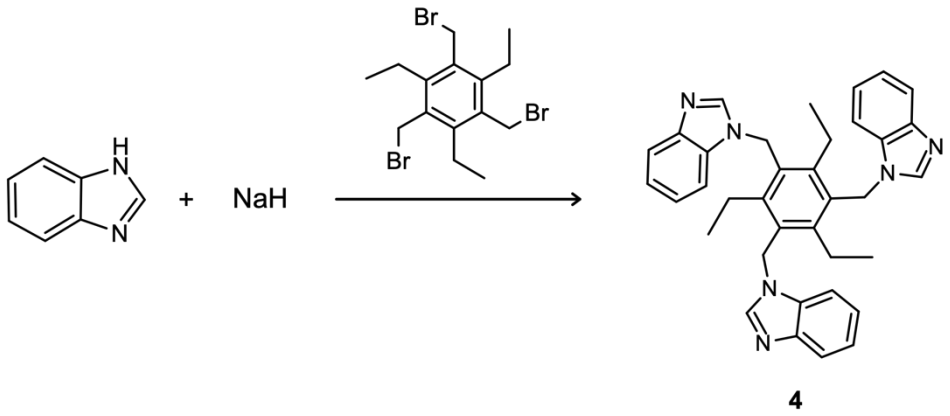

4

Scheme S4. Synthesis of compound **4**.

Synthesis of compound 4 (1,1',1''-((2,4,6-triethylbenzene-1,3,5-triyl)tris(methylene))tris(1*H*-benzo[*d*]imidazole)).[1] All the glassware was oven-dried overnight to remove any moisture. 1*H*-benzo[*d*]imidazole (5.427 mmol, 641.2 mg) and 1,3,5-tris(bromomethyl)-2,4,6-triethylbenzene (1.809 mmol, 797.9 mg) were weighed in air. A flask with 1*H*-benzo[*d*]imidazole was evacuated, flushed with argon three times, and left under vacuum. The flask was introduced into a glove box where 5.609 mmol NaH (134.6 mg) was weighted and added to the flask. The flask was connected to a Schlenk line, put under argon and dry DMF (6 mL) was added. After stirring at ambient temperature for 30 minutes, 1,3,5-tris(bromomethyl)-2,4,6-triethylbenzene in DMF (6 mL) and THF (6 mL) was added dropwise over 2 hours. The mixture was stirred for 20 hours, the solvent was removed under reduced pressure and the residue was washed with water after which a white solid was obtained (859.0 mg, 86%). ^{1}H NMR (500 MHz, CD_3CN) δ 7.68 (d, *J* = 7.90 Hz, 3H), 7.55 (s, 3H), 7.54 (d, *J* = 8.07 Hz, 3H), 7.31 (dt, *J* = 0.88, 7.94 Hz, 3H), 7.26 (dt, *J* = 0.94, 7.58 Hz, 3H), 5.45 (s, 6H), 2.65 (q, *J* = 7.52 Hz, 6H), 0.91 (t, *J* = 7.52 Hz, 9H).

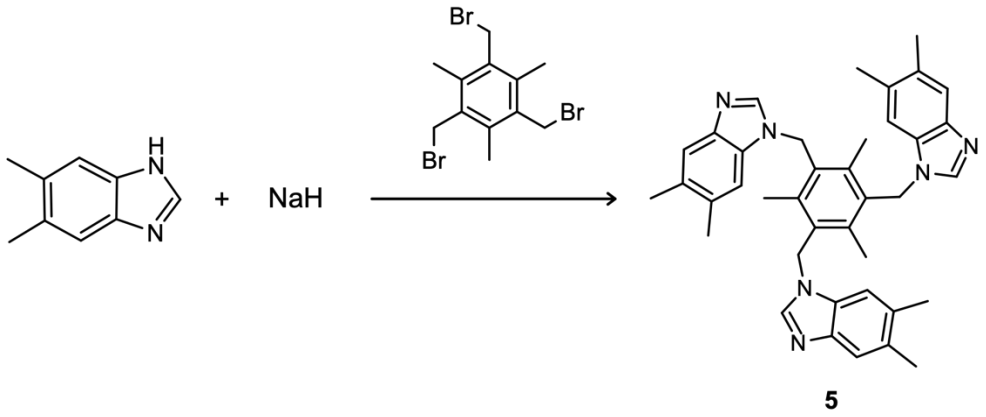

5

Scheme S5. Synthesis of compound **5**.

Synthesis of compound 5 (1,1',1''-((2,4,6-trimethylbenzene-1,3,5-triyl)tris(methylene))tris(5,6-dimethyl-1*H*-benzo[*d*]imidazole)).[1] All the glassware was oven-dried overnight to remove any moisture. 5,6-dimethyl-1*H*-benzo[*d*]imidazole (5.043 mmol, 737.3 mg) and 1,3,5-Tris(bromomethyl)-2,4,6-trimethylbenzene (1.681 mmol, 670.7 mg) were weighed in air. A flask with 5,6-dimethyl-1*H*-benzo[*d*]imidazole was evacuated, flushed with argon three times, and left under vacuum. The flask was introduced into a glove box where 5.213 mmol NaH (125.1 mg) was weighed and added to the flask. The flask was connected to a Schlenk line and put under argon and dry DMF (6 mL) was added. After stirring at ambient temperature for 30 minutes, 1,3,5-Tris(bromomethyl)-2,4,6-trimethylbenzene in 12 mL DMF was added dropwise over 2 hours. The mixture was stirred for 20 hours, the solvent was removed under reduced pressure and the residue was washed with water (2 × 50 mL) after which a light brown solid was obtained (718.2 mg, 72%). ^{1}H NMR (500 MHz, CD_3CN) δ 7.42 (s, 6H), 7.24 (s, 3H), 5.37 (s, 6H), 2.35 (d, *J* = 9.90 Hz, 18H), 2.23 (s, 9H).

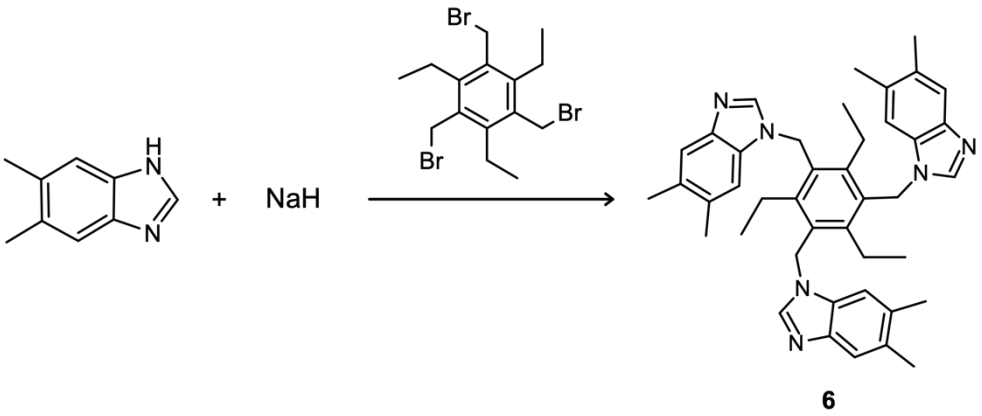

Scheme S6. Synthesis of compound **6**.

Synthesis of compound 6 (1,1',1''-((2,4,6-triethylbenzene-1,3,5-triyl)tris(methylene))tris(5,6-dimethyl-1*H*-benzo[*d*]imidazole)). All the glassware was oven-dried overnight to remove any moisture. 5,6-dimethyl-1*H*-benzo[*d*]imidazole (4.710 mmol, 688.6 mg) and 1,3,5-Tris(bromomethyl)-2,4,6-triethylbenzene (1.570 mmol, 692.5 mg) were weighted in air. A flask with 5,6-dimethyl-1*H*-benzo[*d*]imidazole was evacuated, flushed with argon three times, and left under vacuum. The flask was introduced into a glove box where 4.867 mmol NaH (116.8 mg) was weighted and added to the flask. The flask was connected to a Schlenk line and put under argon and dry DMF (6 mL) was added. After stirring at ambient temperature for 30 minutes, 1,3,5-Tris(bromomethyl)-2,4,6-triethylbenzene in DMF (6 mL) and THF (6 mL) was added dropwise over 2 hours. The mixture was stirred for 20 hours, the solvent was removed under reduced pressure and the residue was washed with water (2 × 50 mL) after which a brown solid was obtained (736.6 mg, 74%). ^{1}H NMR (500 MHz, CD_3CN) δ 7.43 (s, 3H), δ 7.40 (s, 3H), 7.27 (s, 3H), 5.39 (s, 6H), 2.64 (q, *J* = 7.47 Hz, 6H), 2.35 (d, *J* = 14.63 Hz, 18H), 0.91 (t, *J* = 7.48 Hz, 9H). ^{13}C NMR (126 MHz, DMSO-d_6) δ 145.49, 142.19, 141.64, 132.75, 131.00, 130.12, 129.90, 119.53, 110.37, 42.70, 22.93, 20.13, 19.86, 15.15. Elemental analysis found: C 78.07%; H 6.98%; N 13.57%. Calculated for ($C_{42}H_{48}N_6 \cdot 0.5\ H_2O$): C 78.10%; H 7.49 %; N 13.01%.

Synthesis and Characterisation: Silver(I) Cages

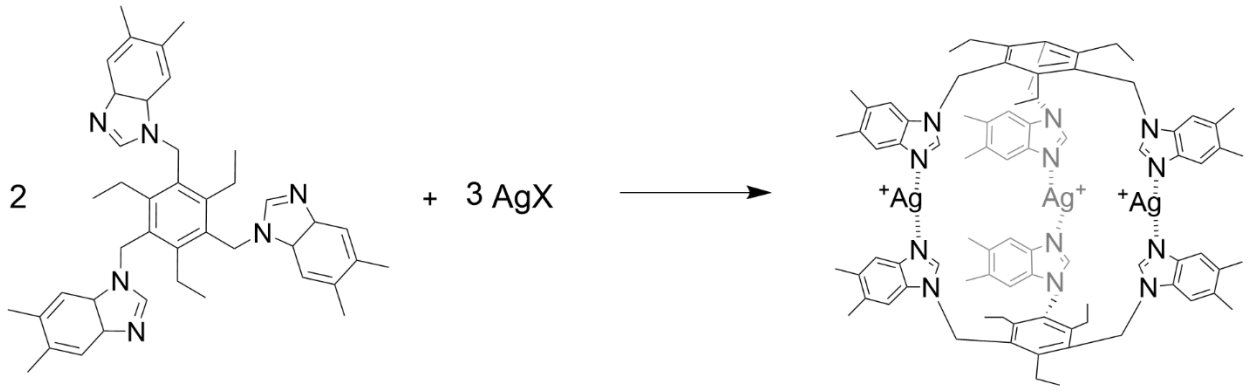

Scheme S7. The general synthesis of silver(I) cages described using ligand **6**. Reactions for all ligands were performed in either CH_3CN or DMSO. $AgPF_6$ was used for NMR analysis, other salts ($AgBF_4$ and $AgSbF_6$) were also used in the crystallization of compounds.

This section describes the synthesis of silver(I) cages. Various silver(I) salts were used in the attempts of obtaining good quality single crystals for the X-ray diffraction studies. Crystallization conditions for each crystal are described below. Furthermore, NMR experiments (^{1}H and ^{1}H-^{15}N HMBC) and HRMS experiments were conducted with samples of cages constructed using silver(I) hexafluorophosphate.

Synthesis of **[BF_4−⊂1−Ag−1][BF_4]$_2$**

The silver complexation of ligand **1** with $AgBF_4$ was performed in small glass vials. Both the ligand **1** (10.0 mg, 0.0277 mmol) and the silver(I) salt (8.1 mg, 0.042 mol) were weighed in their own vials. The ligand and the silver(I) salt were dissolved in MeCN separately (200 μl + 200 μl), and to aid solubility, few drops of DMSO were added to the ligand solution. Once completely dissolved, the ligand was added to the silver(I) salt. The mixture was stirred for 1 hour. The single crystals for the X-ray diffraction experiments (see Figure S1) were grown from diffusion of methanol to the MeCN/DMSO mixture in room temperature.

Synthesis of **[PF_6−⊂1−Ag−1][PF_6]$_2$**

The silver complexation of ligand **1** with $AgPF_6$ was performed in small glass vials. Both the ligand **1** (10.0 mg, 0.0277 mmol) and the silver(I) salt (10.5 mg, 0.0415 mol) were weighed in their own vials. The ligand and the silver(I) salt were dissolved in MeCN separately (200 μl + 200 μl). Once completely dissolved, the

ligand was added to the silver(I) salt. The mixture was stirred for 1 hour. The cages for all ligands with $AgPF_6$ were characterized with mass spectrometry ($[PF_6{-}\subset 1{-}Ag{-}1]^{2+}$ *m/z* 594.0453, see Figure S26). This is a known complex, and therefore, other characterization was not performed.

Synthesis of **$[SbF_6{-}\subset 1{-}Ag{-}1][SbF_6]_2$**

The silver complexation of ligand **1** with $AgSbF_6$ was performed in small glass vials. Both the ligand **1** (10.0 mg, 0.0277 mmol) and the silver(I) salt (14.3 mg, 0.0416 mol) were weighed in their own vials. The ligand and the silver(I) salt were dissolved in MeCN separately (200 μl + 200 μl). Once completely dissolved, the ligand was added to the silver(I) salt. The mixture was stirred for 1 hour. The single crystals for the X-ray diffraction experiments (see Figure S2) were grown from diffusion of methanol to the MeCN in fridge (+4 °C).

Synthesis of **$[1{-}Ag{-}]_n[OTf]_n$**

The silver complexation of ligand **1** with AgOTf was performed in small glass vials. Both the ligand **1** (10.0 mg, 0.0277 mmol) and the silver(I) salt (10.7 mg, 0.0416 mol) were weighed in their own vials. The ligand and the silver(I) salt were dissolved in MeCN separately (200 μl + 200 μl). Once completely dissolved, the ligand was added to the silver(I) salt. The mixture was stirred for 1 hour. The single crystals for the X-ray diffraction experiments (see Figure S3) were grown from evaporation of MeCN in room temperature.

Synthesis of **$[PF_6{-}\subset 2{-}Ag{-}2][PF_6]_2$**

The silver complexation of ligand **2** with $AgPF_6$ was performed in small glass vials. Both the ligand **2** (10.0 mg, 0.0248 mmol) and the silver(I) salt (9.4 mg, 0.037 mol) were weighed in their on vials. The ligand and the silver(I) salt were dissolved in DMSO separately (200 μl + 200 μl). Once completely dissolved, the ligand was added to the silver(I) salt. The mixture was stirred for 1 hour and characterized. For NMR experiments, the solvents were switched to deuterated ones. The NMR experiments (Figure S50 and Figure S51) revealed effectively a 100% conversion from the ligand to the silver(I) complex. The single crystals for the X-ray diffraction experiments were not obtained due to poor solubility preventing any valid crystallization attempts. However, the cages for all ligands with $AgPF_6$ were characterized with mass spectrometry ($[PF_6{-}\subset 2{-}Ag{-}2]^{2+}$ *m/z* 636.0905, see Figure S29). ^{1}H NMR (500 MHz, DMSO-d_6) δ 7.76 (s, 6H), 7.44 (s, 6H), 7.23 (s, 6H), 5.33 (s, 12H), 2.65 (q, unresolved, 12H), 0.79 (t, *J* = 7.05 Hz, 18H).

Synthesis of **$[PF_6{-}\subset 3{-}Ag{-}3][PF_6]_2$**

The silver complexation of ligand **3** with $AgPF_6$ was performed in small glass vials. Both the ligand **3** (10.0 mg, 0.0196 mmol) and the silver(I) salt (7.4 mg, 0.029 mol) were weighed in their own vials. The ligand and

the silver(I) salt were dissolved in MeCN separately (200 μl + 200 μl). Once completely dissolved, the ligand was added to the silver(I) salt. The mixture was stirred for 1 hour and characterized. For NMR experiments, the solvents were switched to deuterated ones. The NMR experiments (Figure S52 and Figure S53) revealed effectively a 100% conversion from the ligand to the silver(I) complex. The single crystals for the X-ray diffraction experiments (see Figure S4) were grown from diffusion of TMBE to the MeCN in room temperature. In addition, the cages for all ligands with $AgPF_6$ were characterized with mass spectrometry ($[PF_6{-}\subset 3{-}Ag{-}3]^{2+}$ *m/z* 743.0927, see Figure S32). ^{1}H NMR (500 MHz, DMSO-d_6) δ 8.09 (d, *J* = 8.11 Hz, 6H), 8.05 (s, 6H), 7.91 (d, *J* = 7.93 Hz, 6H), 7.53 (t, *J* = 7.56 Hz, 6H), 7.46 (t, *J* = 7.54 Hz, 6H), 5.70 (s, 6H), 2.37 (s, 18H).

Synthesis of **$[SbF_6{-}\subset 3{-}Ag{-}3][SbF_6]_2$**

The silver complexation of ligand **3** with $AgSbF_6$ was performed in small glass vials. Both the ligand **3** (10.0 mg, 0.0196 mmol) and the silver(I) salt (10.1 mg, 0.0294 mol) were weighed in their own vials. The ligand and the silver(I) salt were dissolved in MeCN separately (200 μl + 200 μl). Once completely dissolved, the ligand was added to the silver(I) salt. The mixture was stirred for 1 hour. The single crystals for the X-ray diffraction experiments (Figure S5) were grown from diffusion of methanol to the MeCN in fridge (+4 °C).

Synthesis of **$[4{-}Ag{-}4][PF_6]_3$**

The silver complexation of ligand **4** with $AgPF_6$ was performed in small glass vials. Both the ligand **4** (10.0 mg, 0.0181 mmol) and the silver(I) salt (6.9 mg, 0.027 mol) were weighed in their own vials. The ligand and the silver(I) salt were dissolved in MeCN separately (200 μl + 200 μl). Once completely dissolved, the ligand was added to the silver(I) salt. The mixture was stirred for 1 hour and characterized. For NMR experiments, the solvents were switched to deuterated ones. The NMR experiments (Figure S54 and Figure S55) revealed effectively a 100% conversion from the ligand to the silver(I) complex. The single crystals for the X-ray diffraction experiments (Figure S6) were grown from evaporation of the MeCN in fridge (+4 °C). In addition, the cages for all ligands with $AgPF_6$ were characterized with mass spectrometry ($[PF_6{-}\subset 4{-}Ag{-}4]^{2+}$ *m/z* 787.1420, see Figure S36). ^{1}H NMR (500 MHz, CD_3CN) δ 7.95 (s, 6H), 7.93 (*overlapping doublets,* 6H), 7.91 (*overlapping doublets*, 6H), 7.58 (t, *J* = 7.62 Hz, 6H), 7.51 (t, *J* = 7.55 Hz, 6H) 5.56 (s, 12H), 2.62 (q, *J* = 7.23 Hz, 12H), 1.08 (t, *J* = 7.32 Hz, 18H).

Synthesis of **$[4{-}Ag{-}4][SbF_6]_3$**

The silver complexation of ligand **4** with $AgSbF_6$ was performed in small glass vials. Both the ligand **4** (10.0 mg, 0.0181 mmol) and the silver(I) salt (9.3 mg, 0.027 mol) were weighed in their own vials. The ligand and the silver(I) salt were dissolved in MeCN separately (200 μl + 200 μl). Once completely dissolved, the ligand was added to the silver(I) salt. The mixture was stirred for 10 minutes and characterized. The single crystals

for the X-ray diffraction experiments (Figure S7) were grown from evaporation of the MeCN in fridge (+4 °C).

Synthesis of **[BF_4−⊂5−Ag−5][BF_4]$_2$**

The silver complexation of ligand **5** with $AgBF_4$ was performed in small glass vials. Both the ligand **5** (10.0 mg, 0.0168 mmol) and the silver(I) salt (4.9 mg, 0.025 mol) were weighed in their own vials. The ligand and the silver(I) salt were dissolved in DMSO separately (200 μl + 200 μl). Once completely dissolved, the ligand was added to the silver(I) salt. The mixture was stirred for 1 hour. The single crystals for the X-ray diffraction experiments (Figure S8) were grown from diffusion of $CHCl_3$ to the DMSO in room temperature.

Synthesis of **[PF_6−⊂5−Ag−5][PF_6]$_2$**

The silver complexation of ligand **5** with $AgPF_6$ was performed in small glass vials. Both the ligand **5** (10.0 mg, 0.0168 mmol) and the silver(I) salt (6.4 mg, 0.025 mol) were weighed in their own vials. The ligand and the silver(I) salt were dissolved in DMSO separately (200 μl + 200 μl). Once completely dissolved, the ligand was added to the silver(I) salt. The mixture was stirred for 1 hour and characterized. For NMR experiments, the solvents were switched to deuterated ones. The NMR experiments (Figure S56 and Figure S57) revealed effectively a 100% conversion from the ligand to the silver(I) complex. The single crystals for the X-ray diffraction experiments (Figure S9) were grown from diffusion of $CHCl_3$ to the DMSO in room temperature. In addition, the cages for all ligands with $AgPF_6$ were characterized with mass spectrometry ($[PF_6−⊂5−Ag−5]^{2+}$ *m/z* 827.1843, see Figure S39). ^{1}H NMR (500 MHz, CD_3CN) δ 7.82 (s, 6H), 7.68 (d, *J* = 3.47 Hz, 12H), 5.49 (s, 12H), 2.48 (s, 18H), 2.45 (s, 18H), 2.27 (s, 18H).

Synthesis of **[PF_6−⊂6−Ag−6][PF_6]$_2$**

The silver complexation of ligand **6** with $AgPF_6$ was performed in small glass vials. Both the ligand **6** (10.0 mg, 0.0157 mmol) and the silver(I) salt (6.0 mg, 0.024 mol) were weighed in their own vials. The ligand and the silver(I) salt were dissolved in DMSO separately (200 μl + 200 μl). Once completely dissolved, the ligand was added to the silver(I) salt. The mixture was stirred for 1 hour and characterized. For NMR experiments, the solvents were switched to deuterated ones. The NMR experiments (Figure S58 and Figure S59) revealed effectively a 100% conversion from the ligand to the silver(I) complex. The single crystals for the X-ray diffraction experiments (Figure S10) were grown from diffusion of $CHCl_3$ to the DMSO in room temperature. In addition, the cages for all ligands with $AgPF_6$ were characterized with mass spectrometry ($[PF_6−⊂6−Ag−6]^{2+}$ *m/z* 871.2361, see Figure S42). ^{1}H NMR (500 MHz, DMSO-d_6) δ 7.88 (s, 12H), 7.66 (s, 6H), 5.57 (s, 12H), 2.61 (s, 12H), 2.42 (s, 18H), 2.35 (s, 18H), 0.91 (s, 18H).

Synthesis of **[SbF_6−⊂6−Ag−6][SbF_6]$_2$**

The silver complexation of ligand **6** with $AgSbF_6$ was performed in small glass vials. Both the ligand 6 (10.0 mg, 0.0157 mmol) and the silver(I) salt (8.1 mg, 0.023 mol) were weighed in their own vials. The ligand and the silver(I) salt were dissolved in MeCN separately (200 μl + 200 μl). Once completely dissolved, the ligand was added to the silver(I) salt. The mixture was stirred for 1 hour. The single crystals for the X-ray diffraction experiments (Figure S11) were grown from evaporation of the MeCN in fridge (+4 °C).

Synthesis and Characterisation: Iodine(I) Cages

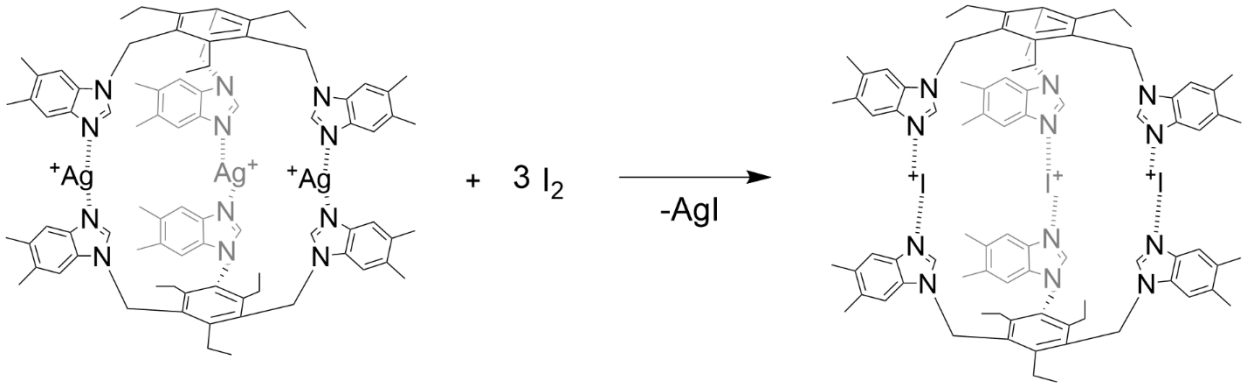

Scheme S8. The general synthesis of iodine(I) cages described using ligand **6**. Reactions for all ligands were performed in either CH_3CN or DMSO.

This section describes the synthesis of iodine(I) cages. The NMR experiments (^1H and ^1H-^{15}N HMBC) and HRMS experiments were conducted with samples of cages constructed using silver(I) hexafluorophosphate. Unfortunately, all crystal structures for the iodine(I) cages remained elusive.

Synthesis of **$[PF_6{-}\subset 1{-}I{-}1][PF_6]_2$**

The cation exchange reaction from **$[PF_6{-}\subset 1{-}Ag{-}1][PF_6]_2$** to **$[PF_6{-}\subset 1{-}I{-}1][PF_6]_2$** was performed in small glass vials. Both the silver(I) cage (10.0 mg, 0.00676 mmol) and the elemental iodine (7.82 mg, 0.0308 mol) were weighed in their own vials. The silver(I) cage and the elemental iodine were dissolved in MeCN separately (200 μl + 200 μl). Once completely dissolved, the elemental iodine was added to the silver(I) cage. The mixture was stirred for 1 hour and the formed silver iodide was filtered from the solution. The cages for all ligands with $AgPF_6$ were characterized with mass spectrometry ($[L_2I_3 + PF_6]^{2+}$ *m/z* 632.0462, see Figure S27). This is a known complex, and therefore, other characterization was not performed.

Synthesis of **$[PF_6{-}\subset 2{-}I{-}2][PF_6]_2$**

The cation exchange reaction from **$[PF_6{-}\subset 2{-}Ag{-}2][PF_6]_2$** to **$[PF_6{-}\subset 2{-}I{-}2][PF_6]_2$** was performed in small glass vials. Both the silver(I) cage (10.0 mg, 0.00640 mmol) and the elemental iodine (7.20 mg, 0.0284 mol) were weighed in their own vials. The silver(I) cage and the elemental iodine were dissolved in DMSO separately (200 μl + 200 μl). Once completely dissolved, the elemental iodine was added to the silver(I) cage. The mixture was stirred for 1 hour, centrifuged for 5 minutes and the formed silver iodide was filtered

from the solution. For NMR experiments (Figure S50 and Figure S51), the solvents were switched to deuterated ones. A conversion from the silver(I) to the iodine(I) complex was revealed by the NMR experiments, however, multiple species were observed due to the highly competitive nature of DMSO and perhaps an incomplete conversion resulting from the low solubility of the ligand and the silver(I) cage. The single crystals for the X-ray diffraction experiments were not obtained due to poor solubility preventing any valid crystallization attempts. However, the cages for all ligands with $AgPF_6$ were characterized with mass spectrometry ($[PF_6{-}\subset 1{-}I{-}1]^{2+}$ *m/z* 665.0902, see Figure S30). ^{1}H NMR (500 MHz, DMSO-d_6) δ 8.99 (s, 6H), 7.74 (s, 6H), 7.61 (s, 6H), 5.50 (s, 12H), 2.66 (q, unresolved, 12H), 0.79 (t, unresolved, 18H).

Synthesis of **$[PF_6{-}\subset 3{-}I{-}3][PF_6]_2$**

The cation exchange reaction from **$[PF_6{-}\subset 3{-}Ag{-}3][PF_6]_2$** to **$[PF_6{-}\subset 3{-}I{-}3][PF_6]_2$** was performed in small glass vials. Both the silver(I) cage (10.0 mg, 0.00562 mmol) and the elemental iodine (5.98 mg, 0.0236 mol) were weighed in their own vials. The silver(I) cage and the elemental iodine were dissolved in DMSO separately (200 μl + 200 μl). Once completely dissolved, the elemental iodine was added to the silver(I) cage. The mixture was stirred for 1 hour, centrifuged for 5 minutes and the formed silver iodide was filtered from the solution. For NMR experiments (Figure S52 and Figure S53), the solvents were switched to deuterated ones A conversion from the silver(I) to the iodine(I) complex was revealed by the NMR experiments, however, multiple species were observed due to the highly competitive nature of DMSO and perhaps an incomplete conversion resulting from the low solubility of the ligand and the silver(I) cage. The single crystals for the X-ray diffraction experiments were not obtained due to poor solubility preventing any valid crystallization attempts. However, the cages for all ligands with $AgPF_6$ were characterized with mass spectrometry ($[PF_6{-}\subset 3{-}I{-}3]^{2+}$ *m/z* 773.0915, see Figure S34). ^{1}H NMR (500 MHz, DMSO-d_6) δ 8.70 (s, 6H), 8.20 (d, unresolved, 6H), 7.96 (d, unresolved, 6H), 7.64 (t, unresolved, 12H), 5.70 (s, 6H), 2.32 (s, 18H).

Synthesis of **$[PF_6{-}\subset 4{-}I{-}4][PF_6]_2$**

The cation exchange reaction from **$[PF_6{-}\subset 4{-}Ag{-}4][PF_6]_2$** to **$[PF_6{-}\subset 4{-}I{-}4][PF_6]_2$** was performed in small glass vials. Both the silver(I) cage (10.0 mg, 0.00536 mmol) and the elemental iodine (5.61 mg, 0.0221 mol) were weighed in their own vials. The silver(I) cage and the elemental iodine were dissolved in MeCN separately (200 μl + 200 μl). Once completely dissolved, the elemental iodine was added to the silver(I) cage. The mixture was stirred for 1 hour and the formed silver iodide was filtered from the solution. For NMR experiments, the solvents were switched to deuterated ones. The NMR experiments (Figure S54 and Figure S55) revealed effectively a 100% conversion from the ligand to the silver(I) complex. The single crystals for the X-ray diffraction experiments were not obtained due to poor solubility preventing any valid crystallization attempts. However, the cages for all ligands with $AgPF_6$ were characterized with mass

spectrometry ($[PF_6{-}\subset 4{-}I{-}4]^{2+}$ *m/z* 815.1360, see Figure S37). ^{1}H NMR (500 MHz, CD_3CN) δ 8.17 (s, 6H), 7.94 (m, 12H), 7.65 (m, 12H), 5.50 (s, 12H), 2.56 (q, *J* = 7.45 Hz, 12H), 1.25 (t, *J* = 7.45 Hz, 18H).

Synthesis of **$[PF_6{-}\subset 5{-}I{-}5][PF_6]_2$**

The cation exchange reaction from **$[PF_6{-}\subset 5{-}Ag{-}5][PF_6]_2$** to **$[PF_6{-}\subset 5{-}I{-}5][PF_6]_2$** was performed in small glass vials. Both the silver(I) cage (10.0 mg, 0.00513 mmol) and the elemental iodine (6.2 mg, 0.024 mol) were weighed in their own vials. The silver(I) cage and the elemental iodine were dissolved in MeCN separately (200 μl + 200 μl). Once completely dissolved, the elemental iodine was added to the silver(I) cage. The mixture was stirred for 1 hour and the formed silver iodide was filtered from the solution. For NMR experiments, the solvents were switched to deuterated ones. The NMR experiments (Figure S56 and Figure S57) revealed effectively a 100% conversion from the ligand to the silver(I) complex. The single crystals for the X-ray diffraction experiments were not obtained due to poor solubility preventing any valid crystallization attempts. However, the cages for all ligands with $AgPF_6$ were characterized with mass spectrometry ($[PF_6{-}\subset 5{-}I{-}5]^{2+}$ *m/z* 857.1865, see Figure S40). ^{1}H NMR (500 MHz, CD_3CN) δ 8.03 (s, 6H), 7.73 (s, 6H), 7.70 (s, 6H), 5.49 (s, 12H), 2.50 (s, 18H), 2.49 (s, 18H), 2.29 (s, 18H).

Synthesis of **$[PF_6{-}\subset 6{-}I{-}6][PF_6]_2$**

The cation exchange reaction from **$[PF_6{-}\subset 6{-}Ag{-}6][PF_6]_2$** to **$[PF_6{-}\subset 6{-}I{-}6][PF_6]_2$** was performed in small glass vials. Both the silver(I) cage (10.0 mg, 0.00492 mmol) and the elemental iodine (5.0 mg, 0.020 mol) were weighed in their own vials. The silver(I) cage and the elemental iodine were dissolved in DMSO separately (200 μl + 200 μl). Once completely dissolved, the elemental iodine was added to the silver(I) cage. The mixture was stirred for 1 hour, centrifuged for 5 minutes and the formed silver iodide was filtered from the solution. For NMR experiments (Figure S58 and Figure S59), the solvents were switched to deuterated ones. A conversion from the silver(I) to the iodine(I) complex was revealed by the NMR experiments, however, multiple species were observed due to the highly competitive nature of DMSO and perhaps an incomplete conversion resulting from the low solubility of the ligand and the silver(I) cage. The single crystals for the X-ray diffraction experiments were not obtained due to poor solubility preventing any valid crystallization attempts. However, the cages for all ligands with $AgPF_6$ were characterized with mass spectrometry ($[PF_6{-}\subset 6{-}Ag{-}6]^{2+}$ *m/z* 899.2325, see Figure S43). ^{1}H NMR (500 MHz, DMSO-d_6) δ 8.61 (s, 6H), 7.93 (s, 6H), 7.64 (s, 6H), 5.54 (s, 12H), 2.59 (q, unresolved, 12H), 2.43 (s, 18H), 2.34 (s, 18H), 0.80 (t, *J* = 7.31 Hz, 18H).

X-Ray Crystallography

The single crystal X-ray data for **$[BF_4{-}\subset{3}{-}Ag{-}3][BF_4]_2$** and **$[PF_6{-}\subset{3}{-}I{-}3][PF_6]_2$** were collected at 120 K using an Agilent Super-Nova diffractometer with an Eos detector using mirror monochromated Mo-K_α (λ = 0.71073 Å) radiation. The single crystal X-ray data for all the other compounds were collected at 120 K using an Agilent Super-Nova dual-wavelength diffractometer with an Atlas detector using mirror-monochromated Cu-K_α (λ = 1.54184 Å) radiation. The program CrysAlisPro[4] was used for the data collection and reduction on both Super-Nova diffractometers. The intensities were corrected for absorption using a gaussian face index absorption correction method.[4] The structures were solved with intrinsic phasing (*SHELXT*)[5] and refined by full-matrix least-squares on F^2 using the *OLEX2* software,[6] which utilizes the *SHELXL*-2015 module.[7] Non-hydrogen atoms were assigned anisotropic displacement parameters unless stated otherwise. Isotropic displacement parameters for all H atoms were constrained to multiples of the equivalent displacement parameters of their parent atoms with Uiso(H) = 1.2 Ueq(parent atom).

X-Ray Experimental Details

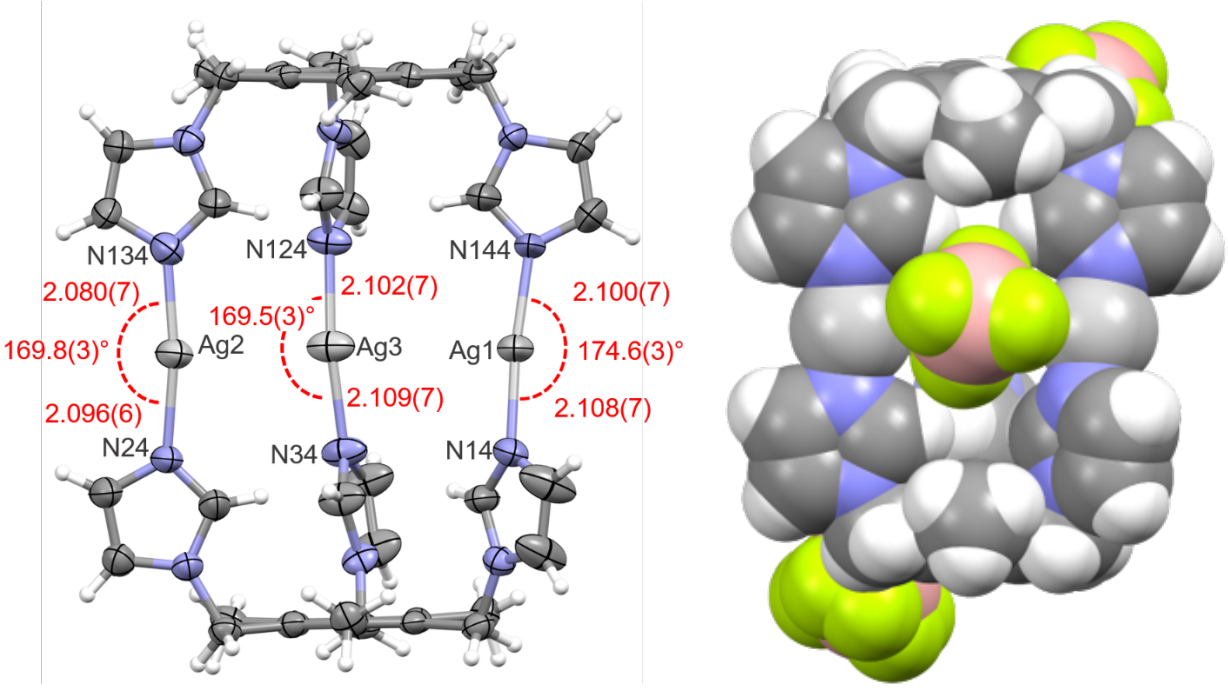

Figure S1. The ellipsoid (left) and spacefill (right) representations of the **[BF_4−⊂1−Ag−1][BF_4]$_2$** Ag-coordination cage (thermal displacement ellipsoids are drawn at a 50% probability level; anions (left) and solvent molecules are omitted for clarity; all lengths are in Å). A polymorph to ConQuest Refcode: UBOGOH.[2]

Crystal data for **[BF_4−⊂1−Ag−1][BF_4]$_2$** (obtained from MeCN/DMSO/MeOH mixture): CCDC-2126429, $[C_{42}H_{48}Ag_3N_{12}](BF_4)_3$, M = 1304.96 gmol^{-1}, colourless yellow, 0.07 × 0.06 × 0.03 mm^3, monoclinic, space group $C2/c$, a = 33.594(2) Å, b = 10.9898(7) Å, c = 34.777(3) Å, β = 117.075(10)°, V = 11432.6 Å^3, Z = 8, D_{calc} = 1.516 gcm^{-3}, $F(000)$ = 5184, μ = 8.86 mm^{-1}, T = 120.00(10) K, θ_{max} = 77.1°, 25435 total reflections, 6167 with $I_o > 2\sigma(I_o)$, R_{int} = 0.074, 11643 data, 692 parameters, 60 restraints, GooF = 1.01, R = 0.072 and wR = 0.207 [$I_o > 2\sigma(I_o)$], 0.81 <$d\Delta\rho$ < -0.92 eÅ^{-3}.

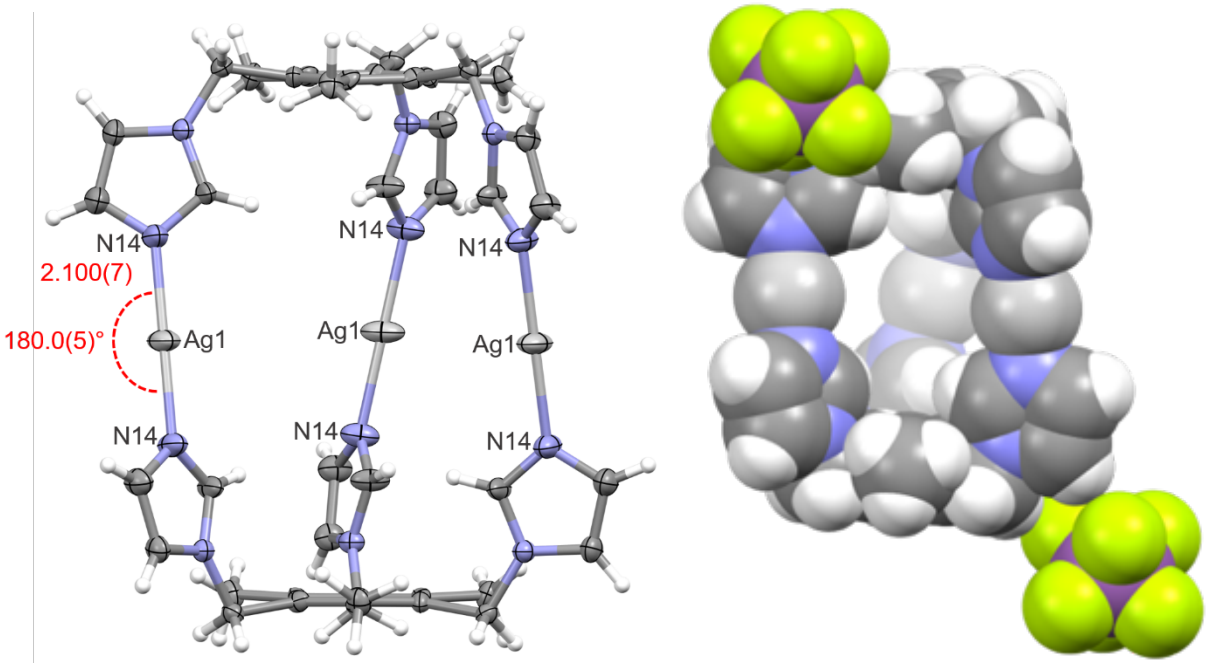

Figure S2. The ellipsoid (left) and spacefill (right) representations of the **[SbF_6⊂1−Ag−1][SbF_6]$_2$** helical Ag-coordination cage. Disordered SbF_6^- was found inside the cage yet could not be adequately modeled and was squeezed (thermal displacement ellipsoids are drawn at a 50% probability level; anions (left) and solvent molecules are omitted for clarity; all lengths are in Å). A polymorph to ConQuest Refcode: BOCQIU.[3]

Crystal data for **[SbF_6⊂1−Ag−1][SbF_6]$_2$** (obtained from MeCN/MeOH): CCDC-2126430, $[C_{42}H_{48}Ag_3N_{12}](F_6Sb)_2^+$, M = 1516.00 gmol^{-1}, colourless block, 0.10 × 0.08 × 0.04 mm^3, trigonal, space group $P321$, a = 11.2651(1) Å, c = 14.4922(2) Å, V = 1592.71 Å^3, Z = 1, D_{calc} = 1.581 gcm^{-3}, $F(000)$ = 735, μ = 14.53 mm^{-1}, T = 120.00(10) K, θ_{max} = 76.9°, 22336 total reflections, 2244 with $I_o > 2\sigma(I_o)$, R_{int} = 0.032, 2246 data, 110 parameters, no restraints, GooF = 1.17, R = 0.036 and wR = 0.095 [$I_o > 2\sigma(I_o)$], 1.95 <$d\Delta\rho$ < -1.25 eÅ^{-3}.

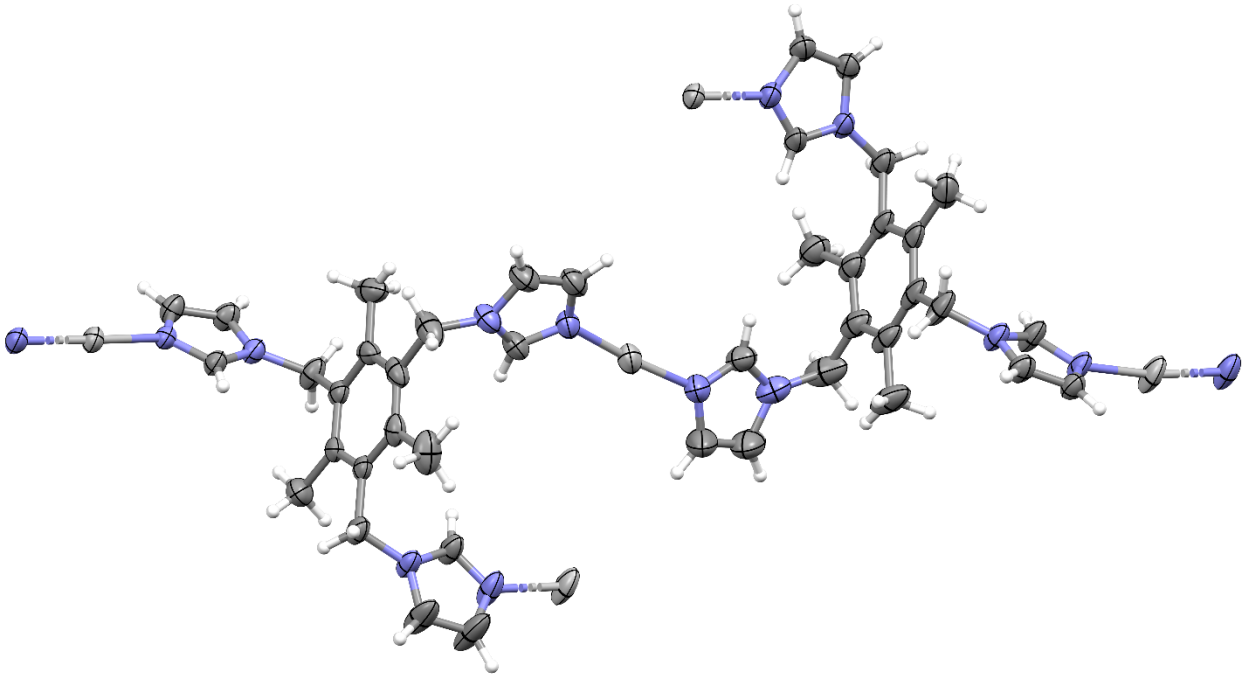

Figure S3. The ellipsoid representation of a polymeric **[1–Ag–]$_n$[OTf]$_n$** structure with N–Ag bond lengths between 2.085 Å - 2.118 Å (thermal displacement ellipsoids are drawn at a 50% probability level; anions and solvent molecules are omitted for clarity; all lengths are in Å).

Crystal data for **[1–Ag–]$_n$[OTf]$_n$** (obtained from MeCN): CCDC- CCDC-2126431, $([C_{42}H_{48}Ag_3N_{12}](CF_3O_3S)_3)_n \cdot (CH_3CN)_2$, M = 1573.85 gmol^{-1}, colourless block, 0.17 × 0.11 × 0.06 mm^3, triclinic, space group *P-1*, a = 10.0952(3) Å, b = 13.0031(4) Å, c = 23.6956(8) Å, α = 98.866(3) °, β = 94.235(3) °, γ = 98.103(3)°, V = 3028.09(17) Å^3, Z = 2, D_{calc} = 1.726 gcm^{-3}, $F(000)$ = 1576, μ = 9.48 mm^{-1}, T = 120.00(10) K, θ_{max} = 76.6°, 21209 total reflections, 10176 with $I_o > 2\sigma(I_o)$, R_{int} = 0.031, 12306 data, 829 parameters, 114 restraints, GooF = 1.04, R = 0.062 and wR = 0.163 [$I_o > 2\sigma(I_o)$], 2.46 <$d\Delta\rho$ < -1.57 eÅ^{-3}.

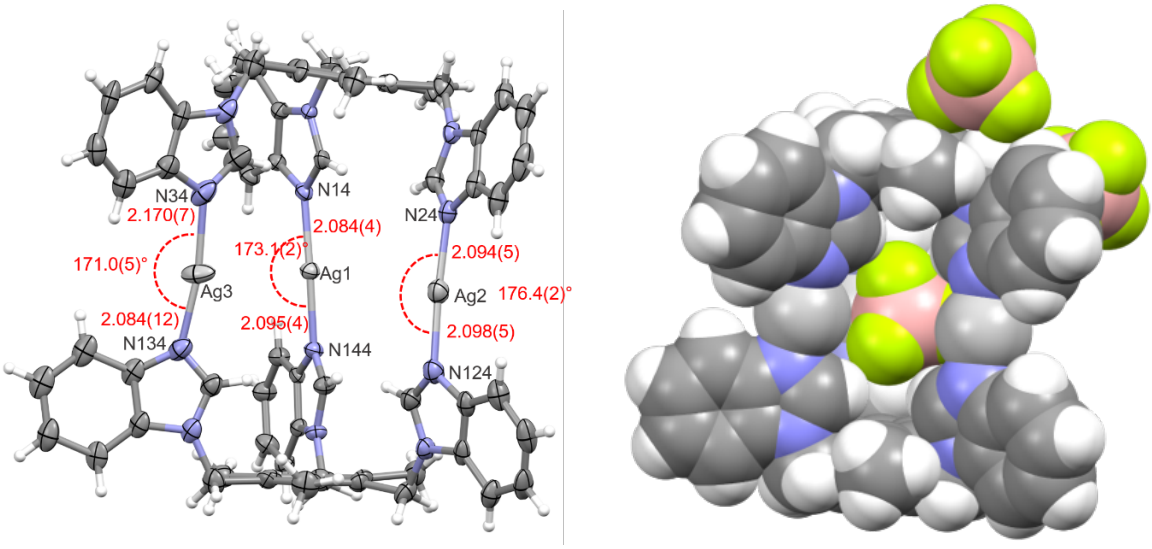

Figure S4 The ellipsoid (left) and spacefill (right) representations of the **[BF$_4$−⊂3−Ag−3][BF$_4$]$_2$** Ag-coordination cage (thermal displacement ellipsoids are drawn at a 50% probability level; anions (left) and solvent molecules are omitted for clarity; all lengths are in Å).

Crystal data for **[BF$_4$−⊂3−Ag−3][BF$_4$]$_2$** (obtained from MeCN/MeOH): CCDC- CCDC-2126432, $[C_{66}H_{60}Ag_3N_{12}][BF_4]_3 \cdot CH_3CN$, M = 1646.35 gmol^{-1}, colourless needle, 0.58 × 0.23 × 0.13 mm^3, tetragonal, space group $P4_2/n$, a = 27.6361(8) Å, c = 18.0738(7) Å, V = 13803.9(10) Å^3, Z = 8, D_{calc} = 1.584 gcm^{-3}, $F(000)$ = 6608, μ = 0.93 mm^{-1}, T = 120.00(10) K, θ_{max} = 26.6°, 14129 total reflections, 8755 with $I_o > 2\sigma(I_o)$, R_{int} = 0.053, 14129 data, 976 parameters, 217 restraints, GooF = 1.02, R = 0.067 and wR = 0.139 [$I_o > 2\sigma(I_o)$], 0.91 <$d\Delta\rho$ < -0.65 eÅ^{-3}.

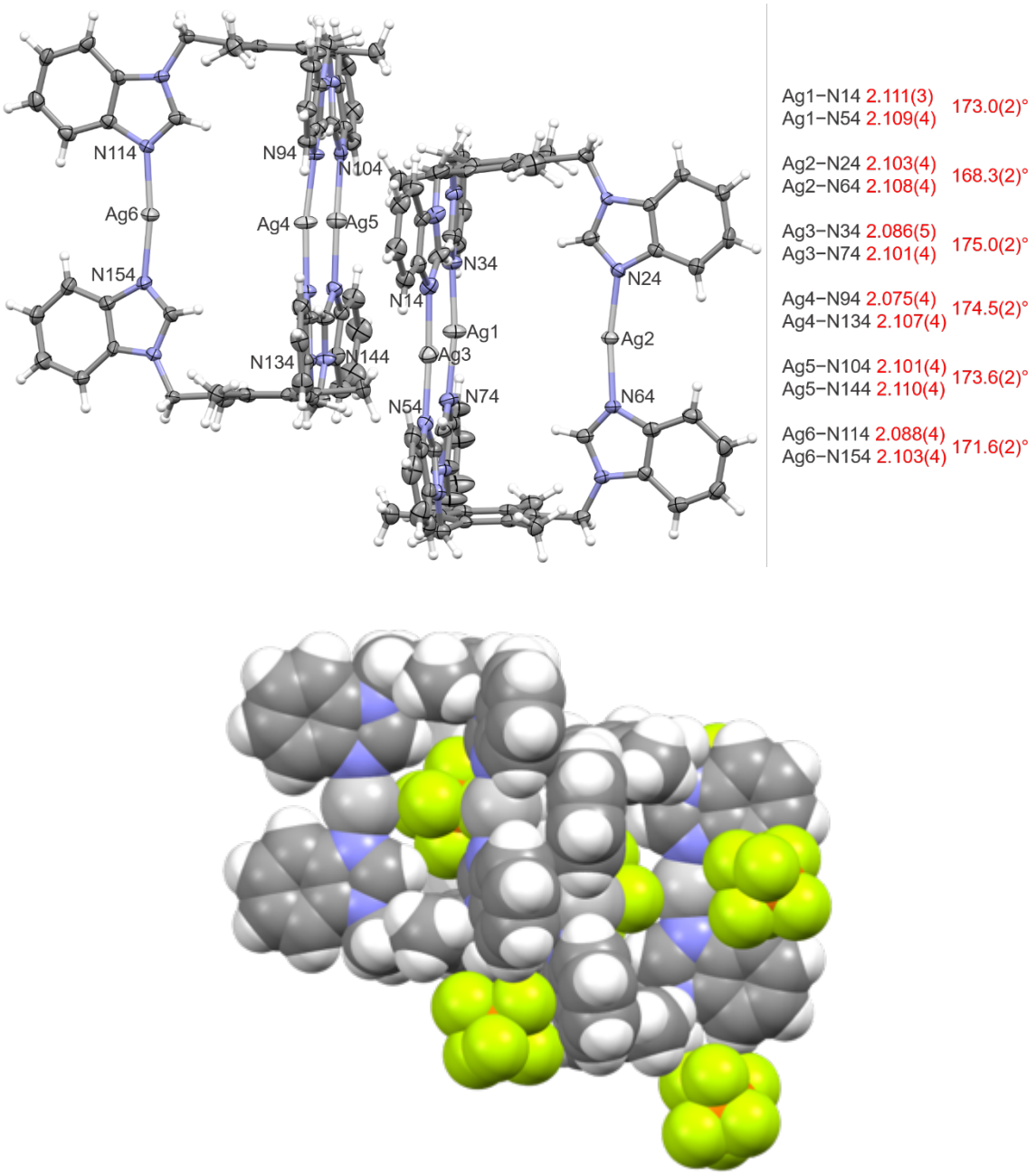

Figure S5. The ellipsoid (top) and spacefill (bottom) in the crystal structure (bottom) of **[PF$_6$−⊂3−Ag−3][PF$_6$]$_2$** with face-to-face π-stacking between cages and slipped π−π interactions between dimers (thermal displacement ellipsoids are drawn at a 50% probability level; anions (top) and solvents omitted for clarity; all lengths are in Å).

Crystal data for **[PF$_6$−⊂3−Ag−3][PF$_6$]$_2$** (obtained from MeCN/TBME): CCDC-2126433, $[C_{66}H_{60}Ag_3N_{12}][PF_6]_3 \cdot CH_3CN$, M = 1861.88 gmol^{-1}, colourless plate, 0.40 × 0.33 × 0.09 mm^3, triclinic, space group *P-1*, a = 15.7817(3) Å, b = 17.6300(6) Å, c = 31.5534(8) Å, α = 99.766(2) °, β = 99.078(2) °, γ = 109.096(2)°, V = 7958.5(4) Å^3, Z = 4, D_{calc} = 1.554 gcm^{-3}, F(000) = 3728, μ = 0.88 mm^{-1}, T = 120.00(10) K, θ_{max} = 29.0°, 67347 total reflections, 21779 with $I_o > 2\sigma(I_o)$, R_{int} = 0.044, 36389 data, 2027 parameters, 542 restraints, GooF = 1.03, R = 0.063 and wR = 0.183 [$I_o > 2\sigma(I_o)$], 1.88 <$d\Delta\rho$ < -1.02 eÅ^{-3}.

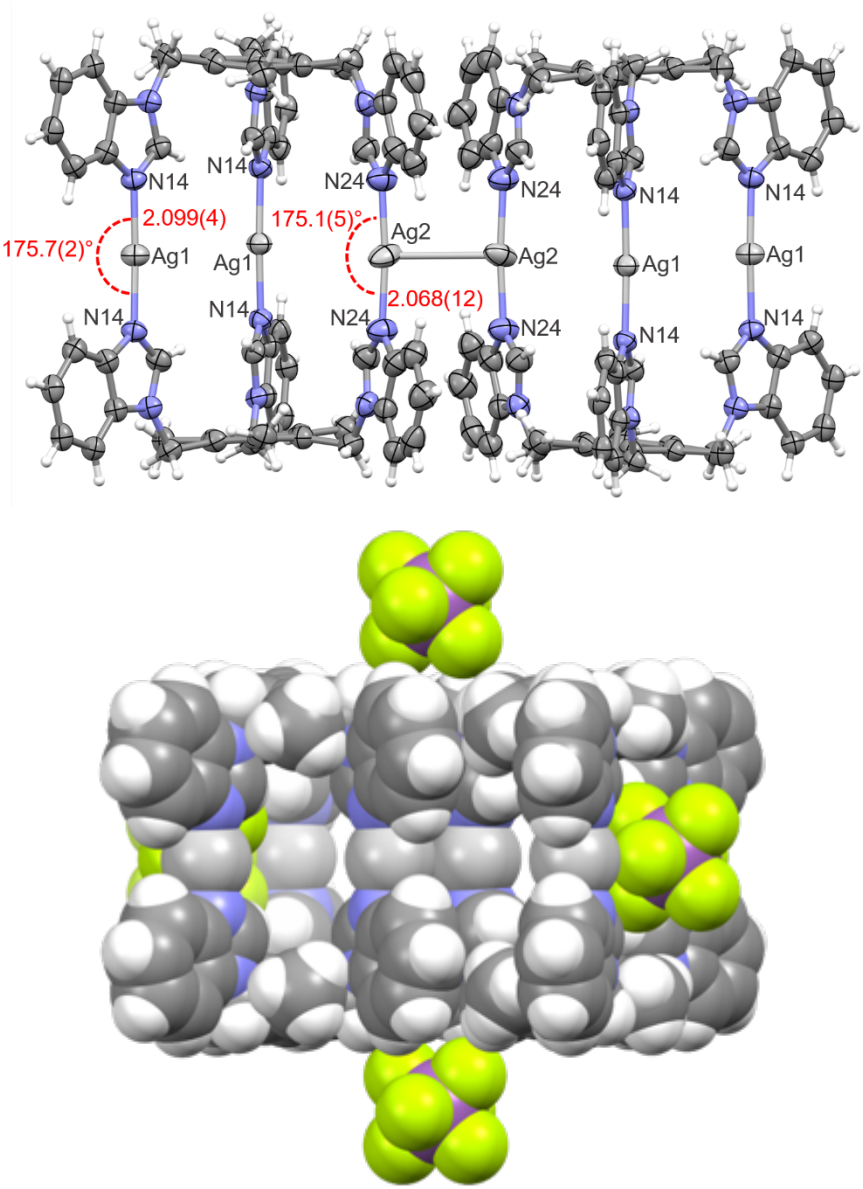

Figure S6. The ellipsoid (top) and spacefill (bottom) representations of the **[SbF$_6$−⊂3−Ag−3][SbF$_6$]$_2$** Ag-coordination cage (thermal displacement ellipsoids are drawn at a 50% probability level; anions (top) and solvent molecules are omitted for clarity; all lengths are in Å).

Crystal data for **[SbF$_6$−⊂3−Ag−3][SbF$_6$]$_2$** (obtained from MeCN/MeOH): CCDC-2126434, $[C_{66}H_{60}Ag_3N_{12}][SbF_6]_3$, M = 1580.62 gmol^{-1}, colourless needle, 0.37 × 0.07 × 0.05 mm^3, tetragonal, space group $I4/mcm$, a = 27.1562(1) Å, c = 19.7887(3) Å, V = 14593.4(2) Å^3, Z = 8, D_{calc} = 1.439 gcm^{-3}, $F(000)$ = 6288, μ = 9.77 mm^{-1}, T = 120.00(10) K, θ_{max} = 74.5°, 69353 total reflections, 3480 with $I_o > 2\sigma(I_o)$, R_{int} = 0.051, 3961 data, 261 parameters, no restraints, GooF = 1.04, R = 0.050 and wR = 0.151 [$I_o > 2\sigma(I_o)$], 1.82 <$d\Delta\rho$ < -0.89 eÅ^{-3}.

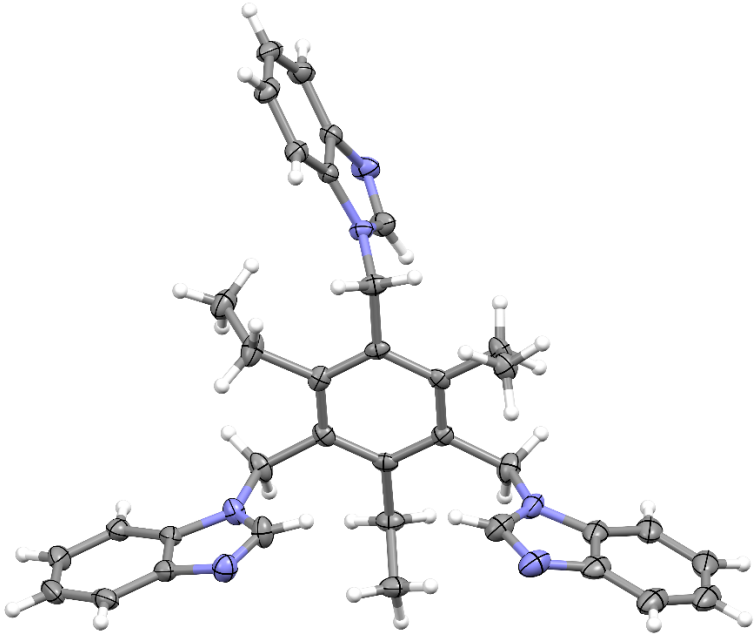

Figure S7. The ellipsoid representation of ligand **4** (thermal displacement ellipsoids are drawn at a 50% probability level; anions (left) and solvent molecules are omitted for clarity; all lengths are in Å).

Crystal data for **4** (obtained from MeCN): CCDC-2126435, $C_{36}H_{36}N_6 \cdot H_2O$, M = 570.72 gmol^{-1}, colourless plate, 0.39 × 0.12 × 0.03 mm^3, monoclinic, space group $P2_1/c$, a = 19.3863(2) Å, b = 11.2138(1) Å, c = 13.9566(1) Å, β = 103.799(1)°, V = 2946.51(5) Å^3, Z = 4, D_{calc} = 1.287 gcm^{-3}, $F(000)$ = 1216, μ = 0.63 mm^{-1}, T = 120.00(10) K, θ_{max} = 76.5°, 6110 total reflections, 5245 with $I_o > 2\sigma(I_o)$, R_{int} = 0.022, 6110 data, 407 parameters, 60 restraints, GooF = 1.03, R = 0.047 and wR = 0.126 [$I_o > 2\sigma(I_o)$], 0.55 <$d\Delta\rho$ < -0.32 eÅ^{-3}.

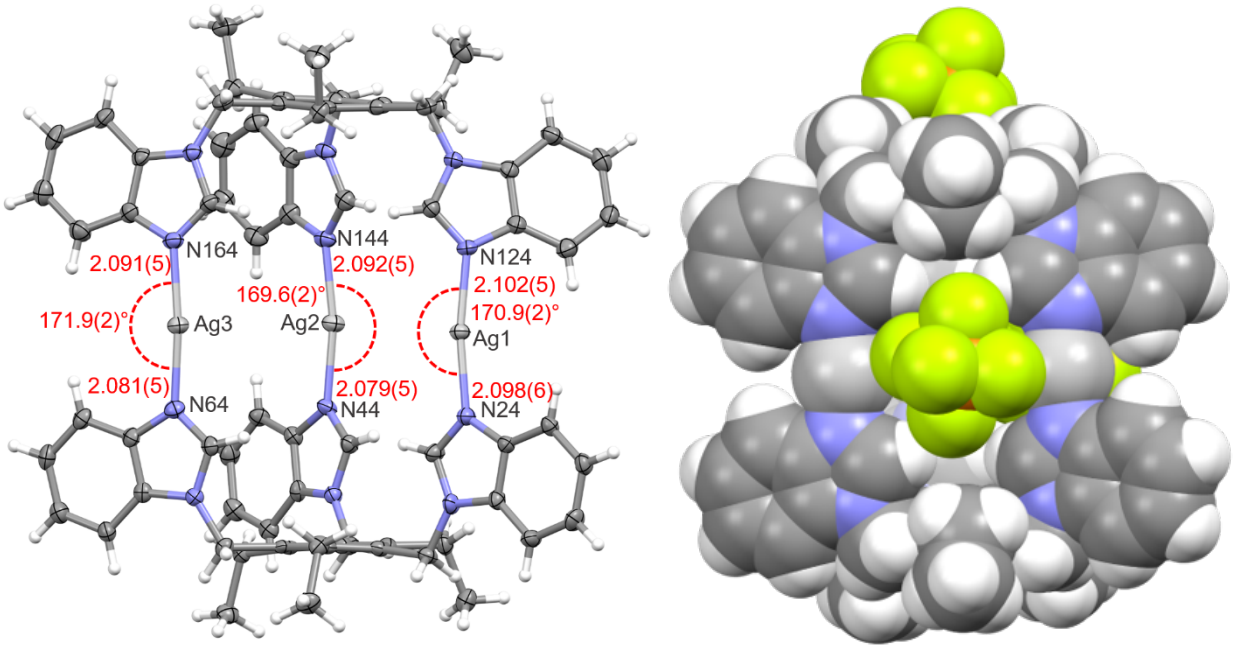

Figure S8. The ellipsoid (left) and spacefill (right) representations of the **[4−Ag−4][PF$_6$]$_3$** Ag-coordination cage (thermal displacement ellipsoids are drawn at a 50% probability level; anions (left) and solvent molecules are omitted for clarity; all lengths are in Å).

Crystal data for **[4−Ag−4][PF$_6$]$_3$** (obtained from MeCN): CCDC-2126436, $[C_{72}H_{72}Ag_3N_{12}][PF_6]_3\cdot(CH_3CN)_4$, M = 2028.15 gmol^{-1}, colourless block, 0.09 × 0.05 × 0.04 mm^3, orthorhombic, space group *Pbca*, a = 24.2463(5) Å, b = 18.9896(4) Å, c = 36.0946(7) Å, V = 16619.9(6) Å^3, Z = 8, D_{calc} = 1.621 gcm^{-3}, F(000) = 8192, μ = 6.99 mm^{-1}, T = 120.00(10) K, θ_{max} = 72.1°, 38547 total reflections, 11290 with $I_o > 2\sigma(I_o)$, R_{int} = 0.050, 11328 data, 1201 parameters, 213 restraints, GooF = 1.06, R = 0.063 and wR = 0.212 [$I_o > 2\sigma(I_o)$], 1.92 <$d\Delta\rho$ < -0.98 eÅ^{-3}.

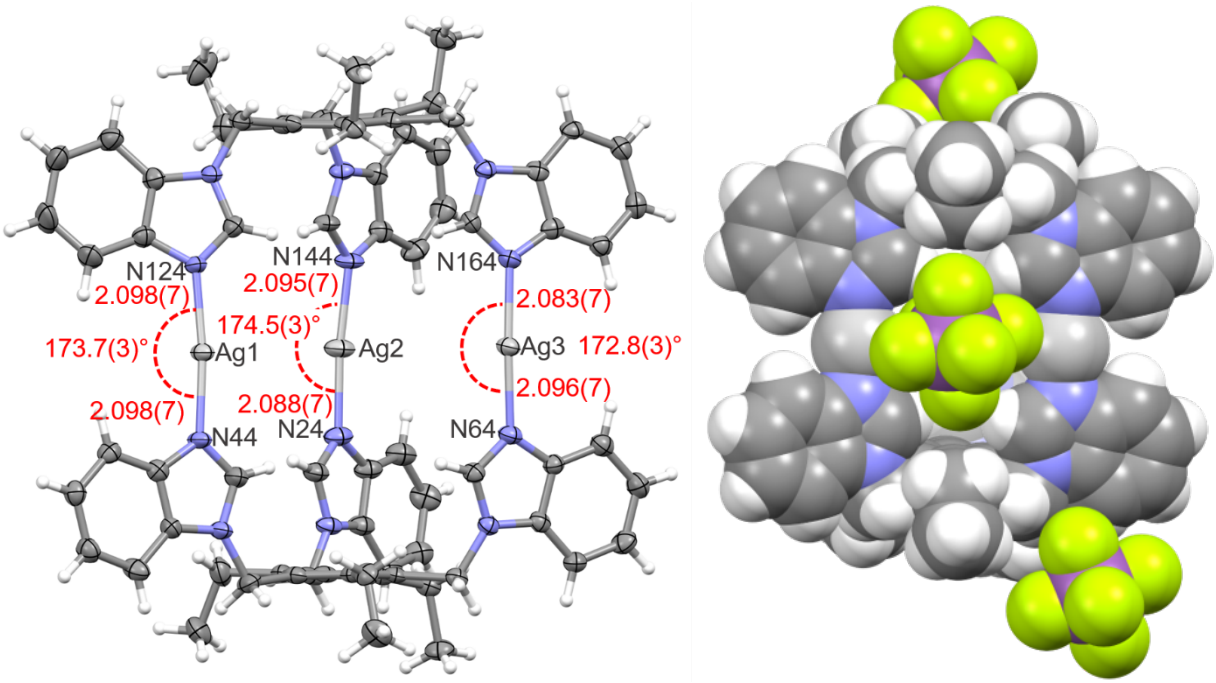

Figure S9. The ellipsoid (left) and spacefill (right) representations of the **[4−Ag−4][SbF$_6$]$_3$** Ag-coordination cage (thermal displacement ellipsoids are drawn at a 50% probability level; anions (left) and solvent molecules are omitted for clarity; all lengths are in Å).

Crystal data for **[4−Ag−4][SbF$_6$]$_3$** (obtained from MeCN): CCDC-2126437, $[C_{72}H_{72}Ag_3N_{12}][SbF_6]_3 \cdot 4(CH_3CN)$, M = 2300.49 gmol^{-1}, colourless block, 0.11 × 0.07 × 0.04 mm^3, triclinic, space group P-1 (No. 2), a = 13.8575(3) Å, b = 18.1569(4) Å, c = 19.1122(3) Å, α = 88.904(2) °, β = 86.763(2) °, γ = 68.015(2)°, V = 4452.00(17) Å^3, Z = 2, D_{calc} = 1.716 gcm^{-3}, F(000) = 2264, μ = 13.08 mm^{-1}, T = 120.00(10) K, θ_{max} = 72.1°, 81954 total reflections, 15020 with $I_o > 2\sigma(I_o)$, R_{int} = 0.059, 17476 data, 1149 parameters, 198 restraints, GooF = 1.09, R = 0.080 and wR = 0.226 [$I_o > 2\sigma(I_o)$], 4.68 <$d\Delta\rho$ < -1.32 eÅ^{-3}.

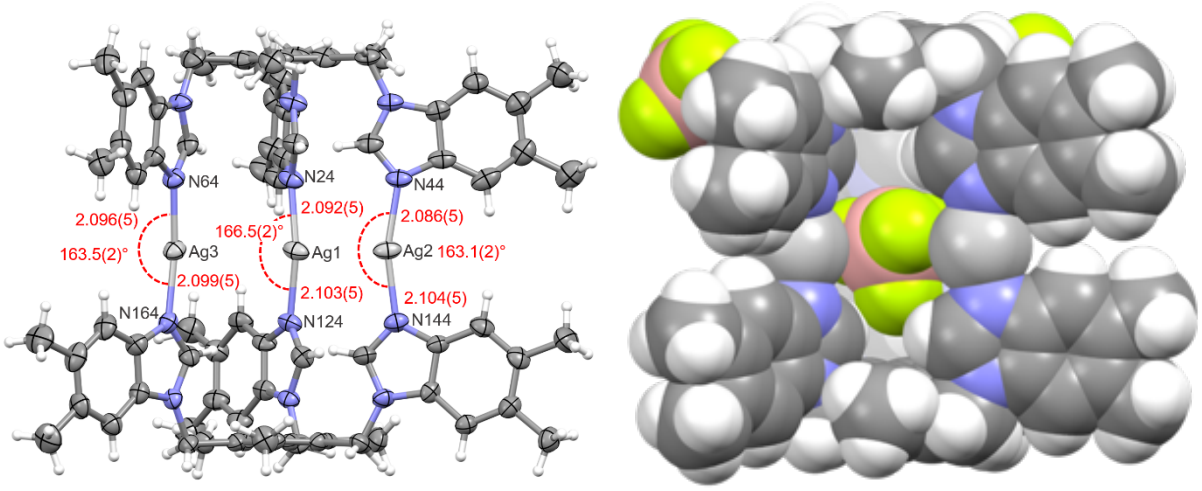

Figure S10. The ellipsoid (left) and spacefill (right) representations of the **[BF_4⊂5−Ag−5][BF_4]$_2$** Ag-coordination cage (thermal displacement ellipsoids are drawn at a 50% probability level; anions (left) and solvent molecules are omitted for clarity; all lengths are in Å).

Crystal data for **[BF_4⊂5−Ag−5][BF_4]$_2$** (obtained from DMSO/$CHCl_3$): CCDC-2126438, $([C_{78}H_{84}Ag_3N_{12}]_2[BF_4]_5)^+$, M = 3460.40 gmol^{-1}, colourless needle, 0.09 × 0.04 × 0.03 mm^3, triclinic, space group *P-1*, a = 17.8788(12) Å, b = 17.8878(13) Å, c = 19.5219(12) Å, α = 65.003(7) °, β = 76.579(5) °, γ = 68.523(7)°, V = 5243.4(7) Å^3, Z = 1, D_{calc} = 1.096 gcm^{-3}, F(000) = 1759, μ = 4.91 mm^{-1}, T = 120.00(10) K, θ_{max} = 72.1°, 33231 total reflections, 12333 with $I_o > 2\sigma(I_o)$, R_{int} = 0.060, 20213 data, 1019 parameters, 124 restraints, GooF = 0.95, R = 0.062 and wR = 0.179 [$I_o > 2\sigma(I_o)$], 1.43 <$d\Delta\rho$ < -1.13 eÅ^{-3}.

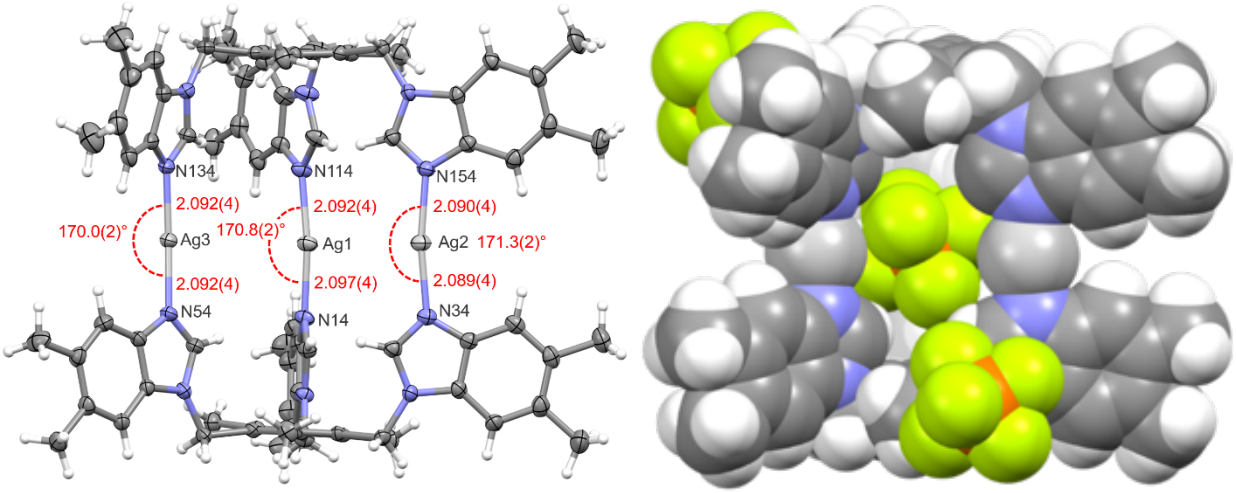

Figure S11. The ellipsoid (left) and spacefill (right) representations of the **[PF_6⊂5−Ag−5][PF_6]$_2$** Ag-coordination cage (thermal displacement ellipsoids are drawn at a 50% probability level, anions (left) and solvent molecules are omitted for clarity; all lengths are in Å).

Crystal data for **[PF_6⊂5−Ag−5][PF_6]$_2$** (obtained from DMSO/$CHCl_3$): CCDC-2126439, $[C_{78}H_{84}Ag_3N_{12}][PF_6]_3 \cdot 6((CH_3)_2SO) \cdot 2(H_2O)$, M = 2470.90 gmol^{-1}, colourless block, 0.13 × 0.09 × 0.08 mm^3, triclinic, space group *P-1*, a = 18.0250(4) Å, b = 18.7080(4) Å, c = 19.9407(4) Å, α = 62.663(2) °, β = 79.563(2) °, γ = 69.602(2)°, V = 5596.9(2) Å^3, Z = 2, D_{calc} = 1.466 gcm^{-3}, $F(000)$ = 2532, μ = 6.36 mm^{-1}, T = 120.00(10) K, θ_{max} = 76.7°, 44929 total reflections, 20051 with $I_o > 2\sigma(I_o)$, R_{int} = 0.030, 22995 data, 1505 parameters, 348 restraints, GooF = 1.04, R = 0.063 and wR = 0.188 [$I_o > 2\sigma(I_o)$], 1.92 <$d\Delta\rho$ < -1.94 eÅ^{-3}.

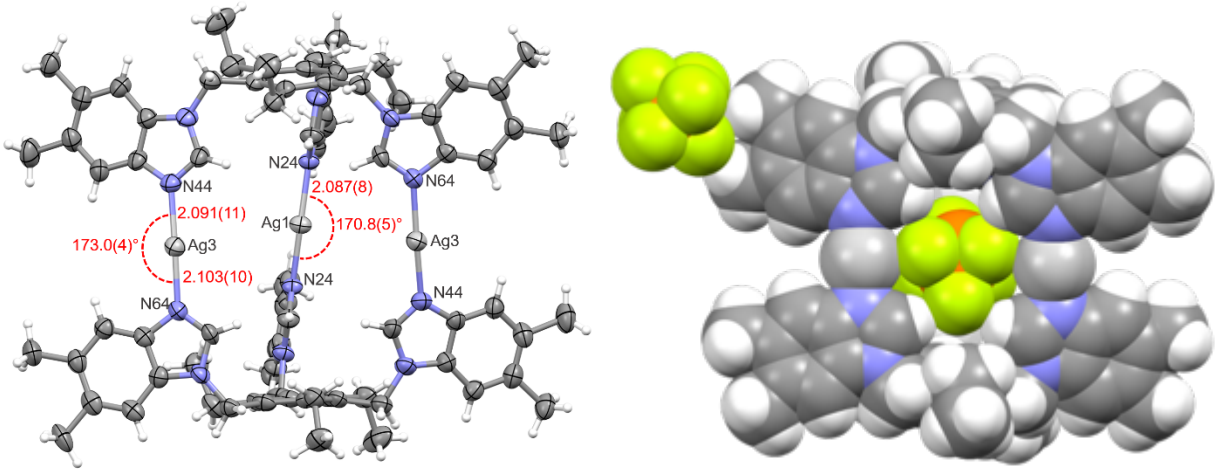

Figure S12. The ellipsoid (left) and spacefill (right) representations of the **[PF_6⊂6−Ag−6][PF_6]$_2$** Ag-coordination cage (thermal displacement ellipsoids are drawn at a 50% probability level; anions (left) and solvent molecules are omitted for clarity; all lengths are in Å).

Crystal data for **[PF_6⊂6−Ag−6][PF_6]$_2$** (obtained from DMSO/$CHCl_3$): CCDC-2126440, $[C_{84}H_{96}Ag_3N_{12}][PF_6]_3$, M = 2032.24 gmol^{-1}, yellow block, 0.12 × 0.07 × 0.04 mm^3, tetragonal, space group I-42d, a = 31.1905(4) Å, c = 18.7751(4) Å, V = 18265.3(6) Å^3, Z = 8, D_{calc} = 1.478 gcm^{-3}, F(000) = 8256, μ = 6.35 mm^{-1}, T = 120.00(10) K, θ_{max} = 76.9°, 19296 total reflections, 6509 with $I_o > 2\sigma(I_o)$, R_{int} = 0.061, 8786 data, 567 parameters, 63 restraints, GooF = 1.00, R = 0.062 and wR = 0.186 [$I_o > 2\sigma(I_o)$], 1.80 <$d\Delta\rho$ < -0.90 eÅ^{-3}.

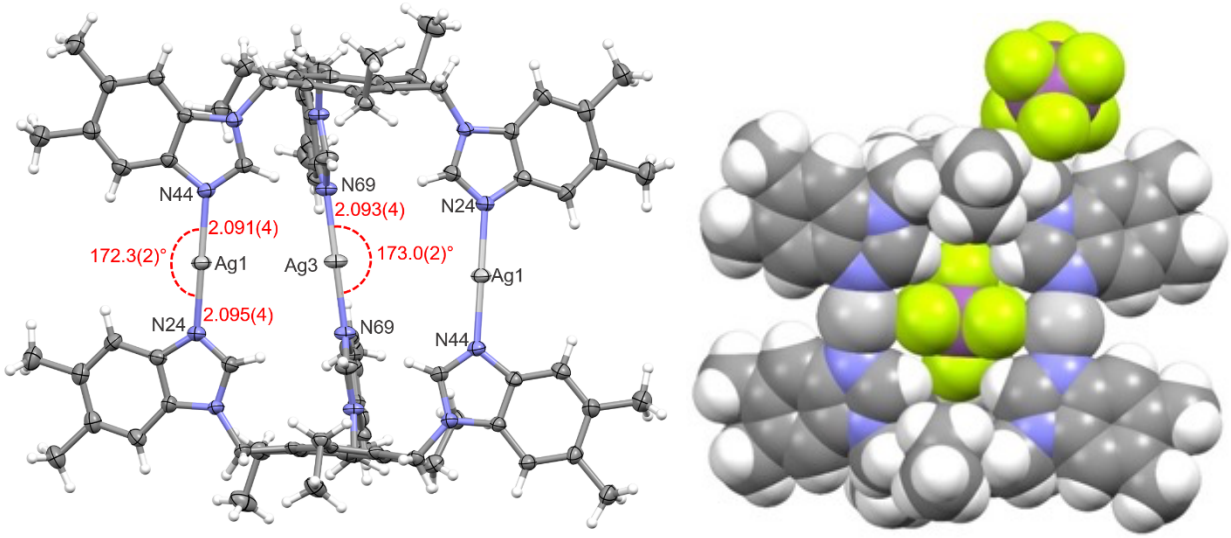

Figure S13. The ellipsoid (left) and spacefill (right) representations of the **[SbF_6⊂6−Ag−6][SbF_6]$_2$** Ag-coordination cage (thermal displacement ellipsoids are drawn at a 50% probability level; anions (left) and solvent molecules are omitted for clarity; all lengths are in Å).

Crystal data for **[SbF_6⊂6−Ag−6][SbF_6]$_2$** (obtained from MeCN): CCDC-2126441, [$C_{84}H_{96}Ag_3N_{12}$][SbF_6]$_3$, M = 2304.58 gmol^{-1}, colourless block, 0.15 × 0.09 × 0.08 mm^3, tetragonal, space group I-42d, a = 31.6145(1) Å, c = 19.0400(1) Å, V = 19030.04(16) Å^3, Z = 8, D_{calc} = 1.609 gcm^{-3}, F(000) = 9120, μ = 12.22 mm^{-1}, T = 120.00(10) K, θ_{max} = 76.9°, 64325 total reflections, 9900 with $I_o > 2\sigma(I_o)$, R_{int} = 0.028, 9982 data, 551 parameters, 6 restraints, GooF = 1.03, R = 0.028 and wR = 0.073 [$I_o > 2\sigma(I_o)$], 1.02 <$d\Delta\rho$ < -1.11 eÅ^{-3}.

Hirshfeld Surface Analysis

Hirshfeld surface[8] plots and 2-D fingerprint calculations were made using *CrystalExplorer*[9] package version 21.5. X-ray crystal structure files ("cifs") were imported, and Hirshfeld surfaces were generated for all host-guest complexes using very high resolution available in Crystal Explorer package version 21.5 and mapped with the d_{norm}. The corresponding contact distances to the Hirshfeld surfaces and fingerprint plots can be found in the following figures.

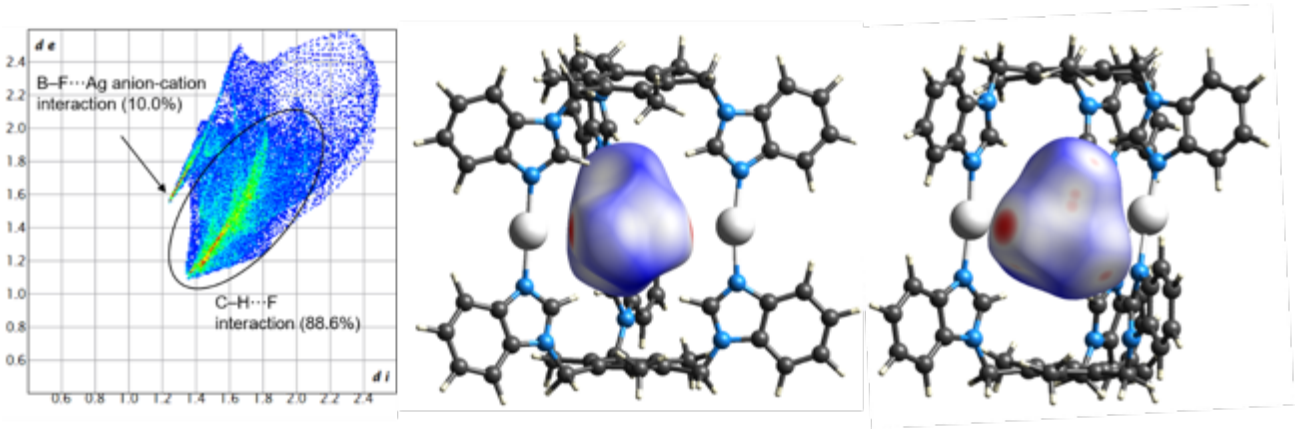

Figure S14. Full fingerprint regions of the tetrafluoroborate anion in the complex **[BF$_4$−⊂3−Ag−3][BF$_4$]$_2$** and two views of the intermolecular contacts to the Hirshfeld surface of the anion. Other interactions contributing to the anion binding: B–F···N (0.5%) and B–F···C (0.9%). In the fingerprint plot, d_i represents the closest internal distance from a given point on the Hirshfeld surface, and d_e is the closest external contact (in Å).

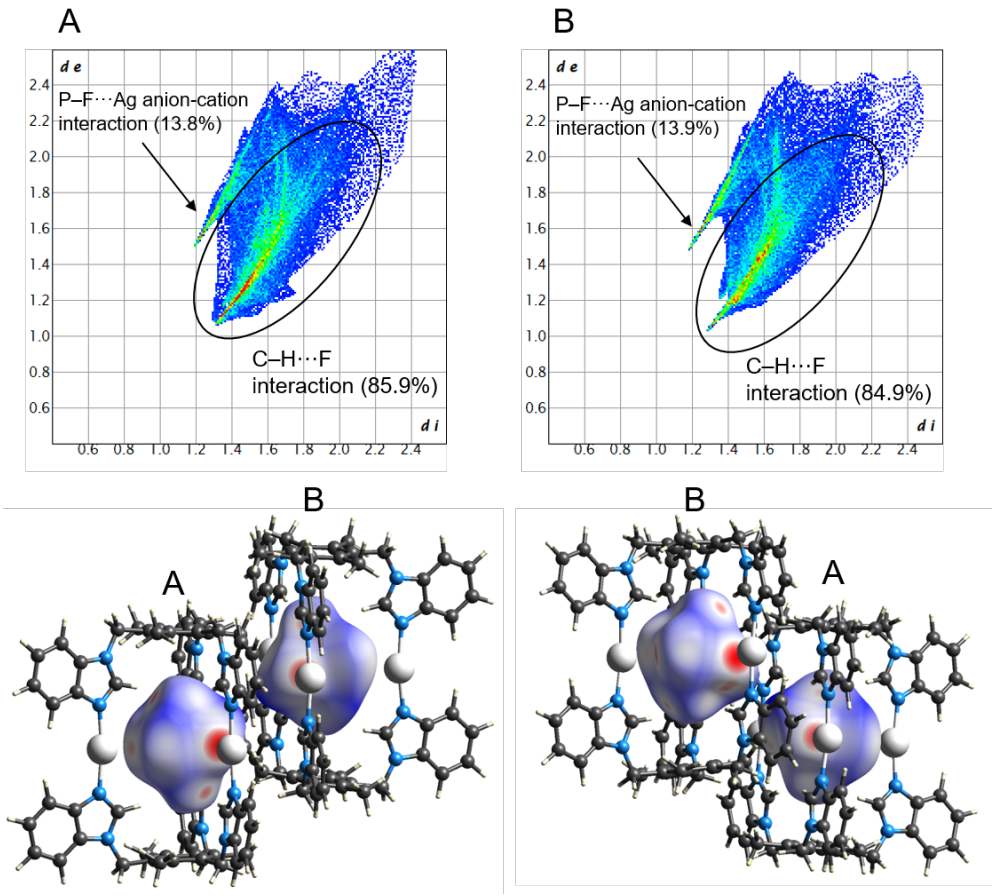

Figure S15. Full fingerprint regions of the hexafluorophosphate anion in the complex **[PF_6−⊂3−Ag−3][PF_6]$_2$** and two views of the intermolecular contacts to the Hirshfeld surface of the anion. Other interactions contributing to the anion binding: P–F···N (A: 0.1%, B: 0.9%) and P–F···C (A: 0.2%, B: 0.3%). In the fingerprint plot, d_i represents the closest internal distance from a given point on the Hirshfeld surface, and d_e is the closest external contact (in Å).

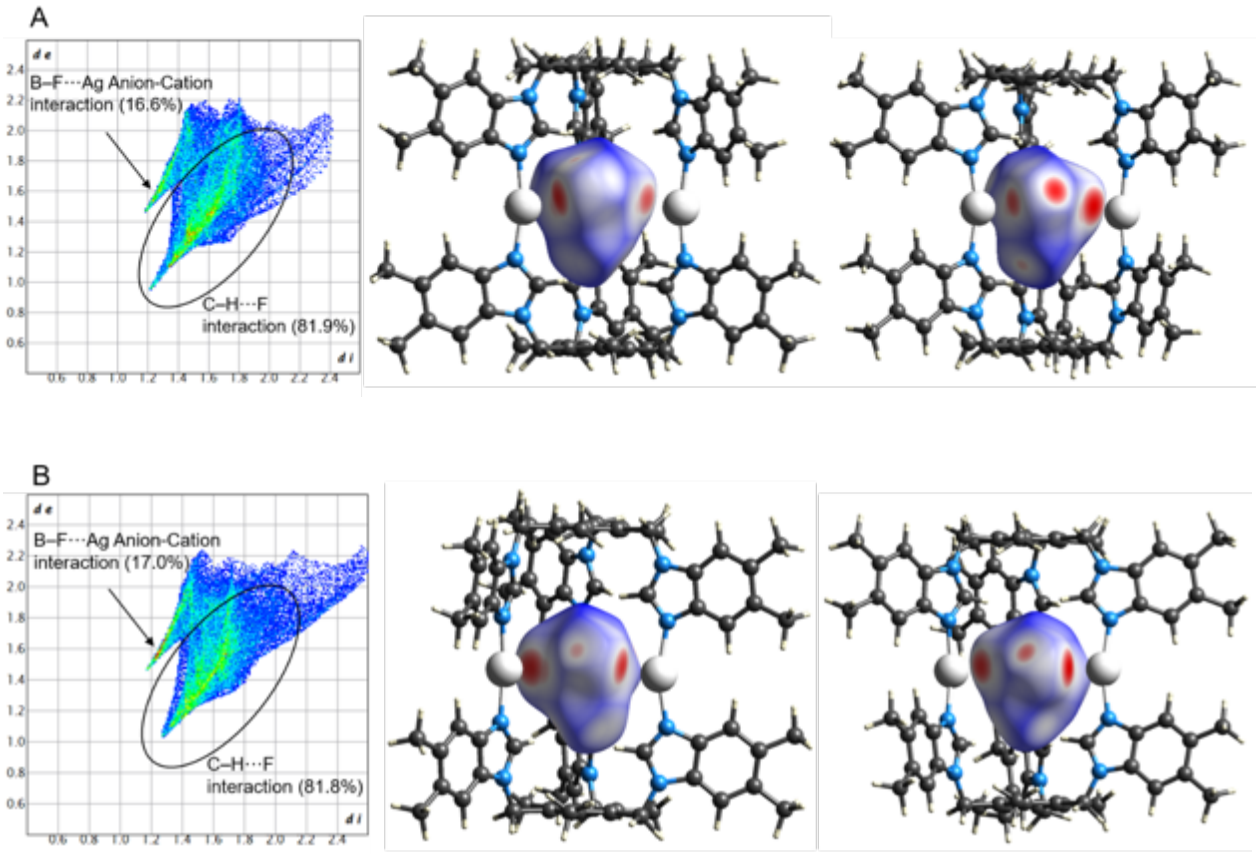

Figure S16. Full fingerprint regions of the tetrafluoroborate anion in the complex **[BF_4−⊂5−Ag−5][BF_4]$_2$** and two views of the intermolecular contacts to the Hirshfeld surface of the anion (disordered over two positions with occupancies A: 35% B: 65%). Other interactions contributing to the anion binding: B–F···C (A: 1.5%, B: 1.2%). In the fingerprint plot, d_i represents the closest internal distance from a given point on the Hirshfeld surface, and d_e is the closest external contact (in Å).

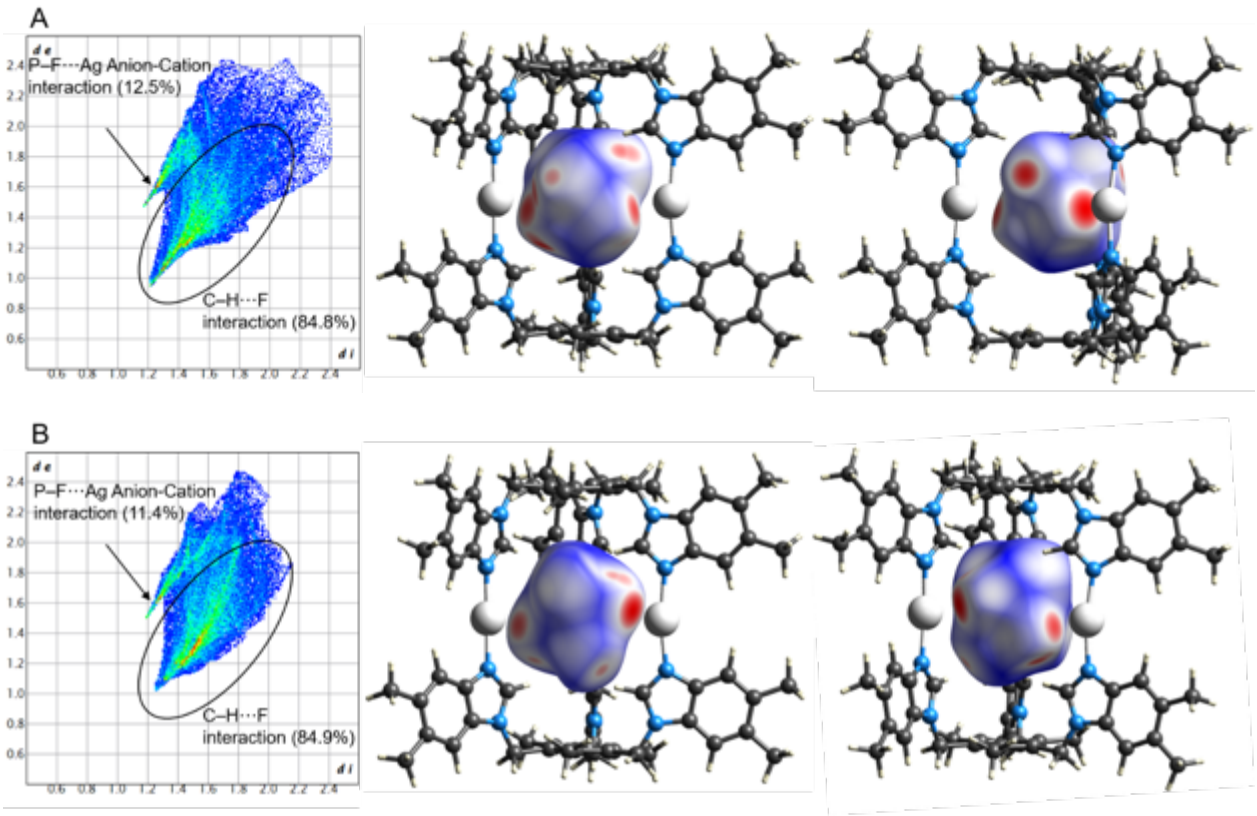

Figure S17. Full fingerprint regions of the hexafluorophosphate anion in the complex **[PF_6−⊂5−Ag−5][PF_6]$_2$** and two views of the intermolecular contacts to the Hirshfeld surface of the anion (disordered over two positions with occupancies A: 48% B: 52%). Other interactions contributing to the anion binding: B–F···N (A: 0.3%, B: 0.2%) and B–F···C (A: 2.4%, B: 3.5%). In the fingerprint plot, d_i represents the closest internal distance from a given point on the Hirshfeld surface, and d_e is the closest external contact (in Å).

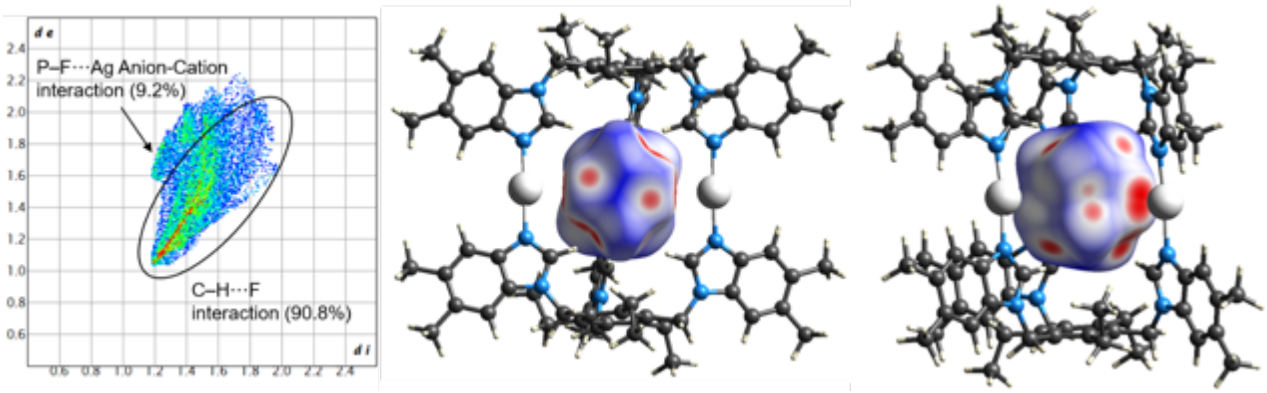

Figure S18. Full fingerprint regions of the hexafluorophosphate anion in the complex **[PF_6−⊂6−Ag−6][PF_6]$_2$** and two views of the intermolecular contacts to the Hirshfeld surface of the anion. In the fingerprint plot d_i represents closest internal distance from a given point on the Hirshfeld surface, and d_e is the closest external contact (in Å). The anion was found in a special position inside the cage due to high symmetry and the two different disordered positions (50:50) could not be modelled separately in the Hirshfeld analysis, and thus, are displayed here together.

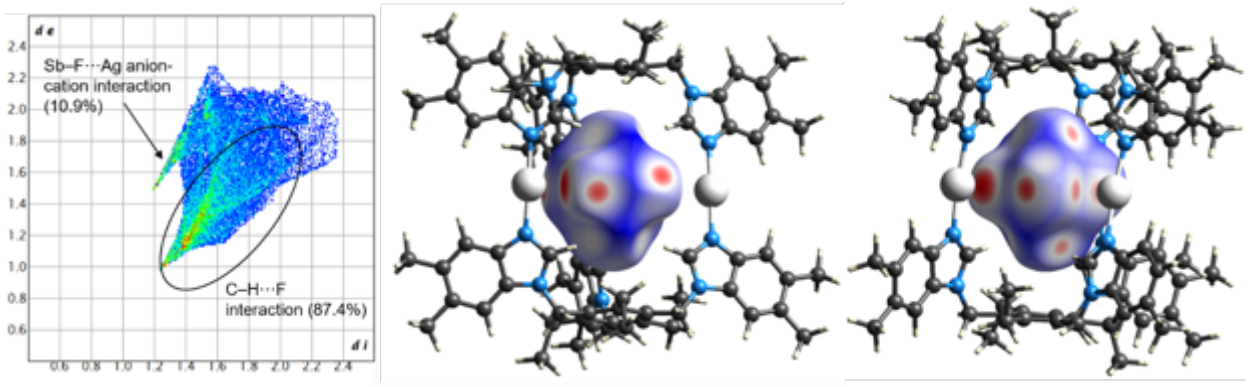

Figure S19. Full fingerprint regions of the hexafluoroantimonate anion in the complex **[SbF_6−⊂6−Ag−6][SbF_6]$_2$** and two views of the intermolecular contacts to the Hirshfeld surface of the anion. Other interactions contributing to the anion binding: Sb–F···C (1.7%). In the fingerprint plot, d_i represents the closest internal distance from a given point on the Hirshfeld surface, and d_e is the closest external contact (in Å).

Computational Methods

General

The cage geometries were modelled at MM-level (MMFF) so that only the N–I distances were fixed to the previously observed bond distances value of 2.25 Å (from single crystal X-ray crystallographic studies of several $[N–I–N]^+$ complexes), all other bond distances are angles were free, using SPARTAN18 software.[10]

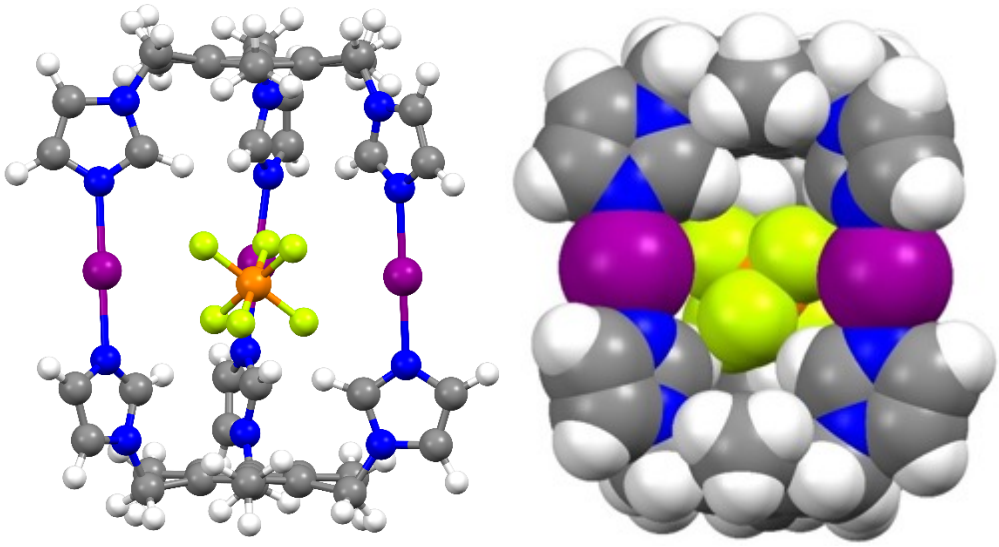

Figure S20. The ball-and-stick (left) and spacefill (right) representations of the modeled structure of **$[PF_6{-}\subset\mathbf{1}{-}I{-}\mathbf{1}][PF_6]_2$** iodine(I) cage.

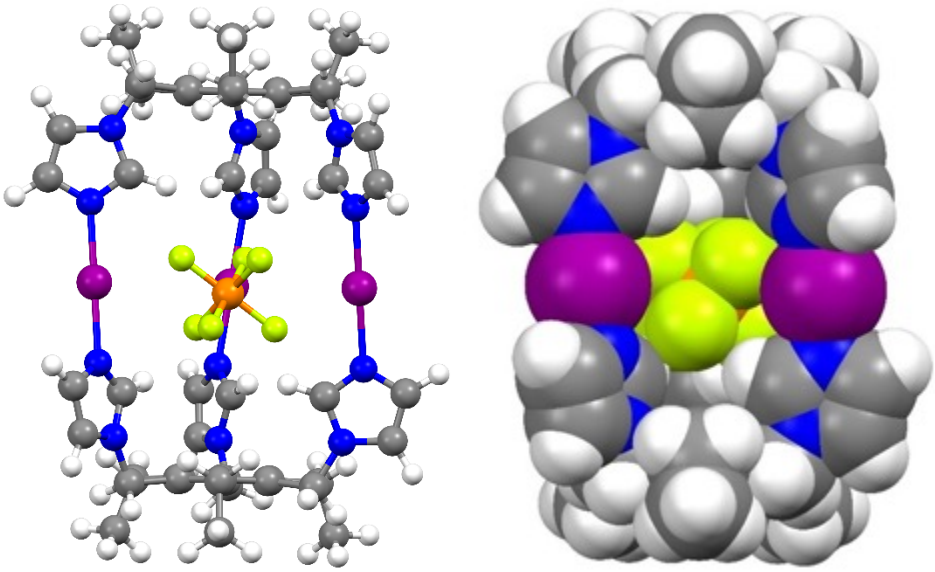

Figure S21. The ball-and-stick (left) and spacefill (right) representations of the modeled structure of **$[PF_6{-}\subset\mathbf{2}{-}I{-}\mathbf{2}][PF_6]_2$** iodine(I) cage.

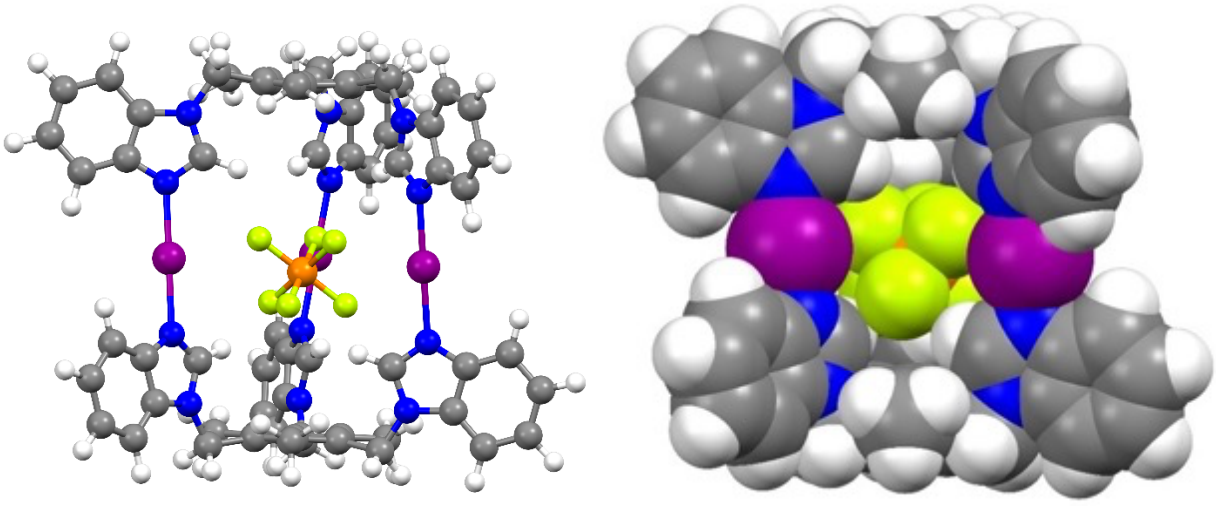

Figure S22. The ball-and-stick (left) and spacefill (right) representations of the modeled structure of **$[PF_6{-}\subset 3{-}I{-}3][PF_6]_2$** iodine(I) cage.

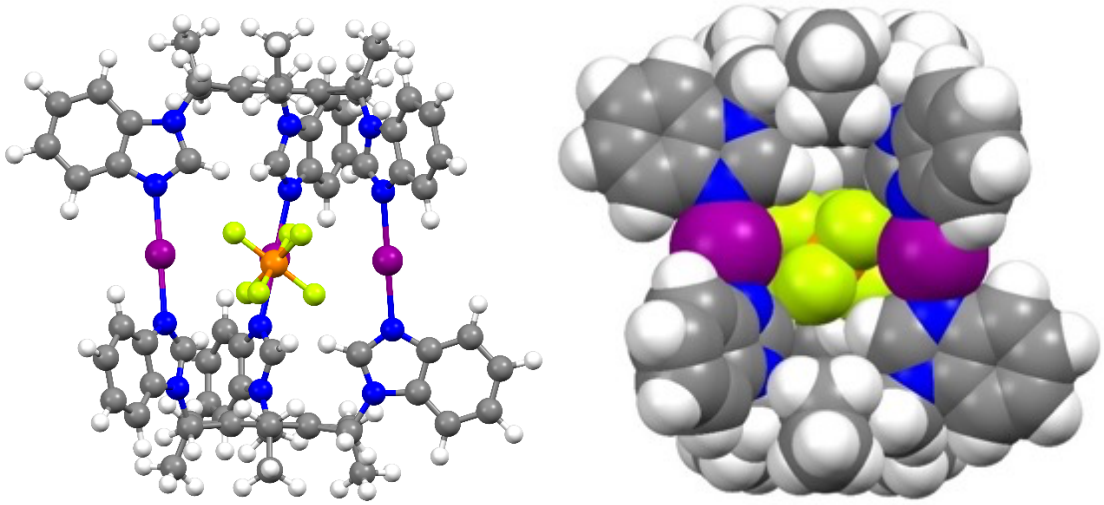

Figure S23.. The ball-and-stick (left) and spacefill (right) representations of the modeled structure of **$[PF_6{-}\subset 4{-}I{-}4][PF_6]_2$** iodine(I) cage.

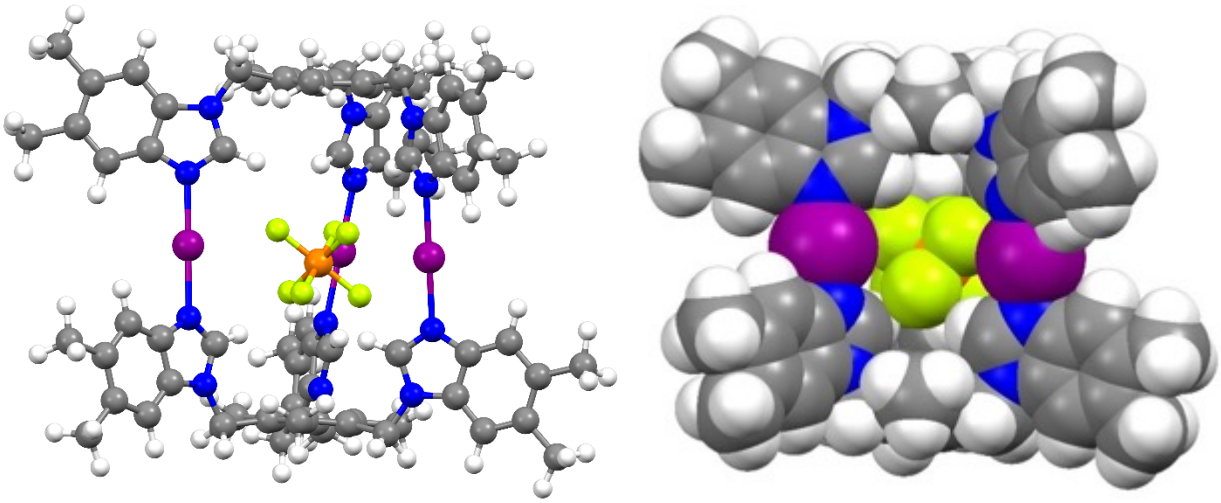

Figure S24. The ball-and-stick (left) and spacefill (right) representations of the modeled structure of **$[PF_6{-}\subset{\mathbf{5}}{-}I{-}\mathbf{5}][PF_6]_2$** iodine(I) cage.

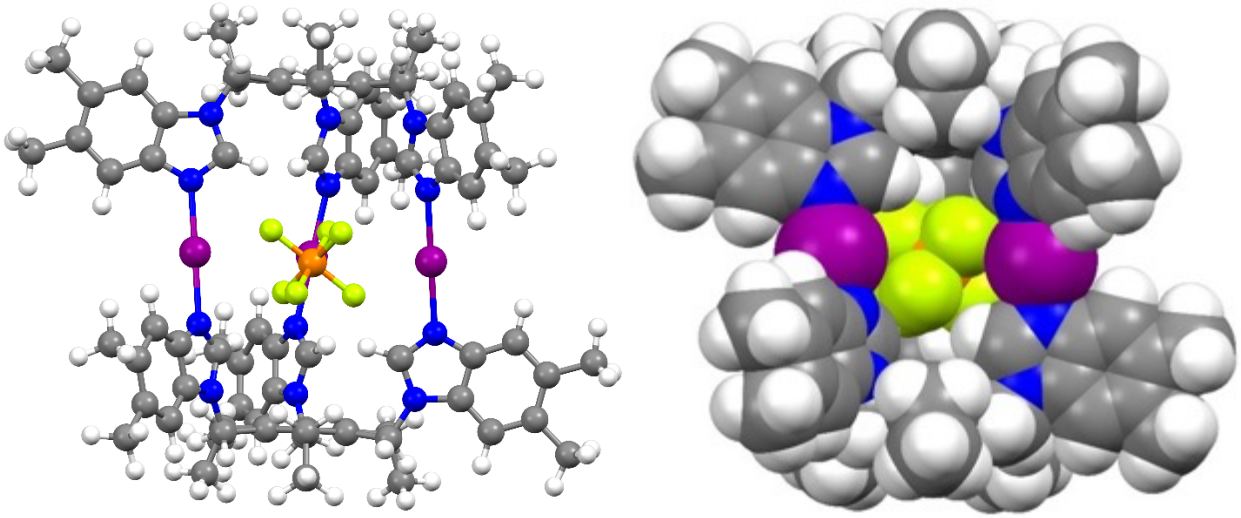

Figure S25. The ball-and-stick (left) and spacefill (right) representations of the modeled structure of **$[PF_6{-}\subset{\mathbf{6}}{-}I{-}\mathbf{6}][PF_6]_2$** iodine(I) cage.

The Cartesian Coordinates

$[PF_6{-}\subset 1{-}I{-}1][PF_6]_2$

C	0.827000	1.155000	5.236000
C	-0.830000	-1.164000	5.278000
C	-0.591000	1.295000	5.280000
C	1.419000	-0.142000	5.279000
C	0.589000	-1.300000	5.235000
C	-1.417000	0.134000	5.235000
C	1.712000	2.388000	5.271000
H	1.234000	3.250000	4.800000
H	2.631000	2.232000	4.699000
C	-2.928000	0.283000	5.270000
H	-3.435000	-0.561000	4.797000
C	1.215000	-2.682000	5.268000
H	0.620000	-3.400000	4.695000
H	2.200000	-2.699000	4.796000
C	-1.214000	2.674000	5.521000
H	-0.605000	3.234000	6.240000
H	-2.205000	2.607000	5.981000
C	2.925000	-0.291000	5.519000
H	3.106000	-1.100000	6.237000
H	3.363000	0.600000	5.980000
C	-1.712000	-2.394000	5.517000
H	-1.159000	-3.219000	5.977000
H	-2.503000	-2.147000	6.236000
N	-1.340000	3.461000	4.289000
N	3.669000	-0.575000	4.286000
N	-2.330000	-2.895000	4.284000
C	-1.435000	3.003000	3.022000
H	-1.406000	1.978000	2.679000
C	3.320000	-0.262000	3.021000
H	2.417000	0.225000	2.678000
C	-1.885000	-2.747000	3.018000
H	-1.012000	-2.209000	2.676000
N	-2.748000	-3.411000	2.255000
N	-1.579000	4.083000	2.260000
N	4.327000	-0.677000	2.257000
C	5.357000	-1.224000	2.953000
C	4.952000	-1.163000	4.259000
C	-1.621000	5.249000	2.957000
C	-1.472000	4.866000	4.262000
C	-3.737000	-4.031000	2.950000
C	-3.481000	-3.712000	4.256000
H	-3.252000	1.158000	4.698000
C	0.831000	1.159000	-5.200000
C	-0.832000	-1.154000	-5.246000

C	1.419000	-0.138000	-5.245000
C	-0.586000	1.303000	-5.244000
C	-1.415000	0.145000	-5.201000
C	0.586000	-1.294000	-5.202000
C	1.715000	2.392000	-5.226000
H	2.684000	2.214000	-4.752000
H	1.270000	3.210000	-4.650000
C	1.212000	-2.676000	-5.229000
H	0.574000	-3.426000	-4.756000
C	-2.926000	0.294000	-5.227000
H	-3.256000	1.222000	-4.753000
H	-3.412000	-0.501000	-4.653000
C	2.923000	-0.286000	-5.480000
H	3.263000	0.473000	-6.195000
H	3.179000	-1.244000	-5.944000
C	-1.210000	2.680000	-5.478000
H	-2.037000	2.595000	-6.194000
H	-0.507000	3.380000	-5.941000
C	-1.712000	-2.382000	-5.482000
H	-2.670000	-2.124000	-5.945000
H	-1.224000	-3.055000	-6.197000
N	3.705000	-0.159000	-4.245000
N	-1.712000	3.292000	-4.243000
N	-1.992000	-3.124000	-4.248000
C	3.290000	-0.373000	-2.978000
H	2.302000	-0.650000	-2.636000
C	-1.320000	3.038000	-2.976000
H	-0.586000	2.321000	-2.634000
C	-1.969000	-2.659000	-2.980000
H	-1.715000	-1.665000	-2.637000
N	-2.339000	-3.685000	-2.218000
N	4.363000	-0.181000	-2.215000
N	-2.023000	3.871000	-2.213000
C	-2.850000	4.693000	-2.909000
C	-2.661000	4.335000	-4.215000
C	5.488000	0.125000	-2.912000
C	5.083000	0.142000	-4.218000
C	-2.637000	-4.812000	-2.916000
C	-2.421000	-4.468000	-4.222000
H	2.143000	-2.700000	-4.654000
I	-2.544000	-3.549000	0.018000
I	-1.801000	3.977000	0.024000
I	4.345000	-0.429000	0.021000
H	-3.448000	5.416000	-2.386000
H	-3.074000	4.691000	-5.147000
H	-1.448000	5.411000	5.194000
H	-1.755000	6.177000	2.436000
H	6.413000	0.280000	-2.389000
H	5.597000	0.322000	-5.149000

H	5.412000	-1.457000	5.190000
H	6.228000	-1.572000	2.431000
H	-2.965000	-5.691000	-2.394000
H	-2.522000	-5.002000	-5.154000
H	-3.966000	-3.964000	5.187000
H	-4.474000	-4.611000	2.428000
H	-3.273000	0.373000	6.304000
H	1.963000	2.641000	6.306000
H	1.309000	-3.027000	6.302000
H	1.411000	-2.978000	-6.262000
H	1.878000	2.717000	-6.258000
H	-3.287000	0.274000	-6.260000
P	0.000000	0.000000	-0.328000
F	0.993000	0.891000	-1.279000
F	0.275000	-1.304000	-1.280000
F	-1.267000	0.415000	-1.279000
F	-0.994000	-0.889000	0.622000
F	-0.273000	1.304000	0.624000
F	1.266000	-0.417000	0.623000

$[PF_6{-}\subset 2{-}I{-}2][PF_6]_2$

C	0.808000	1.175000	5.383000
C	-0.812000	-1.187000	5.397000
C	-0.619000	1.291000	5.399000
C	1.430000	-0.115000	5.398000
C	0.616000	-1.293000	5.381000
C	-1.425000	0.107000	5.382000
C	1.671000	2.437000	5.439000
H	1.176000	3.268000	4.931000
H	2.582000	2.293000	4.846000
C	-2.950000	0.224000	5.437000
H	-3.422000	-0.621000	4.927000
C	1.277000	-2.672000	5.435000
H	0.697000	-3.388000	4.842000
H	2.245000	-2.658000	4.927000
C	-1.274000	2.671000	5.547000
H	-0.751000	3.254000	6.310000
H	-2.307000	2.627000	5.896000
C	2.953000	-0.238000	5.545000
H	3.196000	-0.984000	6.308000
H	3.432000	0.678000	5.895000
C	-1.680000	-2.444000	5.543000
H	-1.126000	-3.317000	5.892000
H	-2.447000	-2.283000	6.306000
N	-1.286000	3.428000	4.289000
N	3.614000	-0.606000	4.287000
N	-2.329000	-2.832000	4.285000

C	-1.427000	2.939000	3.039000
H	-1.505000	1.905000	2.732000
C	3.261000	-0.237000	3.037000
H	2.403000	0.348000	2.732000
C	-1.834000	-2.709000	3.035000
H	-0.899000	-2.258000	2.730000
N	-2.737000	-3.272000	2.237000
N	-1.464000	4.004000	2.242000
N	4.200000	-0.737000	2.240000
C	5.194000	-1.389000	2.897000
C	4.834000	-1.311000	4.215000
C	-1.397000	5.190000	2.901000
C	-1.284000	4.838000	4.218000
C	-3.798000	-3.807000	2.895000
C	-3.551000	-3.535000	4.212000
H	-3.281000	1.085000	4.845000
C	0.858000	1.147000	-5.359000
C	-0.860000	-1.143000	-5.377000
C	1.424000	-0.168000	-5.377000
C	-0.562000	1.322000	-5.376000
C	-1.418000	0.175000	-5.360000
C	0.562000	-1.310000	-5.361000
C	1.777000	2.369000	-5.409000
H	2.722000	2.164000	-4.899000
H	1.348000	3.184000	-4.815000
C	1.160000	-2.717000	-5.412000
H	0.511000	-3.434000	-4.903000
C	-2.936000	0.360000	-5.411000
H	-3.232000	1.280000	-4.900000
H	-3.428000	-0.420000	-4.817000
C	2.940000	-0.346000	-5.520000
H	3.326000	0.336000	-6.282000
H	3.231000	-1.338000	-5.868000
C	-1.166000	2.725000	-5.518000
H	-1.950000	2.719000	-6.281000
H	-0.452000	3.473000	-5.865000
C	-1.772000	-2.367000	-5.522000
H	-2.777000	-2.122000	-5.869000
H	-1.375000	-3.042000	-6.285000
N	3.658000	-0.114000	-4.261000
N	-1.727000	3.229000	-4.259000
N	-1.930000	-3.106000	-4.264000
C	3.230000	-0.386000	-3.010000
H	2.268000	-0.775000	-2.703000
C	-1.279000	2.993000	-3.008000
H	-0.461000	2.354000	-2.701000
C	-1.950000	-2.601000	-3.012000
H	-1.806000	-1.574000	-2.703000
N	-2.204000	-3.637000	-2.216000

N	4.253000	-0.088000	-2.213000
N	-2.049000	3.730000	-2.211000
C	-2.971000	4.479000	-2.870000
C	-2.777000	4.169000	-4.188000
C	5.363000	0.336000	-2.873000
C	4.997000	0.325000	-4.190000
C	-2.391000	-4.809000	-2.877000
C	-2.219000	-4.485000	-4.194000
H	2.081000	-2.754000	-4.819000
I	-2.468000	-3.451000	0.011000
I	-1.755000	3.863000	0.016000
I	4.223000	-0.411000	0.013000
C	1.428000	-3.201000	-6.834000
H	2.118000	-2.542000	-7.369000
H	0.510000	-3.254000	-7.425000
H	1.870000	-4.202000	-6.810000
C	2.063000	2.844000	-6.829000
H	2.568000	2.076000	-7.421000
H	2.709000	3.727000	-6.805000
H	1.148000	3.112000	-7.366000
C	-3.490000	0.371000	-6.832000
H	-3.076000	1.193000	-7.423000
H	-4.578000	0.489000	-6.808000
H	-3.264000	-0.555000	-7.369000
C	-3.491000	0.321000	6.859000
H	-3.087000	1.185000	7.395000
H	-3.246000	-0.567000	7.450000
H	-4.582000	0.418000	6.838000
C	1.463000	-3.191000	6.857000
H	2.108000	-2.535000	7.449000
H	1.924000	-4.183000	6.836000
H	0.512000	-3.273000	7.393000
C	2.027000	2.856000	6.862000
H	2.656000	3.751000	6.841000
H	2.573000	2.073000	7.396000
H	1.135000	3.086000	7.453000
H	-3.622000	5.129000	-2.319000
H	-3.242000	4.504000	-5.103000
H	-1.213000	5.408000	5.132000
H	-1.448000	6.110000	2.350000
H	6.252000	0.575000	-2.321000
H	5.519000	0.561000	-5.105000
H	5.292000	-1.659000	5.128000
H	6.016000	-1.803000	2.345000
H	-2.630000	-5.699000	-2.326000
H	-2.276000	-5.055000	-5.109000
H	-4.080000	-3.760000	5.126000
H	-4.569000	-4.311000	2.343000
P	0.000000	0.000000	-0.215000

F	1.086000	0.773000	-1.167000
F	0.126000	-1.326000	-1.169000
F	-1.212000	0.555000	-1.167000
F	-1.087000	-0.769000	0.738000
F	-0.122000	1.325000	0.740000
F	1.209000	-0.557000	0.738000

$[PF_6{-}\subset 3{-}I{-}3][PF_6]_2$

C	0.854000	1.139000	5.220000
C	-0.855000	-1.142000	5.264000
C	-0.561000	1.311000	5.264000
C	1.416000	-0.170000	5.264000
C	0.560000	-1.309000	5.220000
C	-1.413000	0.169000	5.220000
C	1.765000	2.353000	5.256000
H	1.308000	3.224000	4.780000
H	2.683000	2.175000	4.687000
C	-2.921000	0.351000	5.256000
H	-3.446000	-0.480000	4.780000
C	1.156000	-2.706000	5.255000
H	0.543000	-3.412000	4.686000
H	2.139000	-2.745000	4.780000
C	-1.152000	2.703000	5.511000
H	-0.528000	3.233000	6.239000
H	-2.146000	2.658000	5.967000
C	2.917000	-0.354000	5.510000
H	3.064000	-1.160000	6.239000
H	3.375000	0.529000	5.967000
C	-1.765000	-2.350000	5.510000
H	-1.229000	-3.188000	5.966000
H	-2.536000	-2.075000	6.239000
N	-1.253000	3.499000	4.285000
N	3.657000	-0.665000	4.285000
N	-2.404000	-2.835000	4.285000
C	-1.388000	3.042000	3.023000
H	-1.413000	2.013000	2.692000
C	3.329000	-0.319000	3.023000
H	2.450000	0.217000	2.692000
C	-1.941000	-2.724000	3.022000
H	-1.037000	-2.231000	2.692000
N	-2.813000	-3.349000	2.239000
N	-1.494000	4.110000	2.240000
N	4.307000	-0.762000	2.240000
C	5.323000	-1.367000	2.912000
C	4.920000	-1.310000	4.254000
C	-1.477000	5.293000	2.913000
C	-1.326000	4.916000	4.255000

C	-3.845000	-3.926000	2.912000
C	-3.594000	-3.607000	4.254000
H	-3.226000	1.235000	4.687000
C	0.797000	1.179000	-5.194000
C	-0.798000	-1.180000	-5.239000
C	1.421000	-0.100000	-5.239000
C	-0.623000	1.282000	-5.239000
C	-1.419000	0.101000	-5.194000
C	0.623000	-1.279000	-5.194000
C	1.645000	2.438000	-5.221000
H	2.616000	2.289000	-4.743000
H	1.175000	3.245000	-4.650000
C	1.288000	-2.643000	-5.221000
H	0.674000	-3.410000	-4.743000
C	-2.934000	0.207000	-5.221000
H	-3.290000	1.122000	-4.743000
H	-3.397000	-0.604000	-4.650000
C	2.929000	-0.203000	-5.480000
H	3.230000	0.564000	-6.203000
H	3.210000	-1.154000	-5.943000
C	-1.288000	2.639000	-5.480000
H	-2.103000	2.516000	-6.203000
H	-0.605000	3.358000	-5.943000
C	-1.641000	-2.434000	-5.480000
H	-2.605000	-2.202000	-5.943000
H	-1.127000	-3.078000	-6.203000
N	3.712000	-0.047000	-4.253000
N	-1.815000	3.238000	-4.253000
N	-1.897000	-3.190000	-4.253000
C	3.309000	-0.296000	-2.988000
H	2.334000	-0.624000	-2.657000
C	-1.398000	3.014000	-2.988000
H	-0.627000	2.333000	-2.656000
C	-1.911000	-2.718000	-2.989000
H	-1.707000	-1.709000	-2.657000
N	-2.243000	-3.741000	-2.207000
N	4.361000	-0.072000	-2.207000
N	-2.118000	3.813000	-2.207000
C	-2.997000	4.603000	-2.881000
C	-2.812000	4.246000	-4.223000
C	5.485000	0.294000	-2.882000
C	5.082000	0.313000	-4.224000
C	-2.488000	-4.897000	-2.882000
C	-2.271000	-4.557000	-4.224000
H	2.222000	-2.639000	-4.651000
I	-2.526000	-3.543000	0.016000
I	-1.805000	3.959000	0.017000
I	4.331000	-0.416000	0.016000
C	-1.279000	5.865000	5.275000

H	-1.172000	5.600000	6.321000
C	-1.385000	7.205000	4.872000
H	-1.357000	7.994000	5.629000
C	-1.533000	7.572000	3.518000
H	-1.614000	8.631000	3.266000
C	-1.584000	6.613000	2.498000
H	-1.702000	6.884000	1.456000
C	-3.901000	5.571000	-2.467000
H	-4.028000	5.835000	-1.424000
C	-4.636000	6.187000	-3.489000
H	-5.365000	6.961000	-3.237000
C	-4.457000	5.838000	-4.843000
H	-5.052000	6.354000	-5.601000
C	-3.537000	4.857000	-5.246000
H	-3.406000	4.604000	-6.292000
C	6.775000	0.593000	-2.467000
H	7.067000	0.571000	-1.425000
C	7.676000	0.922000	-3.489000
H	8.710000	1.166000	-3.237000
C	7.284000	0.941000	-4.844000
H	8.028000	1.199000	-5.602000
C	5.974000	0.635000	-5.246000
H	5.690000	0.648000	-6.292000
C	6.519000	-1.935000	2.497000
H	6.812000	-1.968000	1.455000
C	7.324000	-2.459000	3.517000
H	8.282000	-2.918000	3.265000
C	6.933000	-2.404000	4.871000
H	7.602000	-2.822000	5.628000
C	5.719000	-1.825000	5.275000
H	5.436000	-1.786000	6.321000
C	-4.935000	-4.678000	2.497000
H	-5.111000	-4.916000	1.455000
C	-5.791000	-5.114000	3.517000
H	-6.668000	-5.714000	3.265000
C	-5.548000	-4.803000	4.871000
H	-6.245000	-5.173000	5.628000
C	-4.440000	-4.040000	5.275000
H	-4.264000	-3.815000	6.320000
C	-2.438000	-5.491000	-5.247000
H	-2.284000	-5.251000	-6.293000
C	-2.828000	-6.778000	-4.844000
H	-2.976000	-7.552000	-5.602000
C	-3.040000	-7.108000	-3.490000
H	-3.345000	-8.126000	-3.238000
C	-2.874000	-6.164000	-2.468000
H	-3.039000	-6.406000	-1.425000
H	1.492000	-2.941000	-6.254000
H	-3.294000	0.179000	-6.254000

H	1.802000	2.763000	-6.254000
H	2.018000	2.602000	6.290000
H	-3.263000	0.446000	6.290000
H	1.245000	-3.050000	6.290000
P	-0.000000	0.000000	-0.338000
F	0.980000	0.904000	-1.290000
F	0.293000	-1.301000	-1.290000
F	-1.273000	0.397000	-1.290000
F	-0.981000	-0.902000	0.613000
F	-0.291000	1.300000	0.614000
F	1.272000	-0.398000	0.613000

$[PF_6{-}\subset 4{-}I{-}4][PF_6]_2$

C	0.836000	1.160000	5.368000
C	-0.838000	-1.164000	5.385000
C	-0.589000	1.307000	5.385000
C	1.427000	-0.144000	5.385000
C	0.587000	-1.304000	5.368000
C	-1.422000	0.143000	5.368000
C	1.728000	2.401000	5.422000
H	1.253000	3.243000	4.912000
H	2.635000	2.235000	4.829000
C	-2.944000	0.295000	5.422000
H	-3.435000	-0.537000	4.912000
C	1.216000	-2.698000	5.421000
H	0.619000	-3.400000	4.829000
H	2.182000	-2.707000	4.911000
C	-1.211000	2.702000	5.536000
H	-0.677000	3.254000	6.314000
H	-2.247000	2.683000	5.876000
C	2.947000	-0.303000	5.536000
H	3.157000	-1.042000	6.313000
H	3.448000	0.604000	5.876000
C	-1.735000	-2.401000	5.536000
H	-1.200000	-3.289000	5.876000
H	-2.480000	-2.214000	6.313000
N	-1.193000	3.466000	4.285000
N	3.598000	-0.700000	4.285000
N	-2.405000	-2.767000	4.285000
C	-1.375000	2.979000	3.040000
H	-1.509000	1.946000	2.748000
C	3.267000	-0.299000	3.039000
H	2.440000	0.334000	2.748000
C	-1.892000	-2.681000	3.039000
H	-0.931000	-2.280000	2.748000
N	-2.799000	-3.201000	2.220000
N	-1.372000	4.024000	2.220000

N	4.171000	-0.824000	2.219000
C	5.144000	-1.537000	2.851000
C	4.791000	-1.465000	4.205000
C	-1.241000	5.223000	2.851000
C	-1.127000	4.881000	4.206000
C	-3.902000	-3.687000	2.851000
C	-3.663000	-3.417000	4.205000
H	-3.253000	1.164000	4.829000
C	0.829000	1.164000	-5.354000
C	-0.832000	-1.167000	-5.371000
C	1.426000	-0.136000	-5.371000
C	-0.595000	1.304000	-5.371000
C	-1.423000	0.137000	-5.354000
C	0.593000	-1.300000	-5.354000
C	1.717000	2.409000	-5.403000
H	2.666000	2.229000	-4.892000
H	1.267000	3.213000	-4.809000
C	1.227000	-2.691000	-5.404000
H	0.596000	-3.423000	-4.893000
C	-2.945000	0.284000	-5.403000
H	-3.264000	1.195000	-4.892000
H	-3.416000	-0.508000	-4.809000
C	2.947000	-0.277000	-5.519000
H	3.298000	0.407000	-6.296000
H	3.263000	-1.264000	-5.858000
C	-1.234000	2.691000	-5.519000
H	-2.001000	2.654000	-6.296000
H	-0.537000	3.459000	-5.858000
C	-1.714000	-2.413000	-5.519000
H	-2.727000	-2.193000	-5.858000
H	-1.298000	-3.059000	-6.296000
N	3.662000	-0.013000	-4.268000
N	-1.820000	3.178000	-4.267000
N	-1.843000	-3.165000	-4.268000
C	3.250000	-0.322000	-3.020000
H	2.308000	-0.765000	-2.727000
C	-1.346000	2.976000	-3.020000
H	-0.491000	2.381000	-2.726000
C	-1.904000	-2.653000	-3.020000
H	-1.817000	-1.616000	-2.726000
N	-2.114000	-3.679000	-2.202000
N	4.243000	0.009000	-2.202000
N	-2.129000	3.671000	-2.202000
C	-3.104000	4.379000	-2.835000
C	-2.917000	4.073000	-4.190000
C	5.344000	0.499000	-2.836000
C	4.985000	0.490000	-4.190000
C	-2.240000	-4.877000	-2.836000
C	-2.069000	-4.562000	-4.191000

H	2.148000	-2.704000	-4.810000
I	-2.453000	-3.435000	0.009000
I	-1.749000	3.842000	0.009000
I	4.201000	-0.407000	0.009000
C	-3.502000	0.281000	-6.823000
H	-3.112000	1.114000	-7.415000
H	-4.592000	0.371000	-6.796000
H	-3.253000	-0.639000	-7.360000
C	1.508000	-3.172000	-6.823000
H	2.180000	-2.497000	-7.361000
H	0.591000	-3.251000	-7.415000
H	1.975000	-4.161000	-6.797000
C	1.993000	2.893000	-6.823000
H	2.520000	2.139000	-7.415000
H	2.616000	3.792000	-6.796000
H	1.072000	3.137000	-7.360000
C	2.095000	2.815000	6.843000
H	2.746000	3.695000	6.819000
H	2.623000	2.021000	7.379000
H	1.211000	3.069000	7.434000
C	-3.486000	0.406000	6.843000
H	-4.573000	0.530000	6.819000
H	-3.062000	1.260000	7.380000
H	-3.264000	-0.487000	7.434000
C	1.391000	-3.223000	6.843000
H	1.828000	-4.226000	6.819000
H	0.440000	-3.283000	7.379000
H	2.054000	-2.584000	7.434000
C	-0.990000	5.857000	5.192000
H	-0.910000	5.622000	6.248000
C	-0.968000	7.187000	4.742000
H	-0.867000	7.995000	5.470000
C	-1.081000	7.517000	3.375000
H	-1.062000	8.570000	3.085000
C	-1.223000	6.531000	2.389000
H	-1.317000	6.775000	1.338000
C	-4.091000	5.238000	-2.375000
H	-4.216000	5.465000	-1.323000
C	-4.913000	5.797000	-3.362000
H	-5.710000	6.486000	-3.073000
C	-4.735000	5.500000	-4.729000
H	-5.400000	5.968000	-5.459000
C	-3.729000	4.629000	-5.178000
H	-3.601000	4.418000	-6.234000
C	6.582000	0.924000	-2.375000
H	6.840000	0.919000	-1.324000
C	7.476000	1.357000	-3.363000
H	8.472000	1.703000	-3.074000
C	7.130000	1.351000	-4.730000

H	7.868000	1.693000	-5.460000
C	5.873000	0.915000	-5.179000
H	5.626000	0.910000	-6.235000
C	6.268000	-2.206000	2.388000
H	6.525000	-2.247000	1.337000
C	7.051000	-2.823000	3.374000
H	7.953000	-3.365000	3.084000
C	6.709000	-2.755000	4.740000
H	7.358000	-3.248000	5.469000
C	5.568000	-2.071000	5.192000
H	5.324000	-2.023000	6.247000
C	-5.044000	-4.325000	2.389000
H	-5.209000	-4.528000	1.338000
C	-5.969000	-4.695000	3.374000
H	-6.890000	-5.205000	3.084000
C	-5.740000	-4.433000	4.741000
H	-6.491000	-4.749000	5.469000
C	-4.577000	-3.787000	5.192000
H	-4.414000	-3.600000	6.247000
C	-2.145000	-5.543000	-5.179000
H	-2.025000	-5.327000	-6.235000
C	-2.395000	-6.850000	-4.730000
H	-2.469000	-7.660000	-5.460000
C	-2.564000	-7.153000	-3.363000
H	-2.762000	-8.188000	-3.075000
C	-2.491000	-6.162000	-2.376000
H	-2.624000	-6.383000	-1.324000
P	-0.000000	0.000000	-0.186000
F	1.105000	0.744000	-1.140000
F	0.092000	-1.329000	-1.140000
F	-1.197000	0.585000	-1.140000
F	-1.106000	-0.741000	0.768000
F	-0.088000	1.328000	0.768000
F	1.195000	-0.588000	0.768000

$[PF_6{-}\subset 5{-}I{-}5][PF_6]_2$

C	0.850000	1.138000	5.222000
C	-0.852000	-1.147000	5.264000
C	-0.564000	1.306000	5.266000
C	1.416000	-0.170000	5.265000
C	0.563000	-1.311000	5.220000
C	-1.414000	0.162000	5.221000
C	1.759000	2.354000	5.257000
H	1.299000	3.224000	4.783000
H	2.677000	2.179000	4.688000
C	-2.922000	0.341000	5.256000
H	-3.445000	-0.492000	4.780000

C	1.162000	-2.706000	5.254000
H	0.551000	-3.413000	4.684000
H	2.145000	-2.743000	4.779000
C	-1.159000	2.697000	5.512000
H	-0.537000	3.228000	6.241000
H	-2.153000	2.649000	5.968000
C	2.918000	-0.350000	5.510000
H	3.067000	-1.156000	6.238000
H	3.374000	0.533000	5.967000
C	-1.759000	-2.358000	5.508000
H	-1.222000	-3.195000	5.964000
H	-2.531000	-2.085000	6.237000
N	-1.261000	3.493000	4.287000
N	3.657000	-0.659000	4.284000
N	-2.397000	-2.843000	4.282000
C	-1.392000	3.035000	3.024000
H	-1.413000	2.007000	2.693000
C	3.326000	-0.316000	3.022000
H	2.446000	0.217000	2.692000
C	-1.935000	-2.726000	3.020000
H	-1.033000	-2.229000	2.690000
N	-2.806000	-3.352000	2.238000
N	-1.499000	4.104000	2.243000
N	4.305000	-0.757000	2.240000
C	5.323000	-1.357000	2.913000
C	4.924000	-1.299000	4.252000
C	-1.488000	5.286000	2.918000
C	-1.340000	4.909000	4.256000
C	-3.836000	-3.935000	2.911000
C	-3.585000	-3.619000	4.250000
H	-3.229000	1.224000	4.687000
C	0.799000	1.181000	-5.194000
C	-0.800000	-1.175000	-5.240000
C	1.421000	-0.100000	-5.240000
C	-0.621000	1.286000	-5.239000
C	-1.419000	0.107000	-5.195000
C	0.620000	-1.277000	-5.196000
C	1.650000	2.438000	-5.219000
H	2.621000	2.287000	-4.742000
H	1.182000	3.245000	-4.648000
C	1.283000	-2.642000	-5.223000
H	0.667000	-3.408000	-4.746000
C	-2.933000	0.216000	-5.221000
H	-3.288000	1.132000	-4.743000
H	-3.398000	-0.594000	-4.651000
C	2.928000	-0.206000	-5.480000
H	3.231000	0.561000	-6.203000
H	3.209000	-1.157000	-5.943000
C	-1.282000	2.645000	-5.478000

H	-2.097000	2.524000	-6.201000
H	-0.598000	3.363000	-5.940000
C	-1.646000	-2.427000	-5.482000
H	-2.610000	-2.194000	-5.944000
H	-1.133000	-3.072000	-6.205000
N	3.711000	-0.051000	-4.253000
N	-1.808000	3.244000	-4.251000
N	-1.902000	-3.183000	-4.255000
C	3.306000	-0.297000	-2.988000
H	2.330000	-0.622000	-2.657000
C	-1.394000	3.015000	-2.986000
H	-0.624000	2.332000	-2.655000
C	-1.912000	-2.711000	-2.990000
H	-1.705000	-1.704000	-2.658000
N	-2.245000	-3.735000	-2.211000
N	4.358000	-0.074000	-2.208000
N	-2.113000	3.814000	-2.205000
C	-2.988000	4.608000	-2.880000
C	-2.802000	4.255000	-4.219000
C	5.484000	0.287000	-2.883000
C	5.083000	0.304000	-4.222000
C	-2.495000	-4.889000	-2.887000
C	-2.281000	-4.550000	-4.226000
H	2.217000	-2.641000	-4.652000
I	-2.523000	-3.541000	0.014000
I	-1.805000	3.956000	0.019000
I	4.328000	-0.415000	0.016000
C	-1.299000	5.855000	5.278000
H	-1.194000	5.570000	6.319000
C	-1.409000	7.207000	4.887000
C	-1.556000	7.578000	3.516000
C	-1.599000	6.602000	2.500000
H	-1.714000	6.854000	1.453000
C	-3.887000	5.576000	-2.462000
H	-4.002000	5.823000	-1.414000
C	-4.630000	6.210000	-3.478000
C	-4.447000	5.860000	-4.851000
C	-3.521000	4.869000	-5.242000
H	-3.375000	4.606000	-6.283000
C	6.771000	0.581000	-2.465000
H	7.043000	0.556000	-1.417000
C	7.691000	0.909000	-3.481000
C	7.296000	0.927000	-4.854000
C	5.974000	0.620000	-5.244000
H	5.673000	0.627000	-6.286000
C	6.518000	-1.919000	2.494000
H	6.793000	-1.944000	1.447000
C	7.342000	-2.445000	3.509000
C	6.949000	-2.389000	4.881000

C	5.723000	-1.808000	5.273000
H	5.424000	-1.758000	6.314000
C	-4.920000	-4.688000	2.492000
H	-5.080000	-4.912000	1.444000
C	-5.787000	-5.140000	3.506000
C	-5.541000	-4.829000	4.879000
C	-4.424000	-4.058000	5.271000
H	-4.232000	-3.825000	6.312000
C	-2.453000	-5.478000	-5.249000
H	-2.297000	-5.219000	-6.290000
C	-2.848000	-6.777000	-4.860000
C	-3.060000	-7.111000	-3.487000
C	-2.884000	-6.152000	-2.470000
H	-3.041000	-6.376000	-1.422000
H	1.487000	-2.941000	-6.256000
H	-3.293000	0.189000	-6.254000
H	1.807000	2.764000	-6.252000
H	2.012000	2.603000	6.292000
H	-3.265000	0.434000	6.290000
H	1.252000	-3.051000	6.288000
C	-3.050000	-7.817000	-5.940000
H	-2.371000	-8.661000	-5.785000
H	-2.844000	-7.406000	-6.934000
H	-4.086000	-8.170000	-5.937000
C	-3.487000	-8.507000	-3.094000
H	-2.735000	-9.237000	-3.409000
H	-4.452000	-8.751000	-3.550000
H	-3.602000	-8.599000	-2.009000
C	-6.987000	-5.971000	3.111000
H	-6.929000	-6.962000	3.571000
H	-7.034000	-6.112000	2.026000
H	-7.911000	-5.473000	3.419000
C	-6.478000	-5.330000	5.956000
H	-6.154000	-5.005000	6.951000
H	-6.502000	-6.424000	5.958000
H	-7.487000	-4.938000	5.793000
C	8.299000	1.273000	-5.933000
H	9.123000	0.553000	-5.930000
H	8.690000	2.283000	-5.777000
H	7.841000	1.247000	-6.928000
C	9.113000	1.237000	-3.087000
H	9.807000	0.524000	-3.542000
H	9.249000	1.182000	-2.001000
H	9.369000	2.253000	-3.400000
C	8.662000	-3.068000	3.114000
H	9.492000	-2.523000	3.575000
H	8.809000	-3.038000	2.029000
H	8.693000	-4.118000	3.421000
C	7.851000	-2.951000	5.958000

H	8.810000	-2.425000	5.962000
H	8.016000	-4.021000	5.795000
H	7.407000	-2.835000	6.953000
C	-5.248000	6.556000	-5.930000
H	-4.996000	6.174000	-6.925000
H	-5.036000	7.630000	-5.926000
H	-6.318000	6.390000	-5.775000
C	-5.625000	7.277000	-3.083000
H	-5.354000	8.235000	-3.538000
H	-5.647000	7.421000	-1.998000
H	-6.634000	6.991000	-3.398000
C	-1.676000	9.033000	3.122000
H	-0.783000	9.584000	3.430000
H	-2.563000	9.478000	3.583000
H	-1.775000	9.146000	2.037000
C	-1.374000	8.268000	5.966000
H	-0.530000	8.946000	5.804000
H	-1.253000	7.825000	6.960000
H	-2.309000	8.836000	5.969000
P	0.000000	0.000000	-0.337000
F	0.981000	0.904000	-1.288000
F	0.292000	-1.300000	-1.290000
F	-1.273000	0.399000	-1.288000
F	-0.982000	-0.902000	0.614000
F	-0.290000	1.300000	0.616000
F	1.271000	-0.400000	0.615000

$[PF_6{-}\subset 6{-}I{-}6][PF_6]_2$

C	0.831000	1.159000	5.371000
C	-0.835000	-1.170000	5.386000
C	-0.593000	1.302000	5.388000
C	1.427000	-0.143000	5.387000
C	0.590000	-1.305000	5.370000
C	-1.423000	0.136000	5.371000
C	1.721000	2.403000	5.425000
H	1.243000	3.243000	4.916000
H	2.628000	2.240000	4.832000
C	-2.945000	0.283000	5.423000
H	-3.434000	-0.550000	4.913000
C	1.223000	-2.698000	5.422000
H	0.628000	-3.401000	4.828000
H	2.190000	-2.704000	4.912000
C	-1.219000	2.695000	5.539000
H	-0.688000	3.247000	6.318000
H	-2.256000	2.673000	5.877000
C	2.947000	-0.298000	5.538000
H	3.159000	-1.035000	6.316000

H	3.446000	0.611000	5.876000
C	-1.729000	-2.409000	5.536000
H	-1.191000	-3.297000	5.873000
H	-2.473000	-2.225000	6.314000
N	-1.201000	3.459000	4.289000
N	3.598000	-0.695000	4.286000
N	-2.399000	-2.774000	4.284000
C	-1.379000	2.973000	3.043000
H	-1.511000	1.940000	2.751000
C	3.265000	-0.296000	3.042000
H	2.437000	0.335000	2.750000
C	-1.887000	-2.683000	3.039000
H	-0.927000	-2.281000	2.748000
N	-2.795000	-3.202000	2.221000
N	-1.374000	4.019000	2.226000
N	4.169000	-0.822000	2.223000
C	5.143000	-1.532000	2.855000
C	4.792000	-1.458000	4.206000
C	-1.247000	5.217000	2.859000
C	-1.136000	4.875000	4.210000
C	-3.897000	-3.691000	2.853000
C	-3.657000	-3.426000	4.204000
H	-3.257000	1.151000	4.831000
C	0.834000	1.164000	-5.351000
C	-0.836000	-1.160000	-5.369000
C	1.427000	-0.139000	-5.368000
C	-0.589000	1.310000	-5.368000
C	-1.422000	0.146000	-5.352000
C	0.589000	-1.299000	-5.352000
C	1.728000	2.406000	-5.399000
H	2.676000	2.222000	-4.888000
H	1.281000	3.211000	-4.804000
C	1.217000	-2.693000	-5.402000
H	0.584000	-3.423000	-4.892000
C	-2.943000	0.299000	-5.401000
H	-3.258000	1.211000	-4.889000
H	-3.417000	-0.491000	-4.807000
C	2.946000	-0.285000	-5.516000
H	3.300000	0.396000	-6.294000
H	3.259000	-1.274000	-5.854000
C	-1.222000	2.699000	-5.514000
H	-1.988000	2.665000	-6.293000
H	-0.522000	3.465000	-5.851000
C	-1.722000	-2.403000	-5.518000
H	-2.735000	-2.179000	-5.855000
H	-1.310000	-3.049000	-6.297000
N	3.661000	-0.022000	-4.265000
N	-1.809000	3.186000	-4.263000
N	-1.852000	-3.155000	-4.267000

C	3.247000	-0.329000	-3.017000
H	2.304000	-0.769000	-2.724000
C	-1.337000	2.979000	-3.016000
H	-0.484000	2.383000	-2.722000
C	-1.910000	-2.644000	-3.020000
H	-1.820000	-1.608000	-2.725000
N	-2.120000	-3.672000	-2.204000
N	4.241000	0.002000	-2.201000
N	-2.121000	3.674000	-2.198000
C	-3.093000	4.385000	-2.833000
C	-2.905000	4.083000	-4.185000
C	5.343000	0.489000	-2.835000
C	4.987000	0.479000	-4.186000
C	-2.249000	-4.868000	-2.840000
C	-2.081000	-4.553000	-4.191000
H	2.138000	-2.709000	-4.808000
I	-2.453000	-3.432000	0.009000
I	-1.746000	3.841000	0.014000
I	4.199000	-0.409000	0.011000
C	-1.004000	5.848000	5.198000
H	-0.928000	5.593000	6.249000
C	-0.980000	7.190000	4.760000
C	-1.091000	7.524000	3.376000
C	-1.229000	6.522000	2.395000
H	-1.321000	6.747000	1.339000
C	-4.076000	5.244000	-2.370000
H	-4.187000	5.455000	-1.313000
C	-4.908000	5.818000	-3.351000
C	-4.726000	5.520000	-4.736000
C	-3.710000	4.642000	-5.174000
H	-3.566000	4.421000	-6.225000
C	6.578000	0.911000	-2.372000
H	6.818000	0.900000	-1.315000
C	7.491000	1.345000	-3.353000
C	7.142000	1.338000	-4.738000
C	5.873000	0.898000	-5.175000
H	5.609000	0.884000	-6.227000
C	6.264000	-2.199000	2.390000
H	6.504000	-2.231000	1.334000
C	7.063000	-2.822000	3.369000
C	6.719000	-2.752000	4.754000
C	5.569000	-2.061000	5.193000
H	5.310000	-2.000000	6.244000
C	-5.036000	-4.328000	2.387000
H	-5.183000	-4.519000	1.331000
C	-5.974000	-4.710000	3.367000
C	-5.740000	-4.448000	4.751000
C	-4.566000	-3.798000	5.191000
H	-4.384000	-3.606000	6.242000

C	-2.161000	-5.529000	-5.181000
H	-2.042000	-5.292000	-6.232000
C	-2.414000	-6.848000	-4.744000
C	-2.582000	-7.156000	-3.360000
C	-2.501000	-6.150000	-2.377000
H	-2.630000	-6.353000	-1.321000
C	-2.514000	-7.940000	-5.788000
H	-1.752000	-8.705000	-5.610000
H	-2.354000	-7.545000	-6.797000
H	-3.509000	-8.396000	-5.765000
C	-2.859000	-8.575000	-2.917000
H	-2.038000	-9.233000	-3.215000
H	-3.797000	-8.932000	-3.354000
H	-2.956000	-8.641000	-1.828000
C	-7.235000	-5.414000	2.920000
H	-7.287000	-6.415000	3.361000
H	-7.263000	-5.531000	1.832000
H	-8.116000	-4.835000	3.212000
C	-6.754000	-4.875000	5.791000
H	-6.432000	-4.597000	6.801000
H	-6.880000	-5.962000	5.773000
H	-7.716000	-4.387000	5.606000
C	8.137000	1.798000	-5.780000
H	9.030000	1.165000	-5.757000
H	8.419000	2.841000	-5.601000
H	7.716000	1.740000	-6.790000
C	8.858000	1.814000	-2.909000
H	9.636000	1.181000	-3.346000
H	8.963000	1.762000	-1.820000
H	9.017000	2.855000	-3.206000
C	8.304000	-3.561000	2.923000
H	9.196000	-3.107000	3.365000
H	8.420000	-3.526000	1.834000
H	8.243000	-4.615000	3.213000
C	7.594000	-3.417000	5.794000
H	8.599000	-2.983000	5.776000
H	7.653000	-4.494000	5.607000
H	7.192000	-3.279000	6.803000
C	-5.622000	6.154000	-5.778000
H	-5.360000	5.819000	-6.788000
H	-5.519000	7.243000	-5.755000
H	-6.666000	5.876000	-5.600000
C	-5.998000	6.767000	-2.906000
H	-5.839000	7.758000	-3.343000
H	-6.006000	6.883000	-1.817000
H	-6.979000	6.385000	-3.205000
C	-1.070000	8.969000	2.931000
H	-0.128000	9.443000	3.222000
H	-1.910000	9.514000	3.373000

H	-1.158000	9.053000	1.842000
C	-0.842000	8.280000	5.801000
H	0.061000	8.869000	5.616000
H	-0.761000	7.861000	6.810000
H	-1.720000	8.933000	5.784000
C	1.496000	-3.174000	-6.822000
H	2.172000	-2.501000	-7.359000
H	0.580000	-3.249000	-7.415000
H	1.960000	-4.165000	-6.796000
C	2.005000	2.889000	-6.818000
H	2.529000	2.134000	-7.411000
H	2.632000	3.787000	-6.791000
H	1.085000	3.138000	-7.355000
C	-3.500000	0.299000	-6.820000
H	-3.107000	1.130000	-7.412000
H	-4.590000	0.393000	-6.794000
H	-3.255000	-0.622000	-7.358000
C	-3.488000	0.392000	6.844000
H	-3.067000	1.247000	7.381000
H	-3.264000	-0.501000	7.435000
H	-4.576000	0.513000	6.820000
C	1.400000	-3.223000	6.842000
H	2.060000	-2.583000	7.434000
H	1.839000	-4.226000	6.818000
H	0.448000	-3.286000	7.379000
C	2.087000	2.817000	6.847000
H	2.735000	3.699000	6.823000
H	2.617000	2.024000	7.383000
H	1.202000	3.069000	7.438000
P	0.000000	0.000000	-0.179000
F	1.109000	0.740000	-1.132000
F	0.086000	-1.329000	-1.134000
F	-1.194000	0.591000	-1.133000
F	-1.110000	-0.736000	0.774000
F	-0.082000	1.328000	0.775000
F	1.192000	-0.594000	0.774000

HRMS, IM-MS, and CID

Measurements were performed with a Water's Synapt G2-S Q-TOF traveling wave ion mobility mass spectrometer (Manchester, UK) equipped with a Z-spray electrospray ionization source. Solutions of the different ligands, $AgPF_6$, and I_2 with 5 mM concentration in DMSO were prepared. Silver(I) complexes were formed via the addition of $AgPF_6$ solution to the respective ligand solution and stirred for 10 minutes. The cation exchange was completed by the addition of I_2 solution to the previously prepared silver(I) complexes followed by centrifugation for 20 minutes and filtering. The final sample concentration of 100 μM was achieved via dilution with acetonitrile and the injection flow rate was 2 μL/min. A capillary voltage of 1.20 kV was used with the sample cone and source offset both set to 15 eV. The source and desolvation temperatures were 100 °C and 250 °C, respectively. The drift cell was operated with N_2 as the drift gas and was turned on 45 minutes prior to measuring to allow the pressures to settle. A wave velocity of 550 m/s and a wave height of 25 V was used for the measurements. Collision-induced dissociation (CID) was completed in the transfer cell with N_2 as the collision gas. IMS and CID were performed with mass selected ions as indicated in the spectra. Data for the survival yield (SY) analysis was obtained by taking measurements with increasing CID voltage until the parent ion was fragmented completely. Data was exported and processed in Origin pro 2020 (OriginLab corporation). The relative parent ion intensity was plotted against collision voltage and the curves were fit with a signmoidal gaussian with the equation y = a/(1+exp(-k*(x-xc))) to obtain the 50% SY voltage (SY50%).

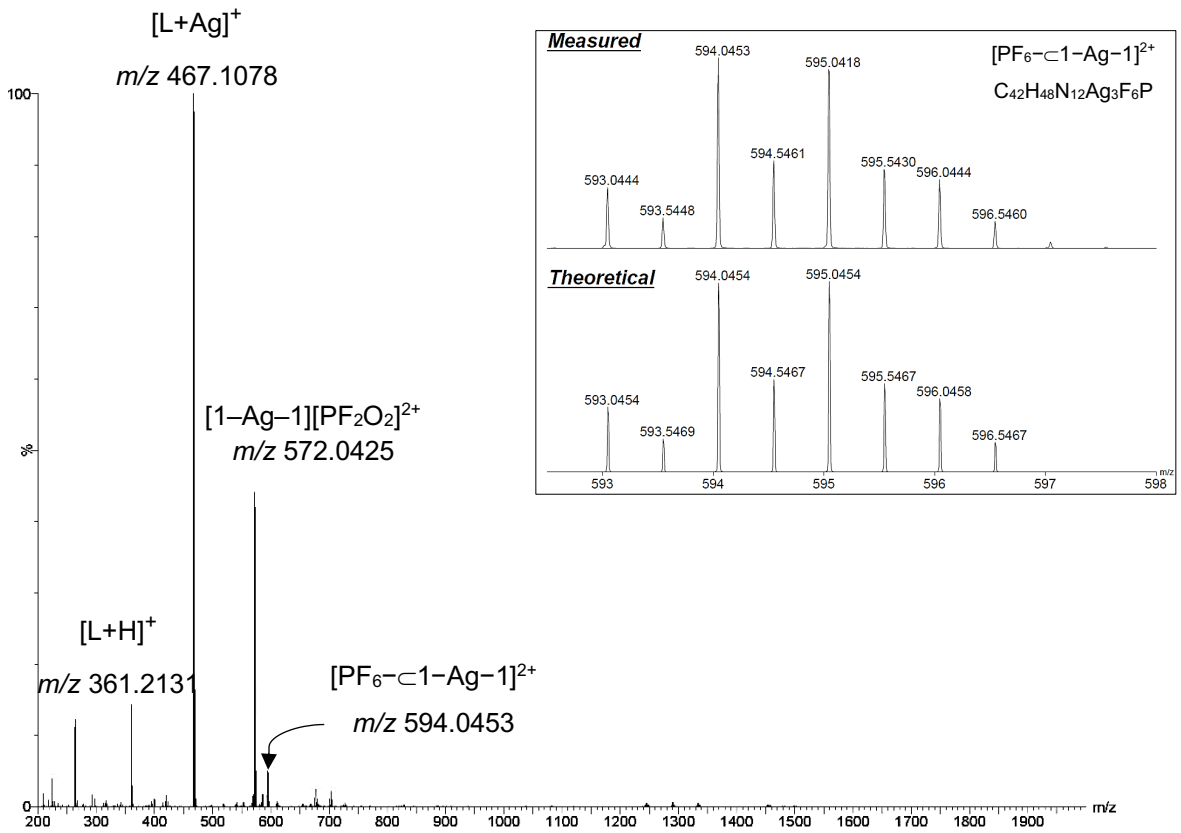

Figure S26. ESI-TOF mass spectrum of **$[PF_6{-}\subset 1{-}Ag{-}1][PF_6]_2$**. Inset: Isotope pattern of the $[PF_6{-}\subset 1{-}Ag{-}1]^{2+}$ ion. Hydrolysis of the anion results in $[1{-}Ag{-}1][PF_2O_2]^{2+}$ seen for all complexes.

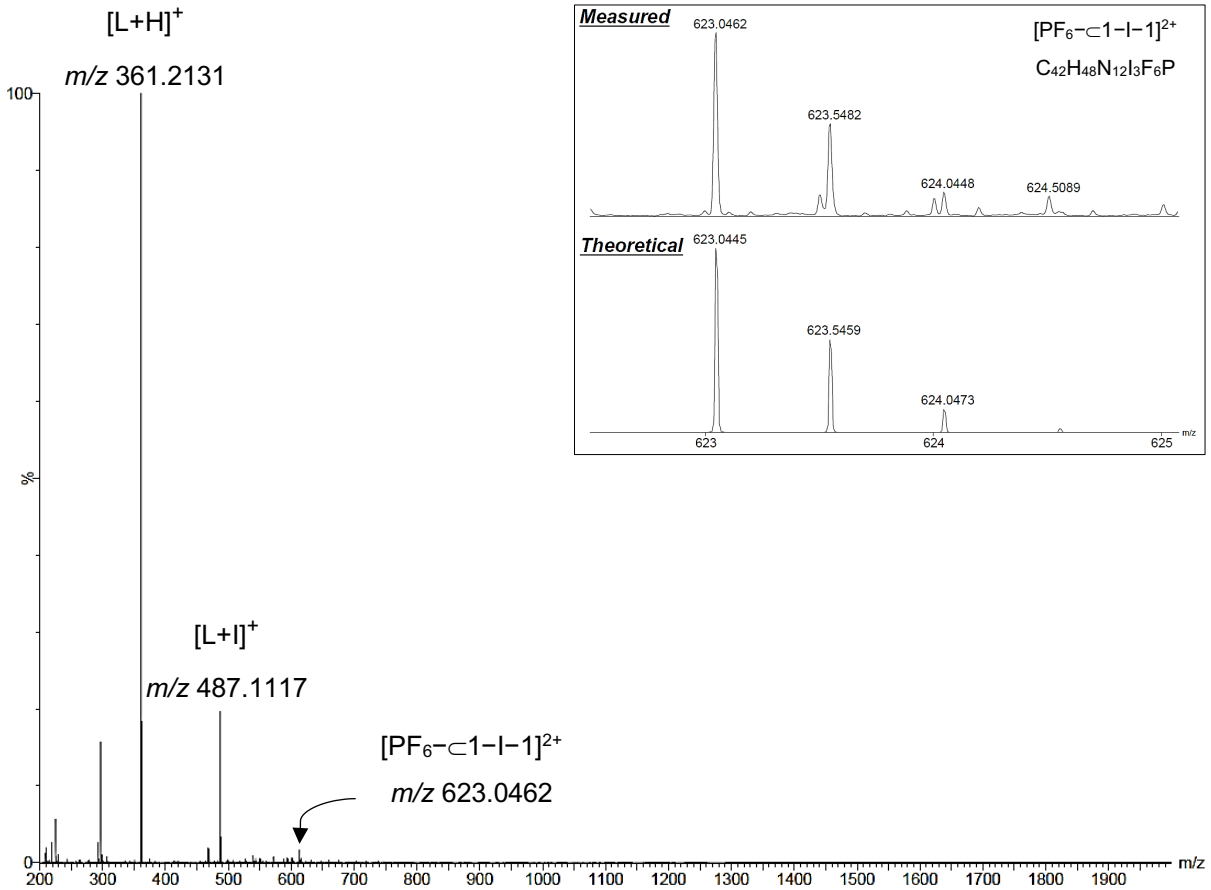

Figure S27. ESI-TOF mass spectrum of **[PF_6−⊂1−I−1][PF_6]$_2$**. Inset: Isotope pattern of the [PF_6−⊂1−I−1]$^{2+}$ ion.

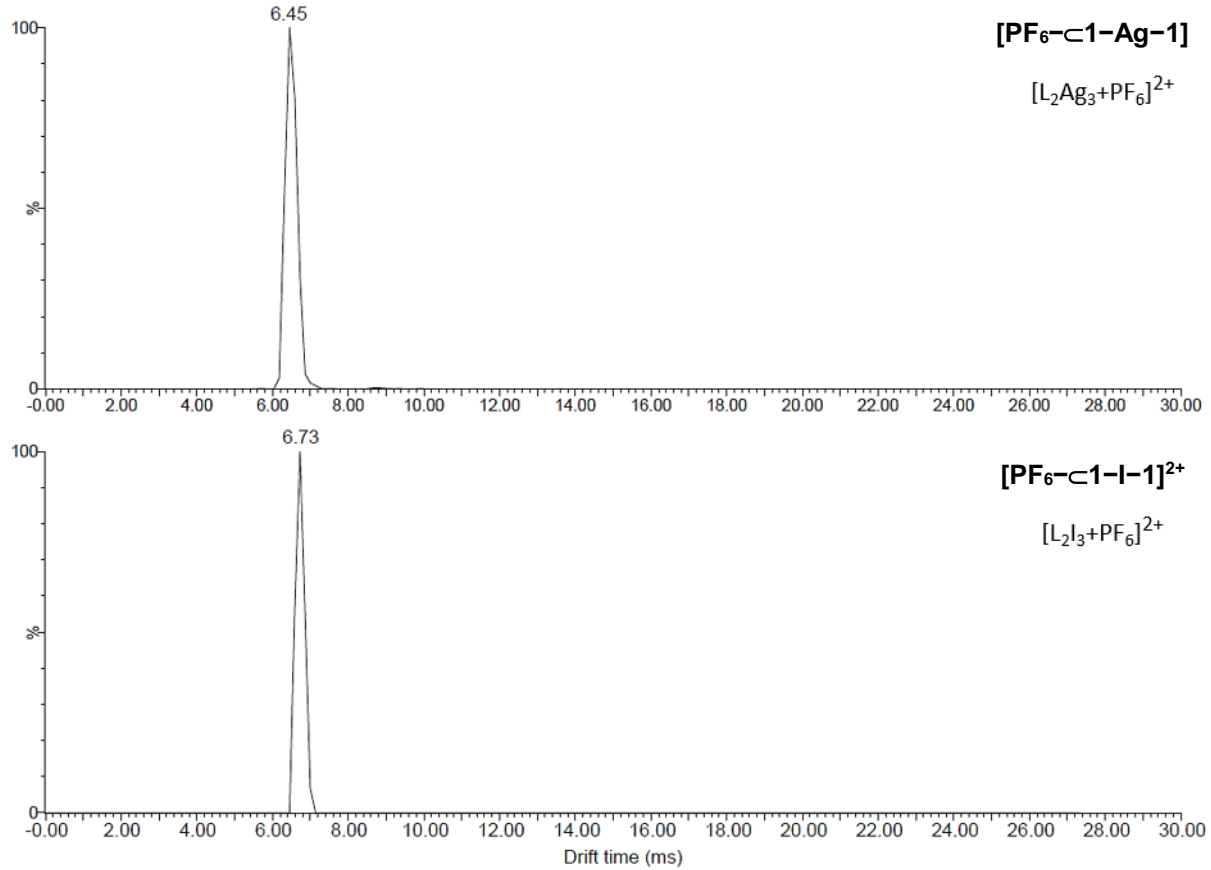

Figure S28. Comparison of arrival time distributions of $[PF_6{-}\subset 1{-}Ag{-}1]^{2+}$ (top) and $[PF_6{-}\subset 1{-}I{-}1]^{2+}$ (bottom). Both arrival time distributions are narrow peaks consistent with a single species and appear at very similar times indicating two closely analogous structures.

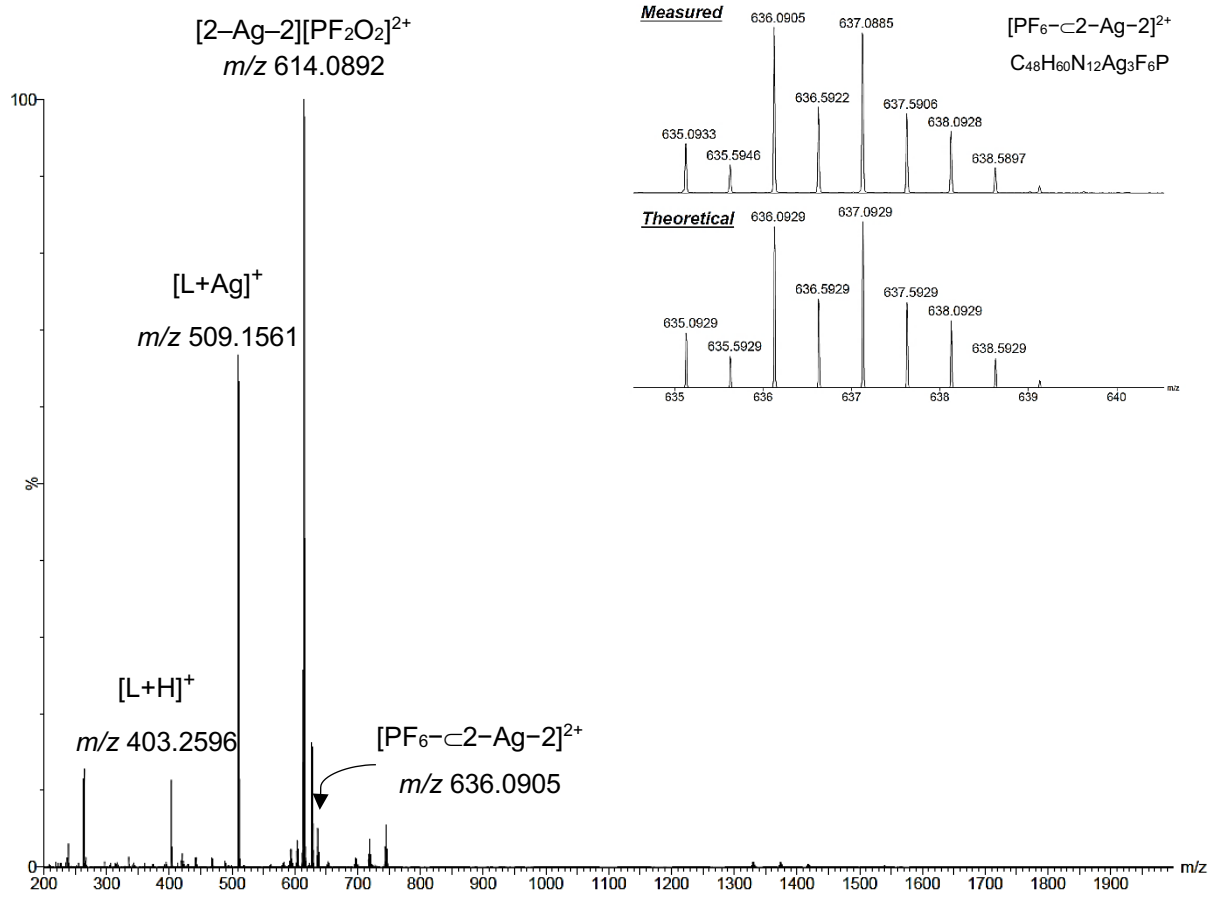

Figure S29. ESI-TOF mass spectrum of **$[PF_6{-}\subset 2{-}Ag{-}2][PF_6]_2$**. Inset: Isotope pattern of the $[PF_6{-}\subset 2{-}Ag{-}2]^{2+}$ ion.

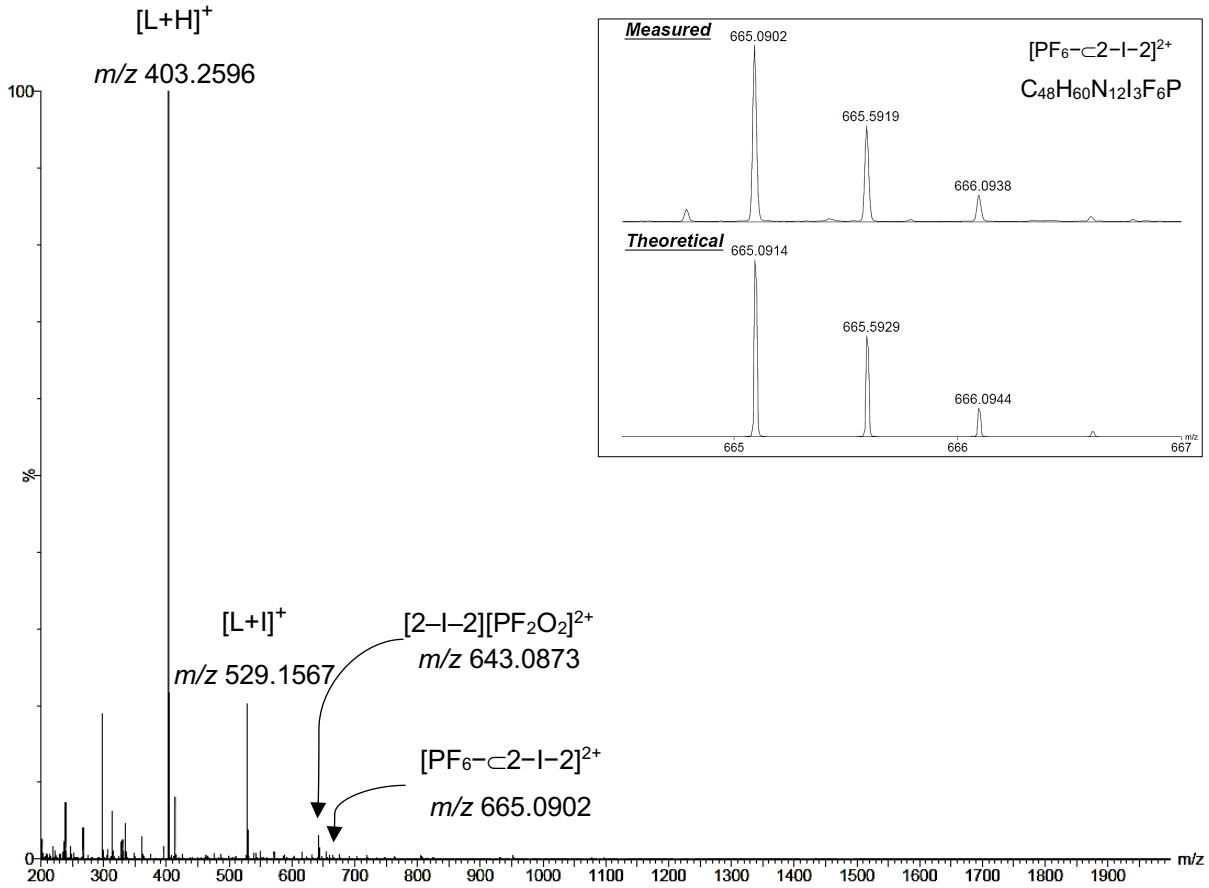

Figure S30. ESI-TOF mass spectrum of **$[PF_6{-}\subset 2{-}I{-}2][PF_6]_2$**. Inset: Isotope pattern of the $[PF_6{-}\subset 2{-}I{-}2]^{2+}$ ion.

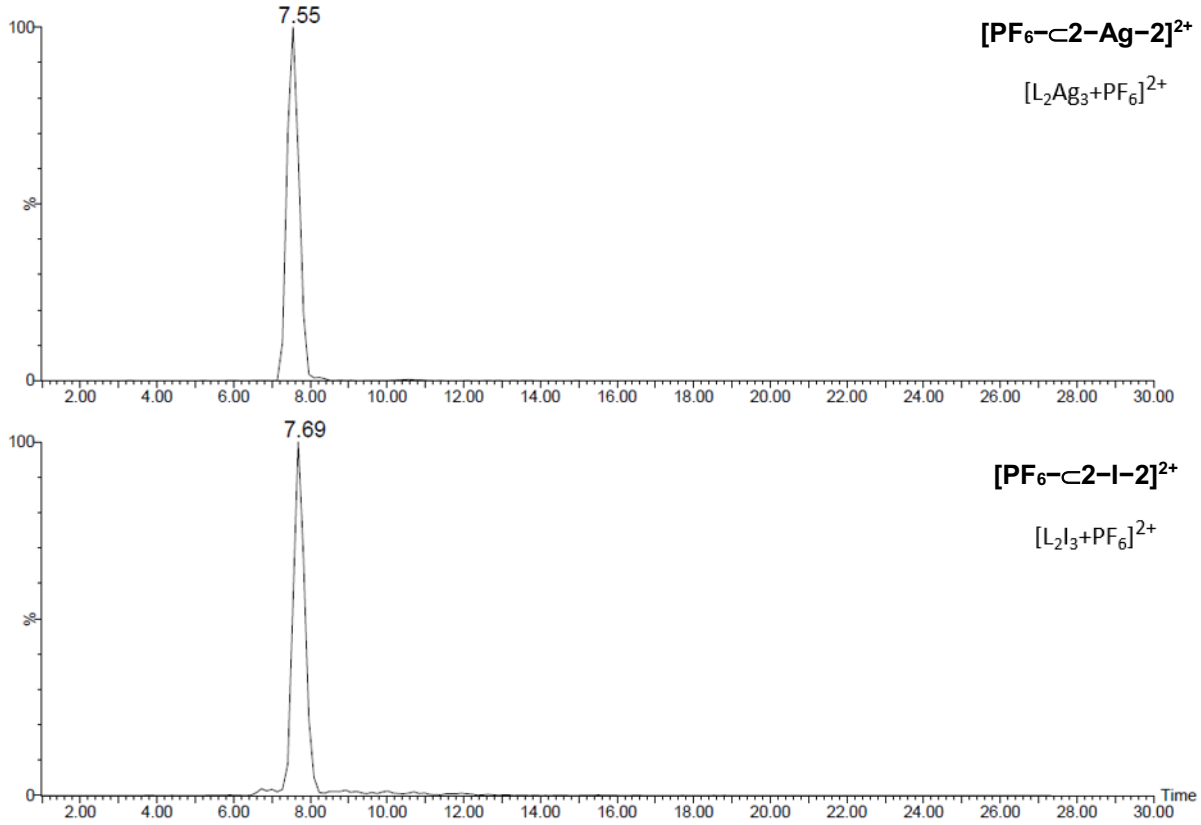

Figure S31. Comparison of arrival time distributions of $[PF_6{-}\subset 2{-}Ag{-}2]^{2+}$ (top) and $[PF_6{-}\subset 2{-}I{-}2]^{2+}$ (bottom).

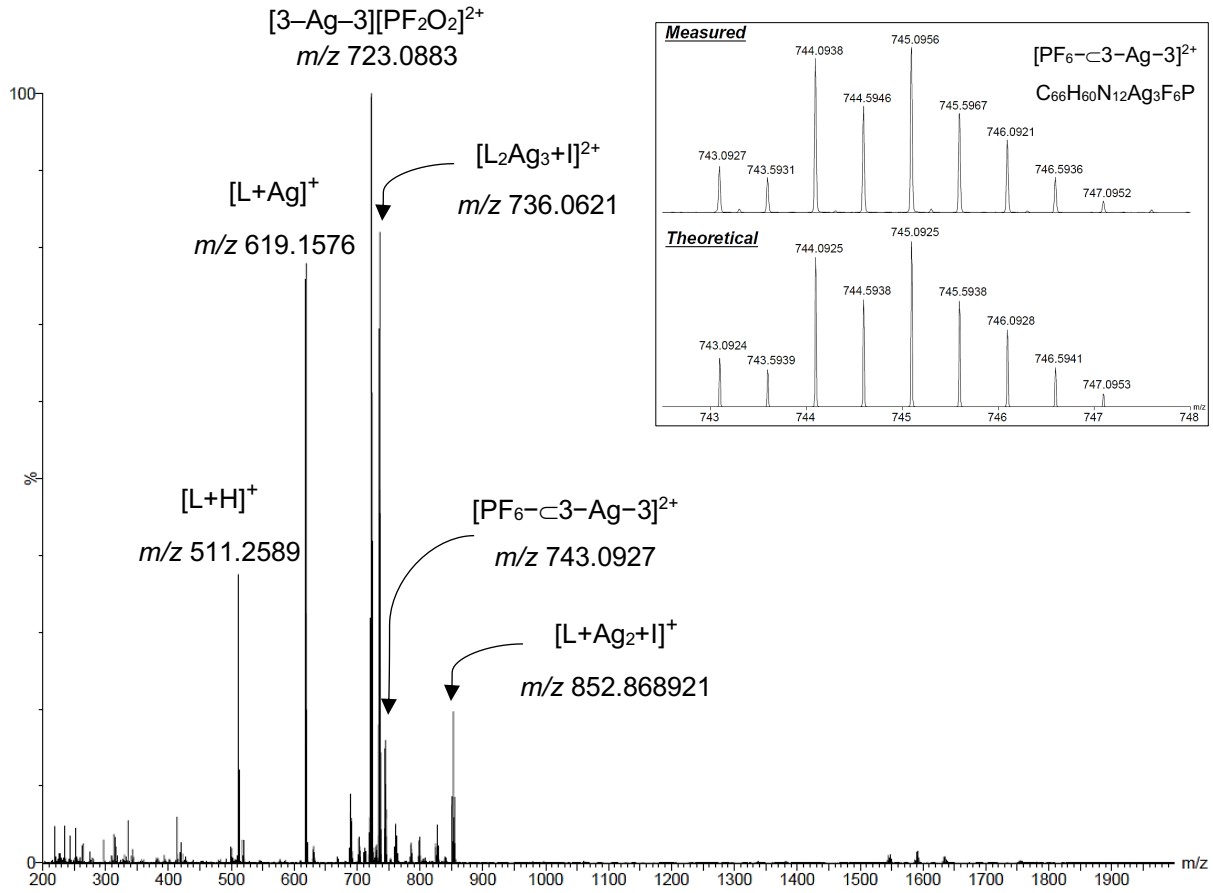

Figure S32. ESI-TOF mass spectrum of **$[PF_6{-}\subset 3{-}Ag{-}3][PF_6]_2$**. Inset: Isotope pattern of the $[PF_6{-}\subset 3{-}Ag{-}3]^{2+}$ ion.

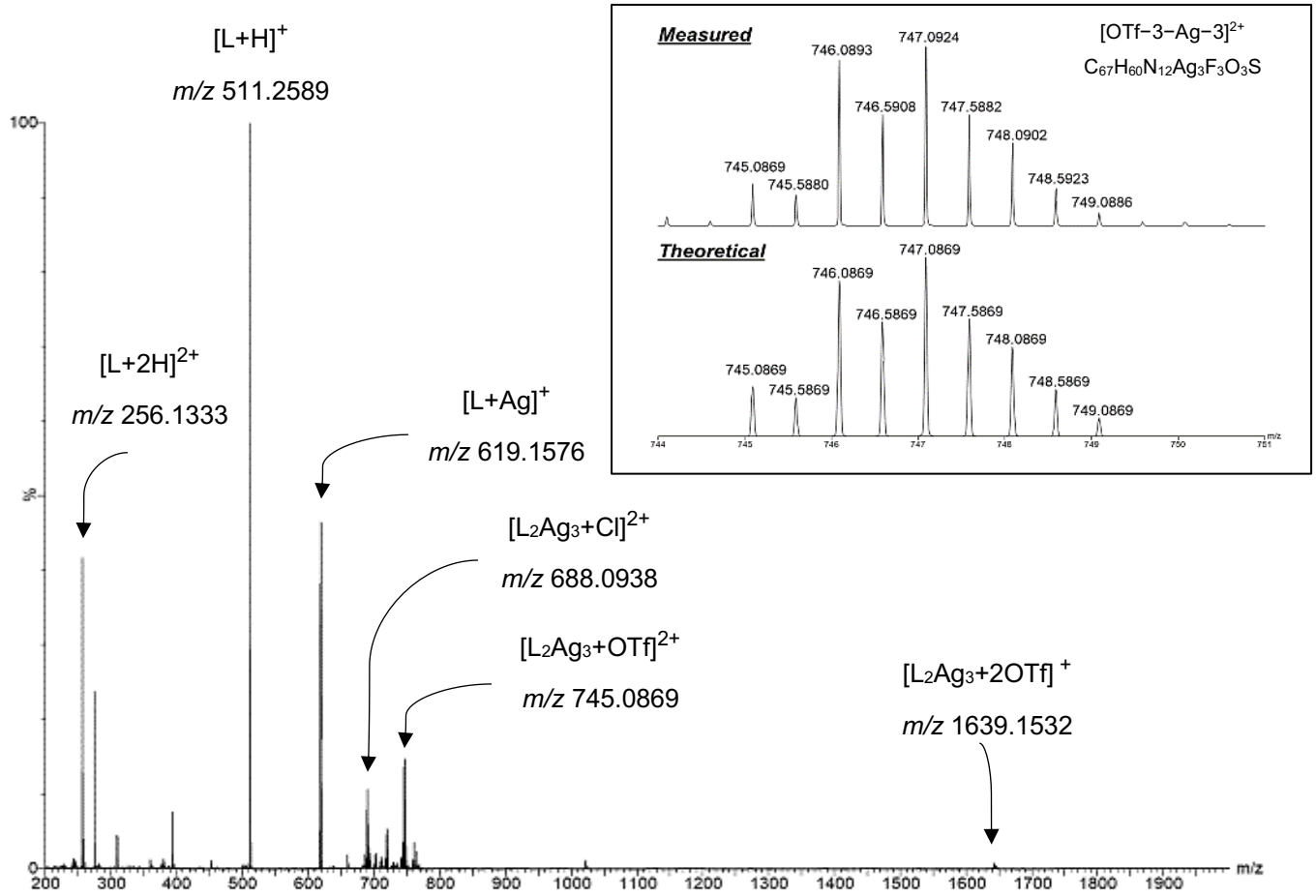

Figure S33. ESI-TOF mass spectrum of **[3−Ag−3][OTf]$_3$**. Inset: Isotope pattern of the [OTf-3−Ag−3]$^{2+}$ ion.

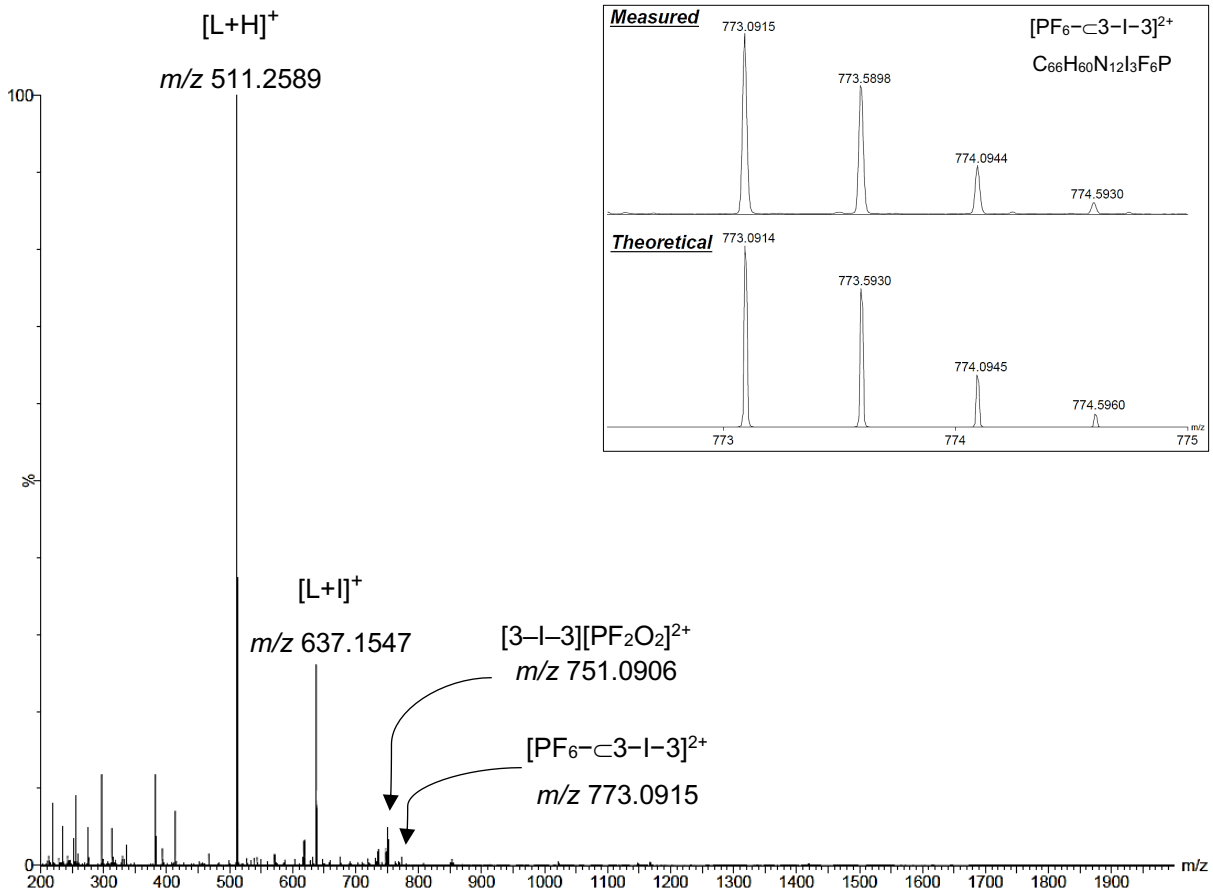

Figure S34. ESI-TOF mass spectrum of **$[PF_6{-}\subset 3{-}I{-}3][PF_6]_2$**. Inset: Isotope pattern of the $[PF_6{-}\subset 3{-}I{-}3]^{2+}$ ion.

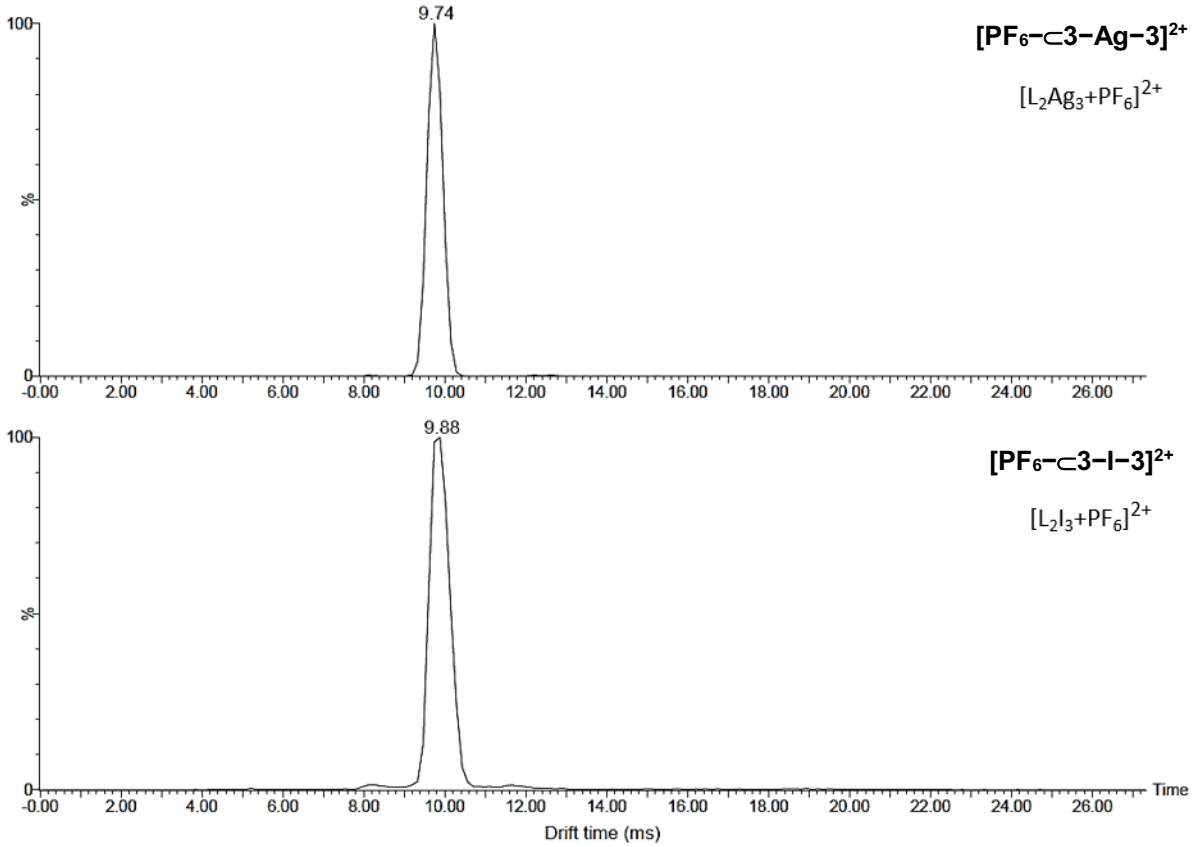

Figure S35. Comparison of arrival time distributions of $[PF_6{-}\subset 3{-}Ag{-}3]^{2+}$ (top) and $[PF_6{-}\subset 3{-}I{-}3]^{2+}$ (bottom).

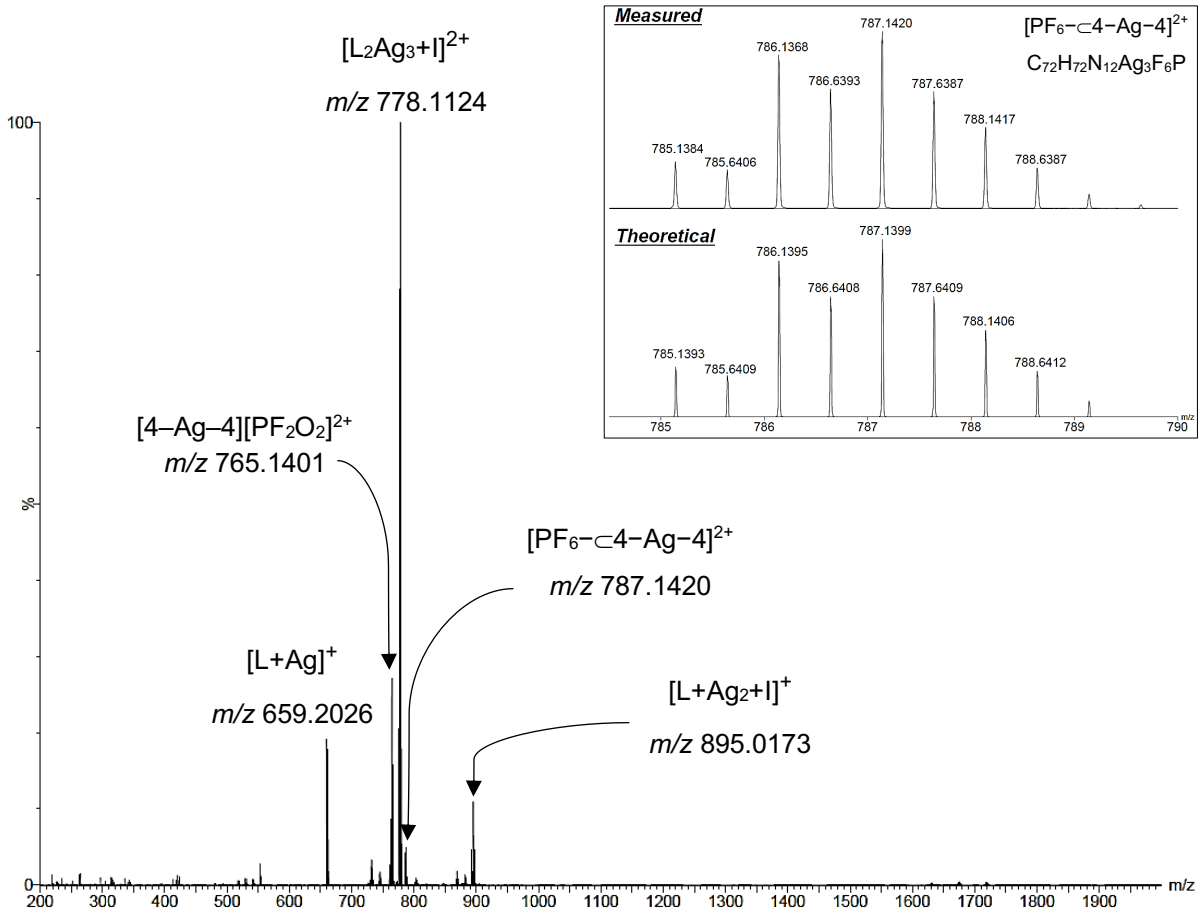

Figure S36. ESI-TOF mass spectrum of **[PF_6−⊂4−Ag−4][PF_6]$_2$**. Inset: Isotope pattern of the $[PF_6−⊂4−Ag−4]^{2+}$ ion.

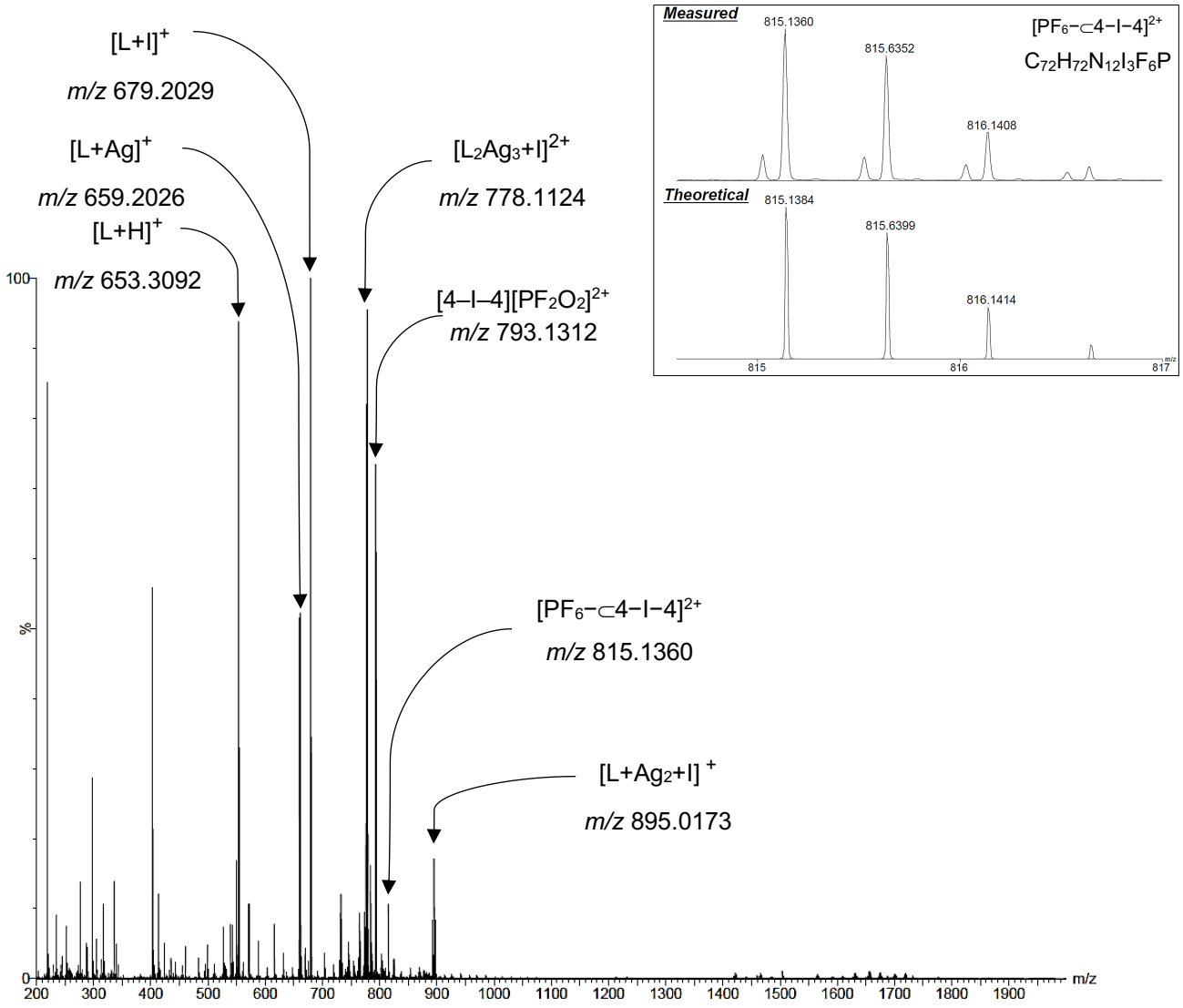

Figure S37. ESI-TOF mass spectrum of **[PF_6−⊂4−I−4][PF_6]$_2$**. Inset: Isotope pattern of the [PF_6−⊂4−I−4]$^{2+}$ ion.

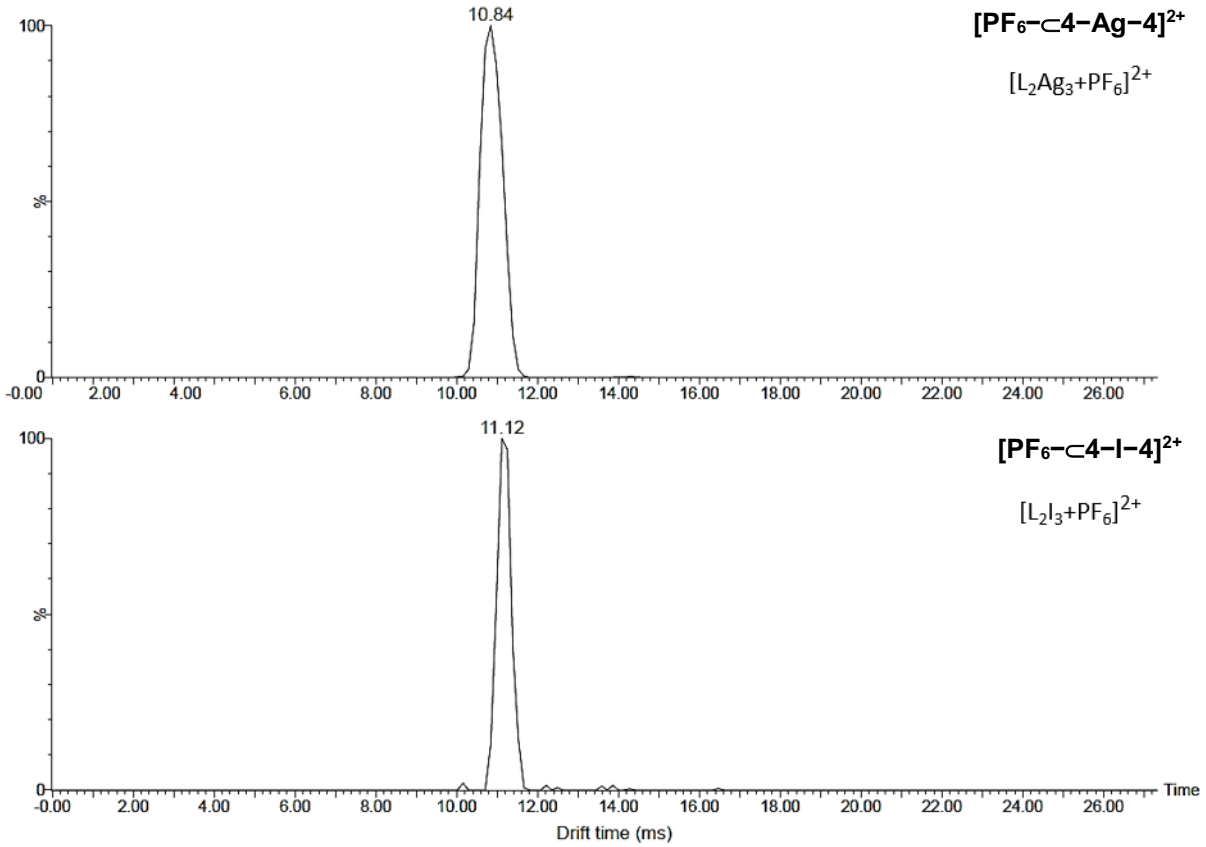

Figure S38. Comparison of arrival time distributions of $[PF_6{-}\subset 4{-}Ag{-}4]^{2+}$ (top) and $[PF_6{-}\subset 4{-}I{-}4]^{2+}$ (bottom).

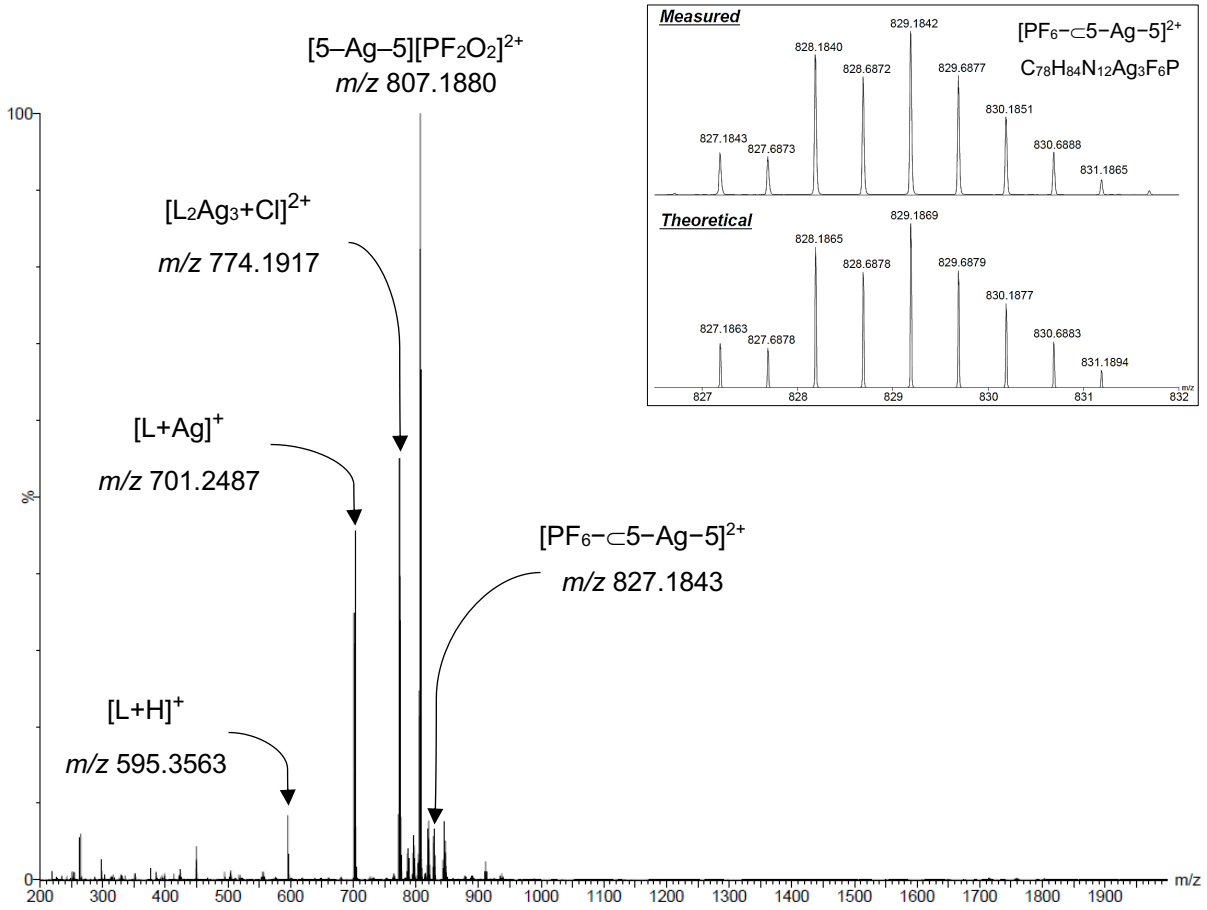

Figure S39. ESI-TOF mass spectrum of **[PF_6−⊂5−Ag−5][PF_6]$_2$**. Inset: Isotope pattern of the [PF_6−⊂5−Ag−5]$^{2+}$ ion.

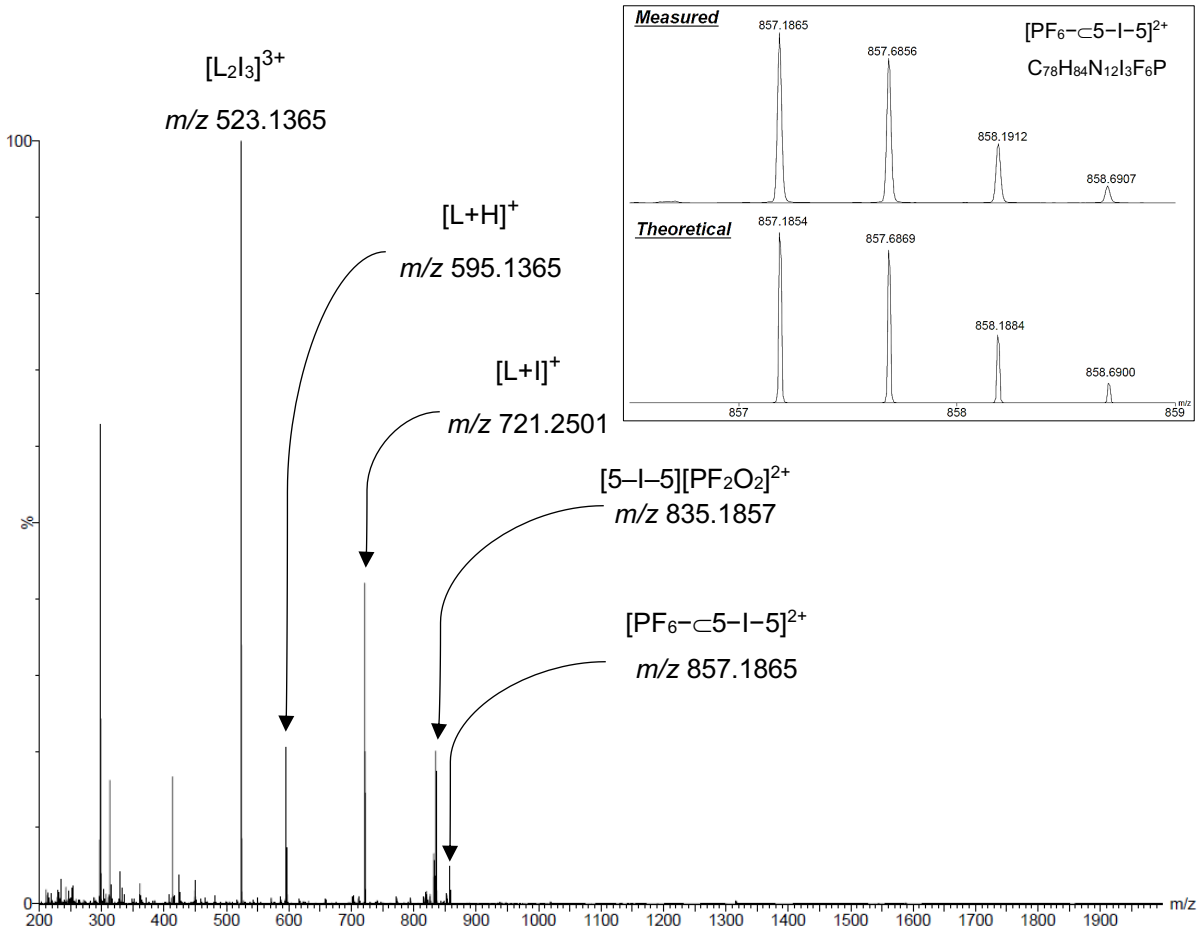

Figure S40. ESI-TOF mass spectrum of **$[PF_6{-}\subset 5{-}I{-}5][PF_6]_2$**. Inset: Isotope pattern of the $[PF_6{-}\subset 5{-}I{-}5]^{2+}$ ion.

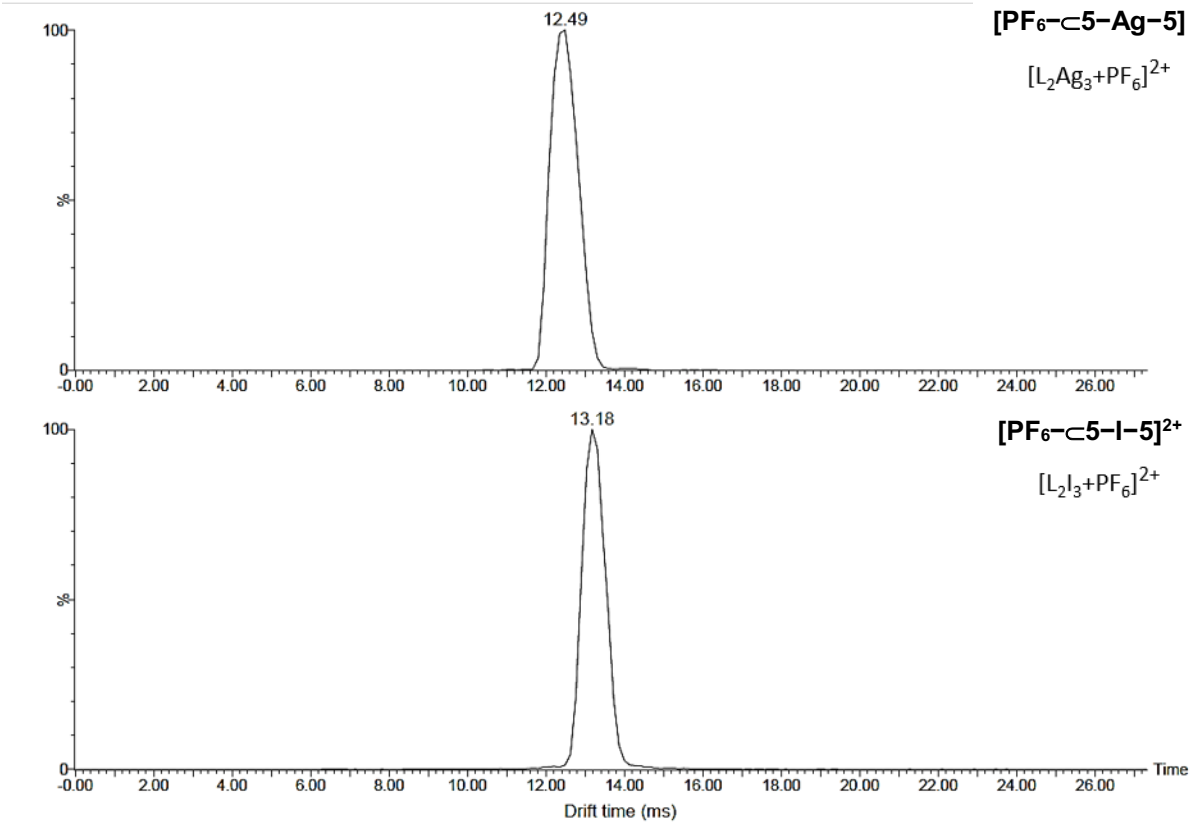

Figure S41. Comparison of arrival time distributions of $[PF_6{-}\subset 5{-}Ag{-}5]^{2+}$ (top) and $[PF_6{-}\subset 5{-}I{-}5]^{2+}$ (bottom).

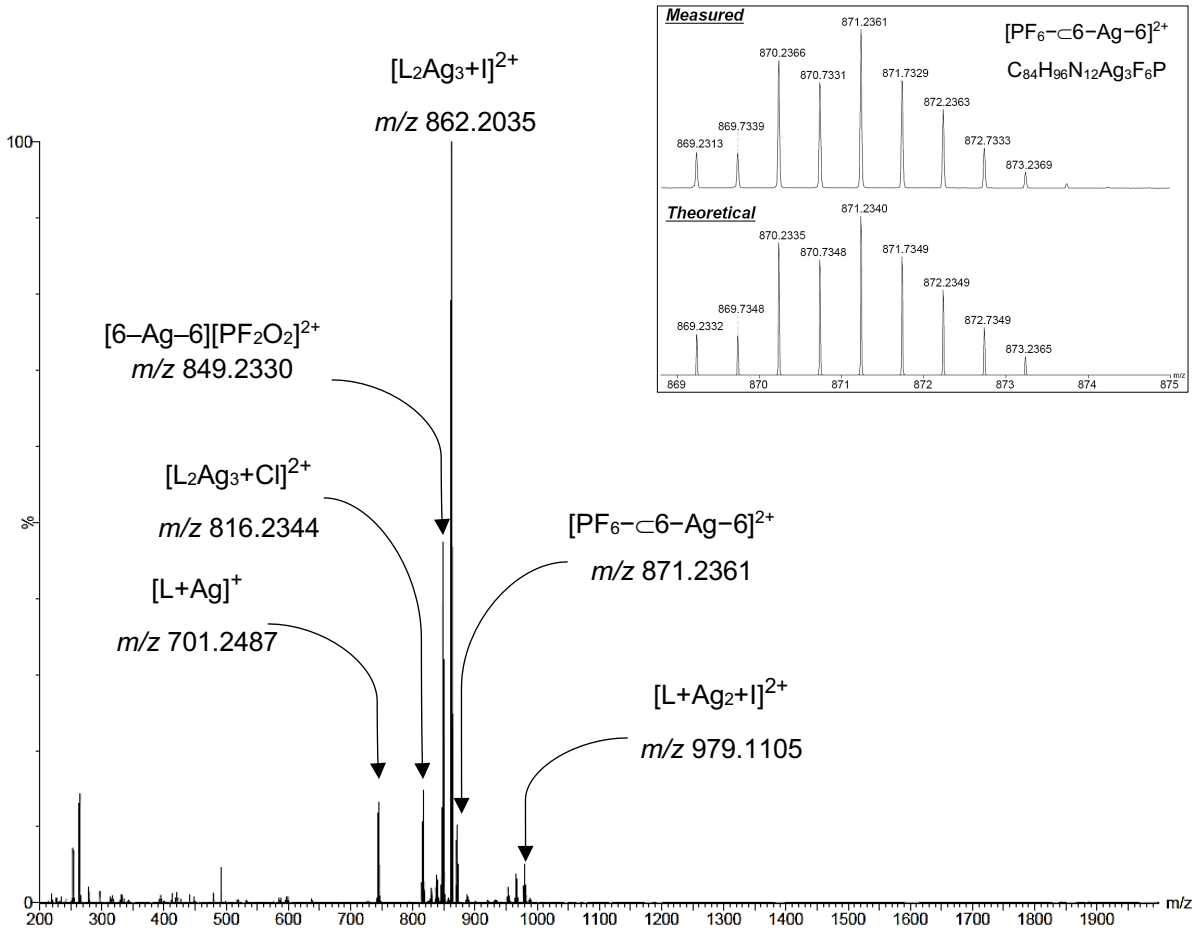

Figure S42. ESI-TOF mass spectrum of **$[PF_6{-}\subset 6{-}Ag{-}6][PF_6]_2$**. Inset: Isotope pattern of the $[PF_6{-}\subset 6{-}Ag{-}6]^{2+}$ ion.

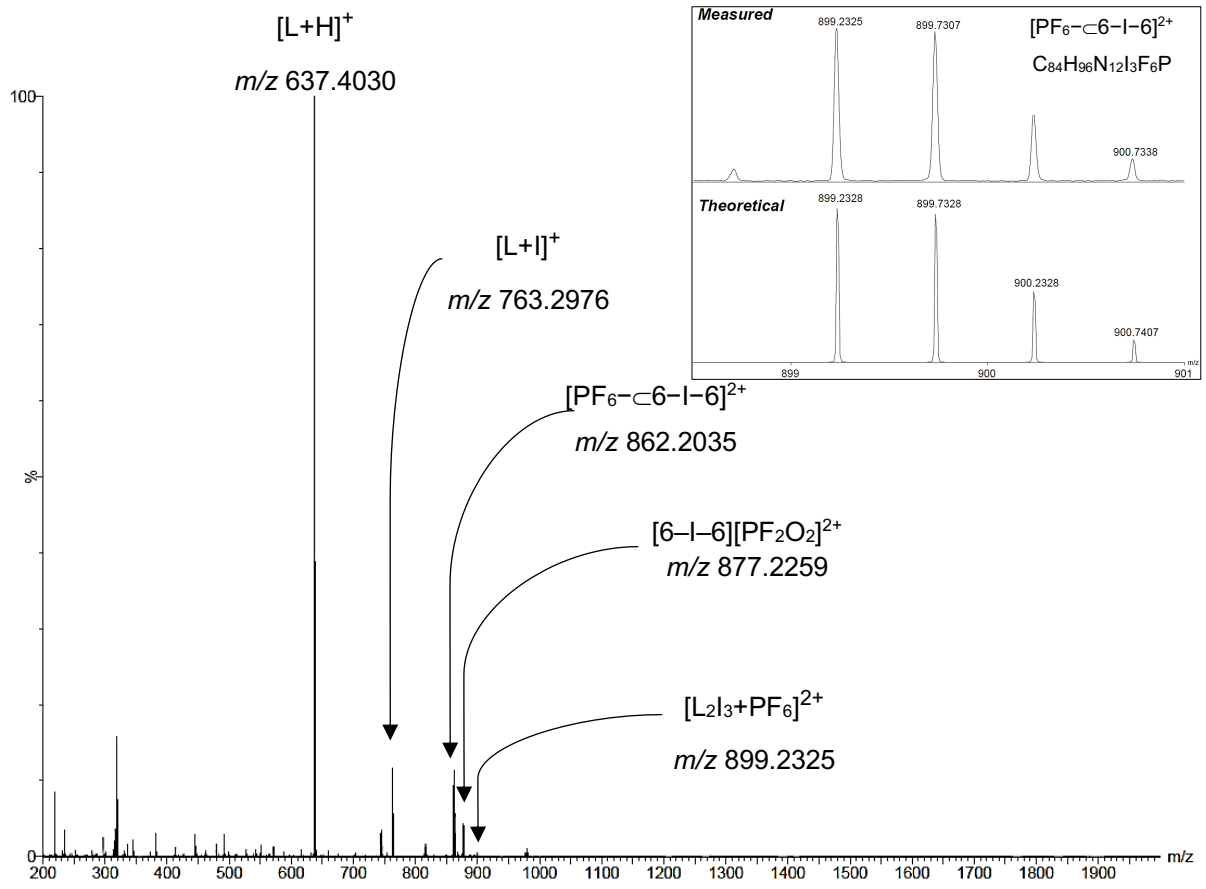

Figure S43. ESI-TOF mass spectrum of **$[PF_6{-}\subset 6{-}I{-}6][PF_6]_2$**. Inset: Isotope pattern of the $[PF_6{-}\subset 6{-}I{-}6]^{2+}$ ion.

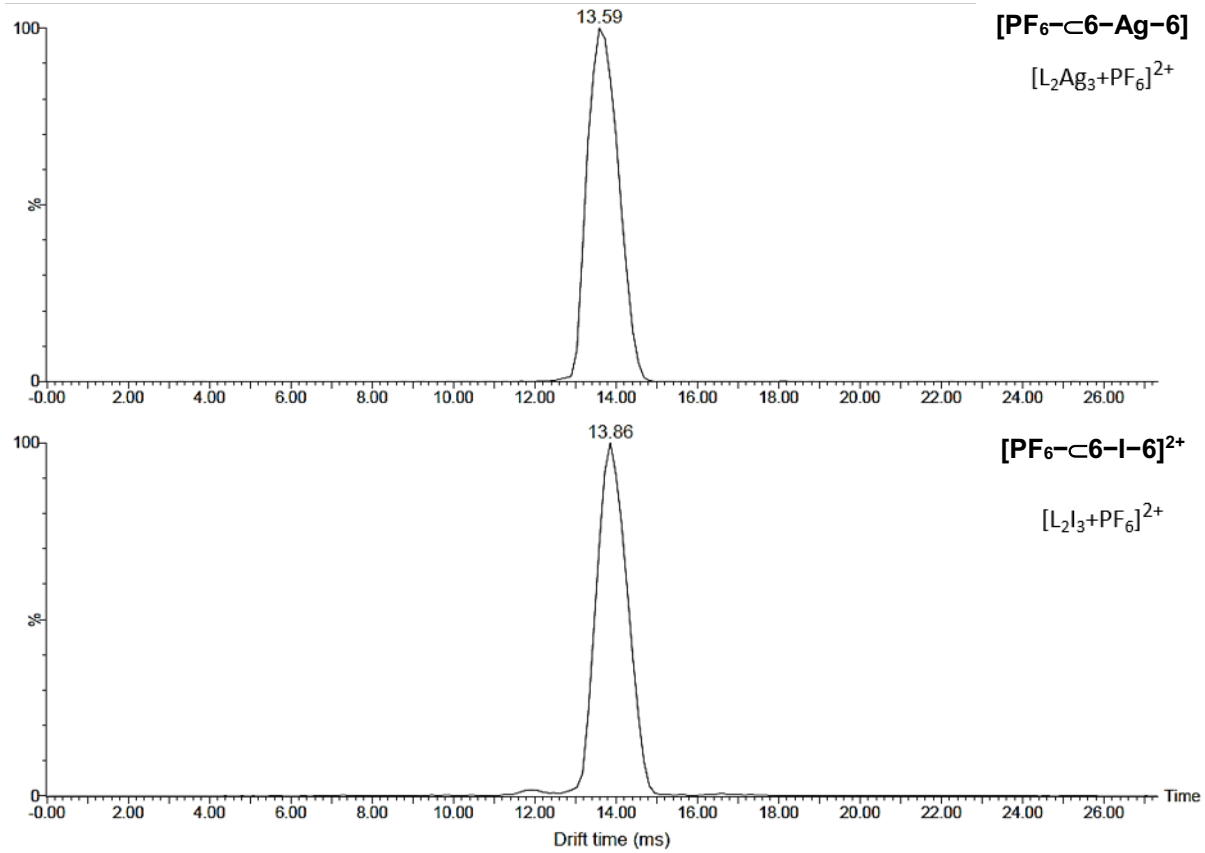

Figure S44. Comparison of arrival time distributions of $[PF_6{-}\subset 6{-}Ag{-}6]^{2+}$ (top) and $[PF_6{-}\subset 6{-}I{-}6]^{2+}$ (bottom).

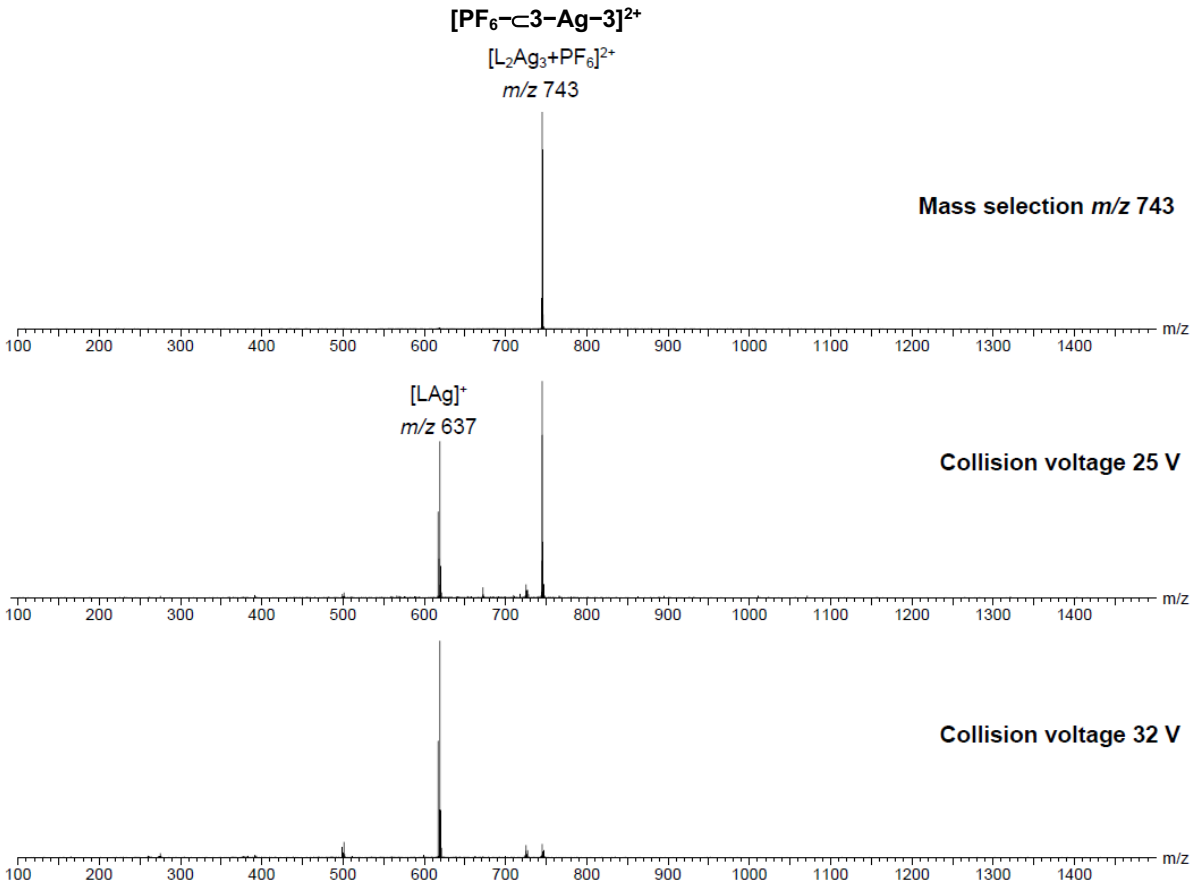

Figure S45. Collision-induced dissociation (CID) spectra of $[PF_6{-}\subset 3{-}Ag{-}3]^{2+}$ with increasing collision energies (from top to bottom). The second expected singly charged fragment, $[LAg_2PF_6]^+$, undergoes a rapid subsequent loss of an $AgPF_6$ ion pair and forms a second $[LAg]^+$ ion.

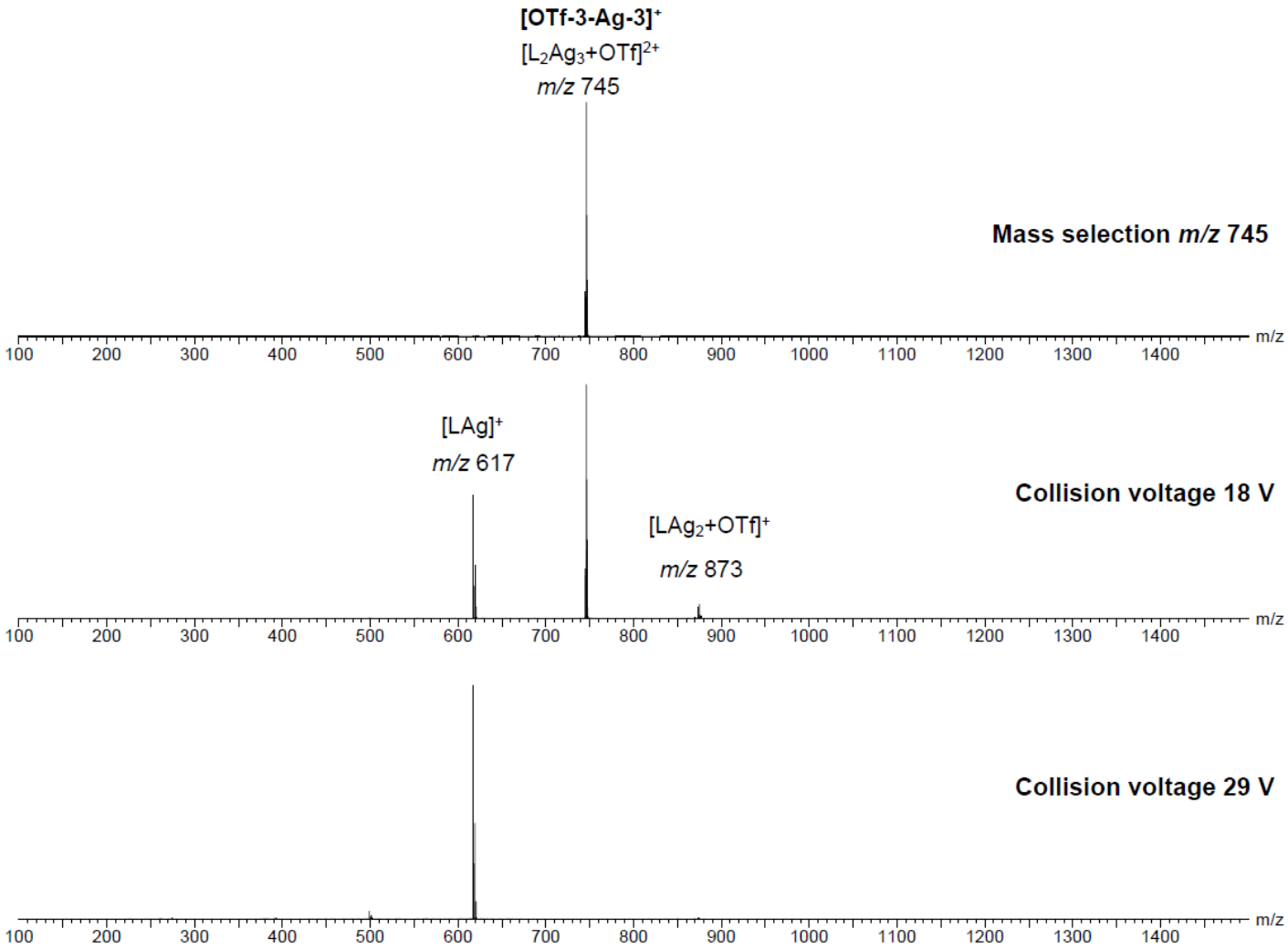

Figure S46. CID spectra of $[OTf\text{-}3\text{−}Ag\text{−}3]^{2+}$with increasing collision energies (from top to bottom).

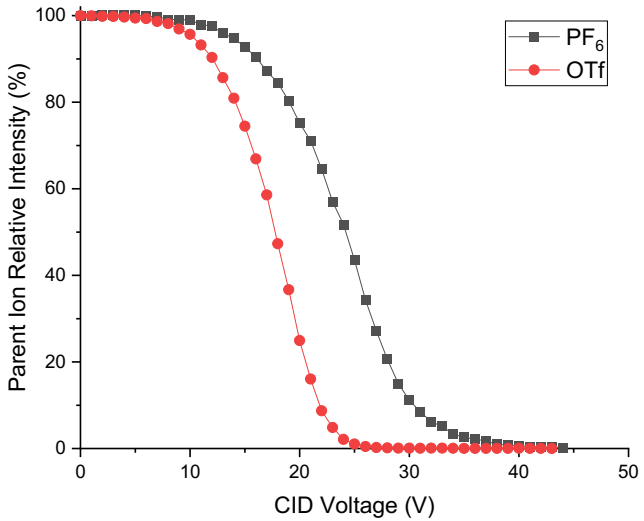

Figure S47. Survivor yield (SY) curve of $[Y{-}3{-}Ag{-}3]^{2+}$ where Y is the respective counterion. The SY shows a greater relative gas-phase stability of $[PF_6{-}\subset 3{-}Ag{-}3]^{2+}$ (SY50 = 26 V) compared to $[OTf{-}3{-}Ag{-}3]^{2+}$ (SY50 = 18 V). This is due to the encapsulation of the PF_6 which does not occur for the OTf.

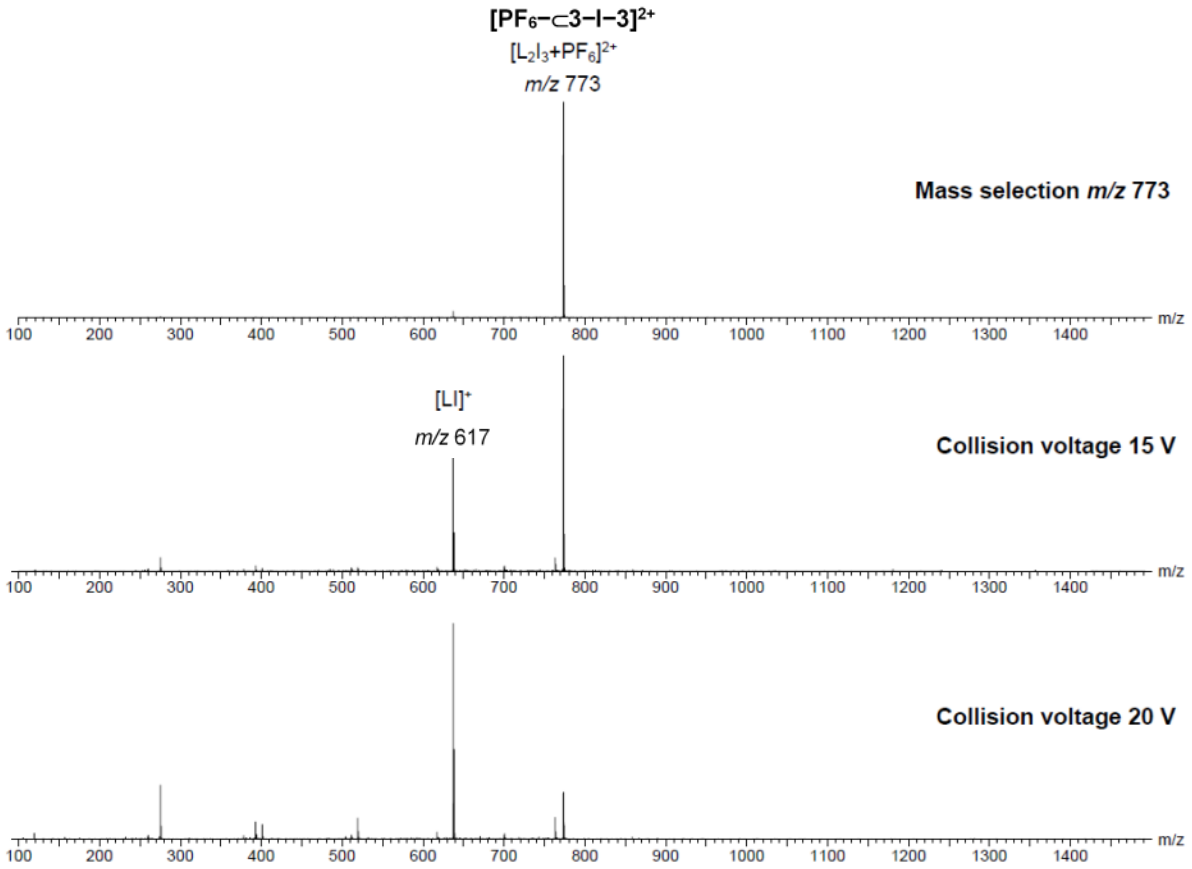

Figure S48. CID spectra of $[PF_6{-}\subset 3{-}I{-}3]^{2+}$ with increasing collision energies (from top to bottom). The second expected singly charged fragment, $[LI_2PF_6]^+$, undergoes a rapid subsequent loss of an IPF_6 ion pair and forms a second $[LI]^+$ ion.

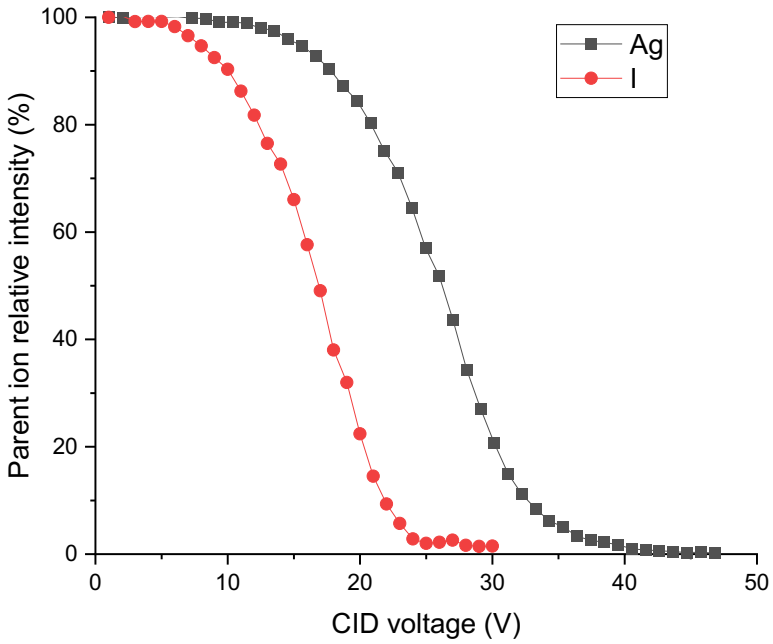

Figure S49. Survivor yield (SY) curve of $[PF_6{-}\subset 3{-}X{-}3]^{2+}$ where X is the respective metal. The SY shows a greater relative gas-phase stability of $[PF_6{-}\subset 3{-}Ag{-}3]^{2+}$ (SY50 = 26 V) compared to $[PF_6{-}\subset 3{-}I{-}3]^{2+}$ (SY50 = 17 V).

^{1}H NMR and ^{1}H-^{15}N HMBC Spectra of Synthesised Compounds

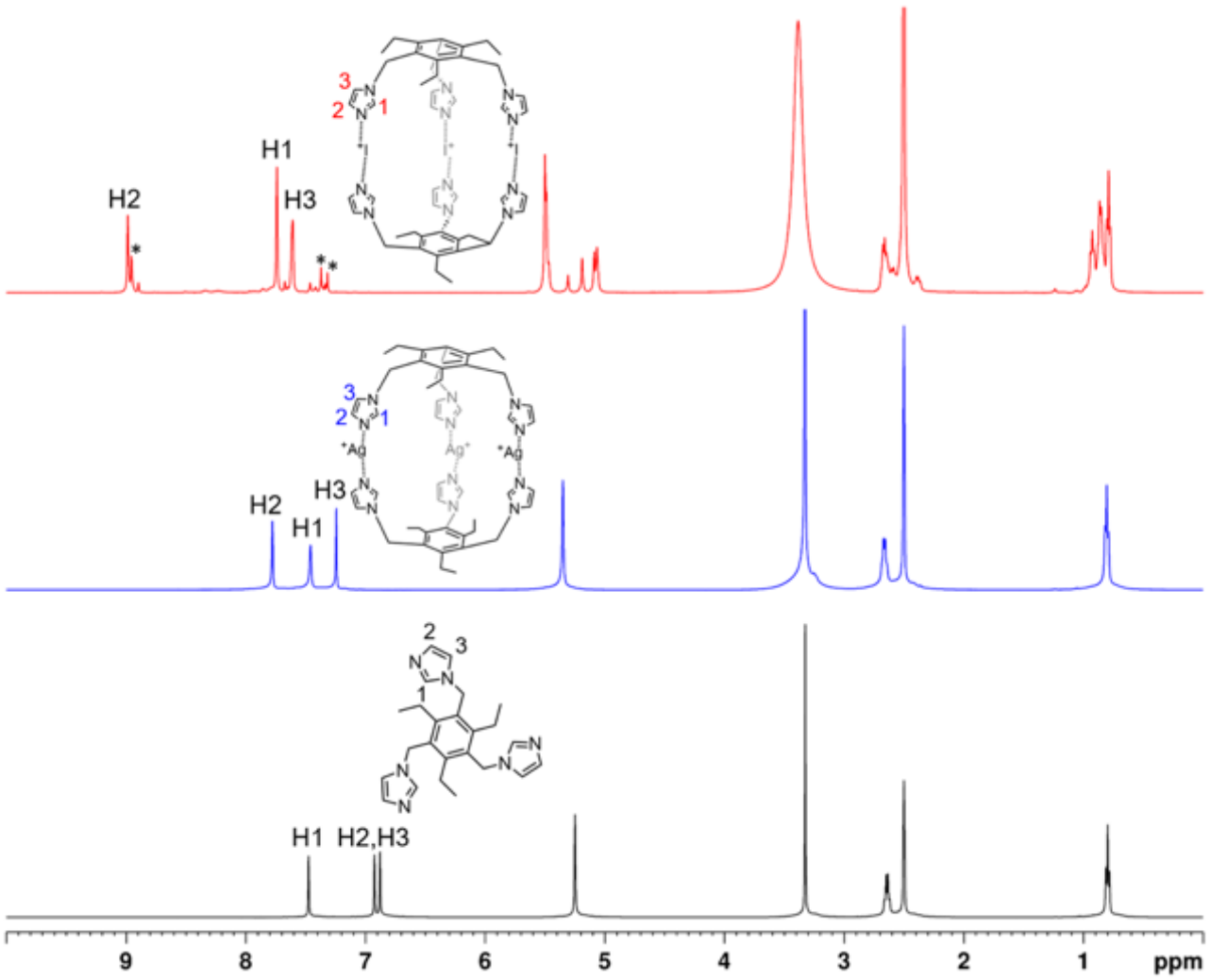

Figure S50. ^{1}H NMR spectra of **2**, **[PF$_6$⊂2−Ag−2][PF$_6$]$_2$** and **[PF$_6$⊂2−I−2][PF$_6$]$_2$** in DMSO-d_6 (303 K, 500 MHz) with minor incompletely exchanged intermediates or cage dissociation due to interactions with DMSO (*) in the iodine(I) complex.

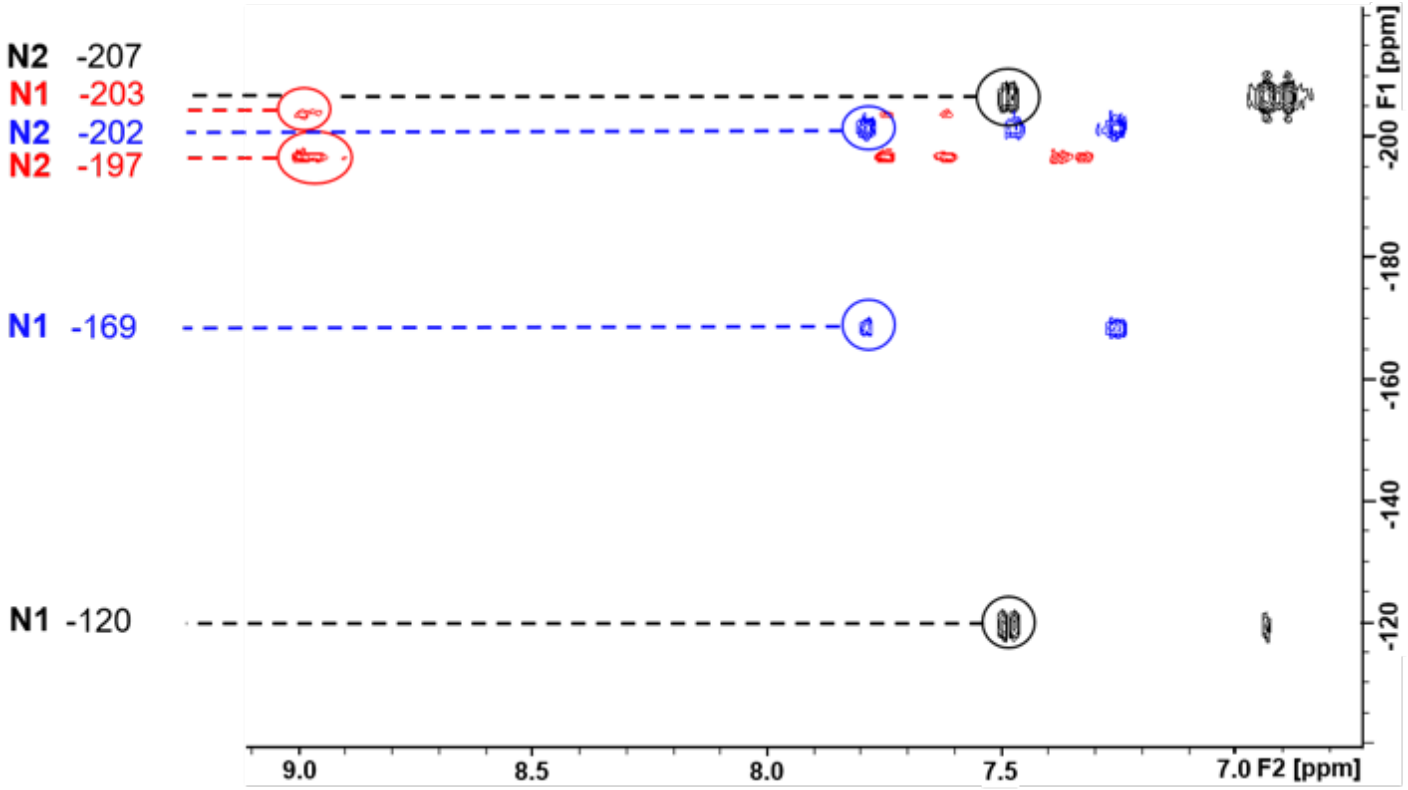

Figure S51. ^{1}H-^{15}N HMBC correlation spectra of the uncomplexed **2** (black), the silver complex **[PF$_6$−⊂2−Ag−2][PF$_6$]$_2$** (blue) and the iodine(I) complex **[PF$_6$−⊂2−I−2][PF$_6$]$_2$** (red) in DMSO-*d*$_6$ (303 K, 500 MHz).

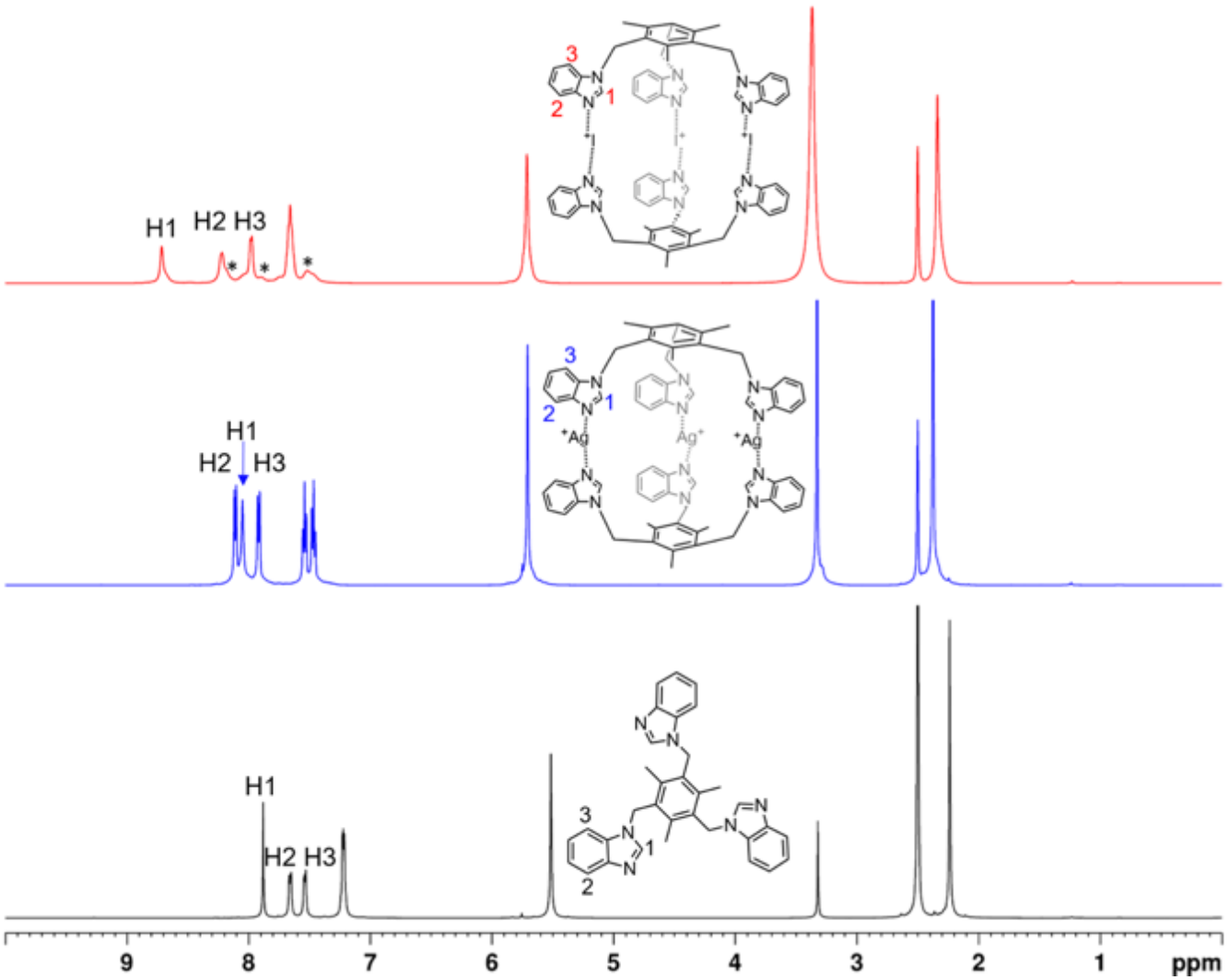

Figure S52. ^{1}H NMR spectra of **3**, **[PF$_6$⊂3−Ag−3][PF$_6$]$_2$** and **[PF$_6$⊂3−I−3][PF$_6$]$_2$** in DMSO-*d*$_6$ (303 K, 500 MHz) with minor incompletely exchanged intermediates or cage dissociation due to interactions with DMSO (*) in the iodine(I) complex.

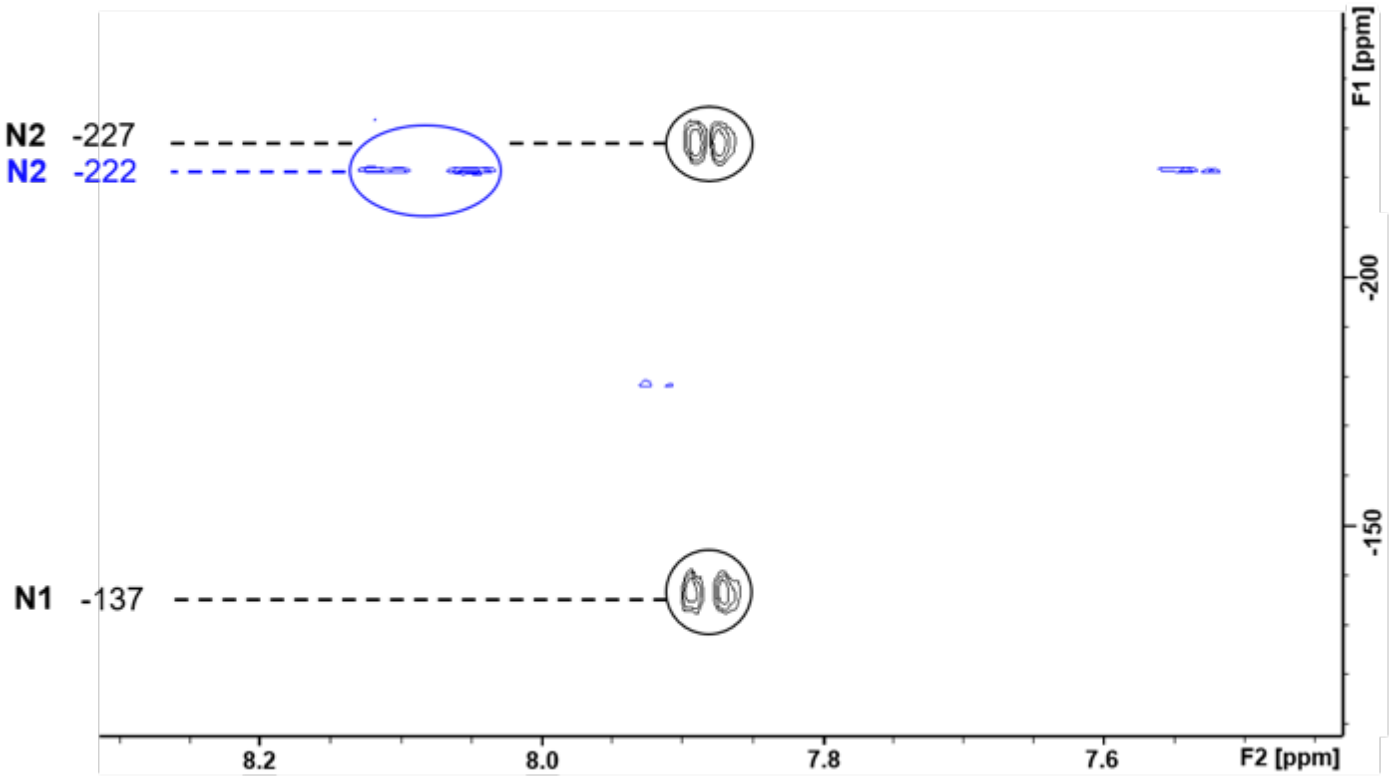

Figure S53. ^{1}H-^{15}N HMBC correlation spectra of the uncomplexed **3** (black) and the silver complex **[PF_6−⊂3−Ag−3][PF_6]$_2$** (blue) in DMSO-*d6* (303 K, 500 MHz).

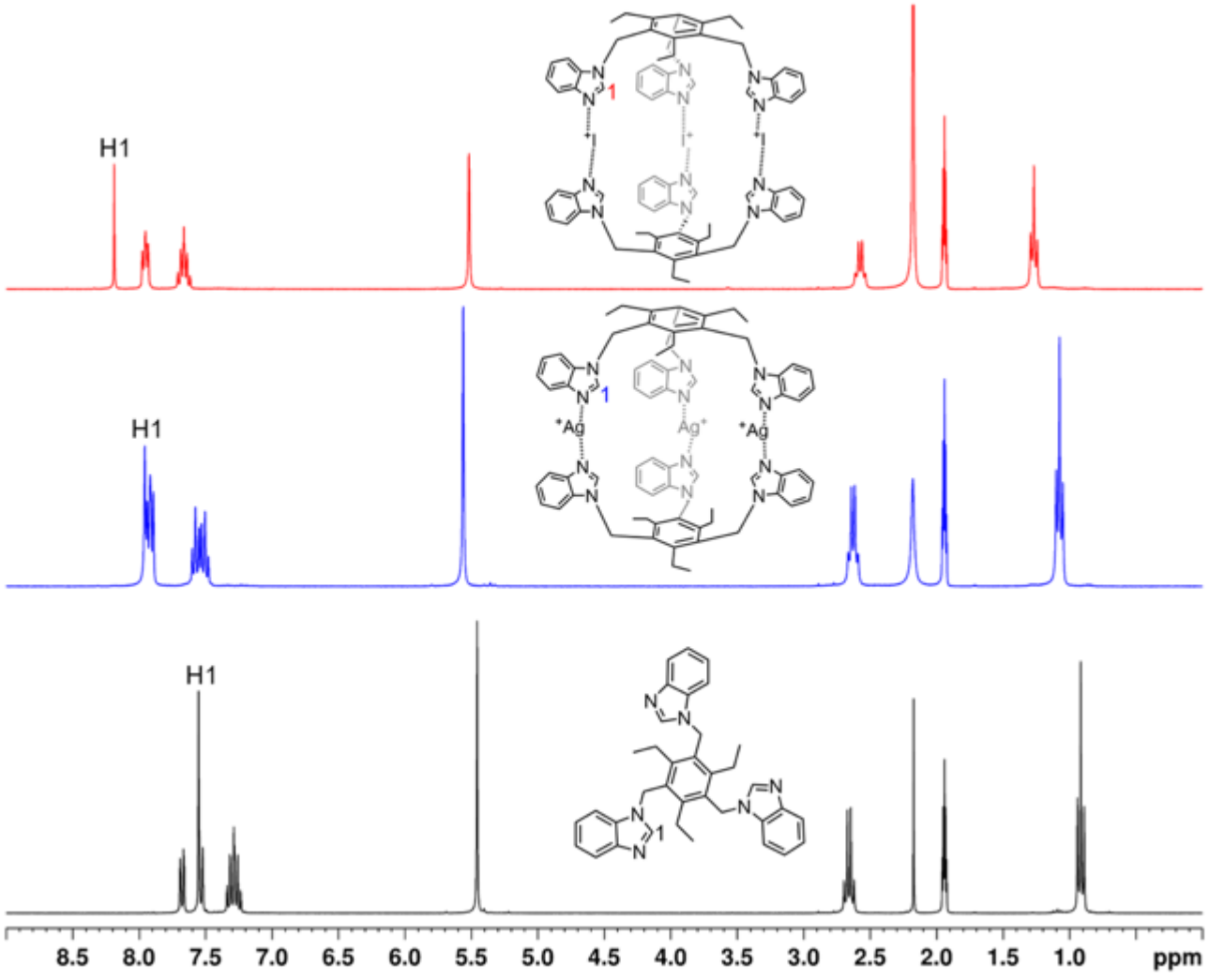

Figure S54. ^{1}H NMR spectra of **4**, **[PF$_6$⁻⊂4−Ag−4][PF$_6$]$_2$** and **[PF$_6$⁻⊂4−I−4][PF$_6$]$_2$** in CD_3CN (303 K, 500 MHz).

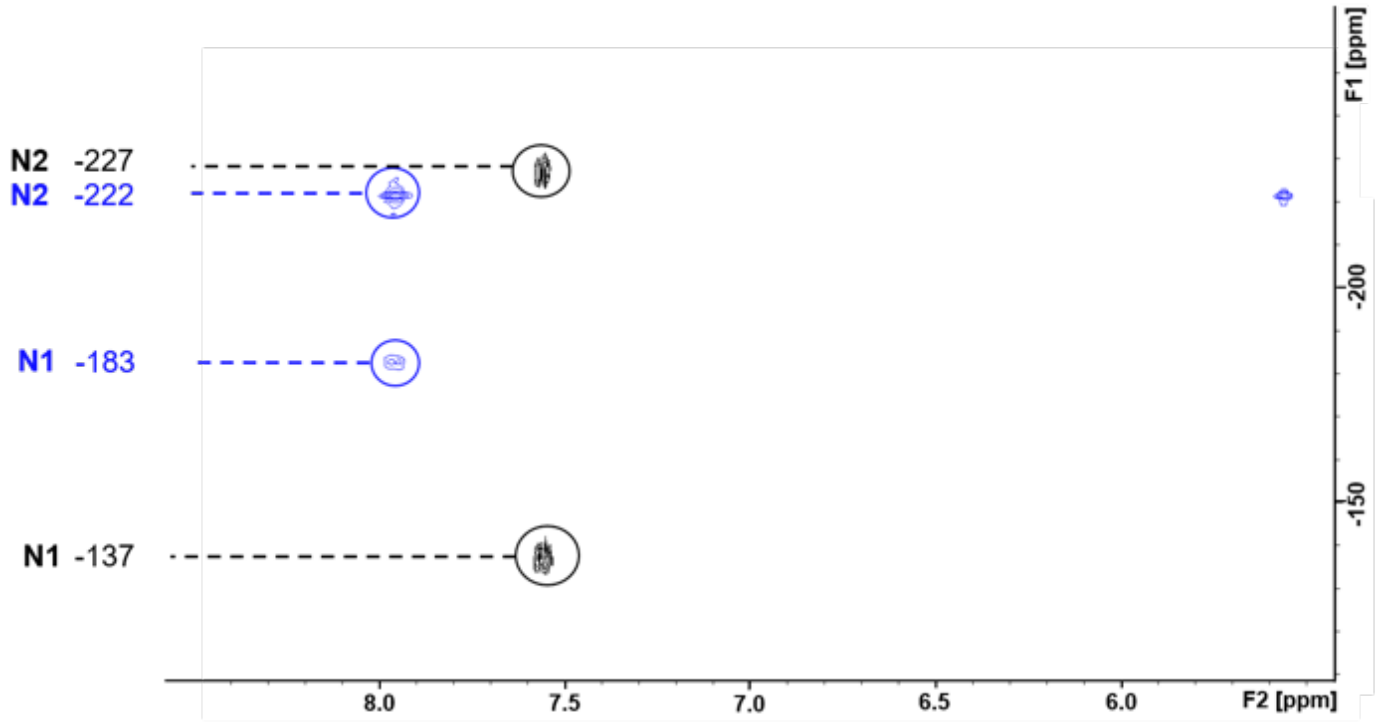

Figure S55. ^{1}H-^{15}N HMBC correlation spectra of the uncomplexed **4** (black) and the silver complex **$[PF_6{-}\subset 4{-}Ag{-}4][PF_6]_2$** (blue) in CD_3CN (303 K, 500 MHz).

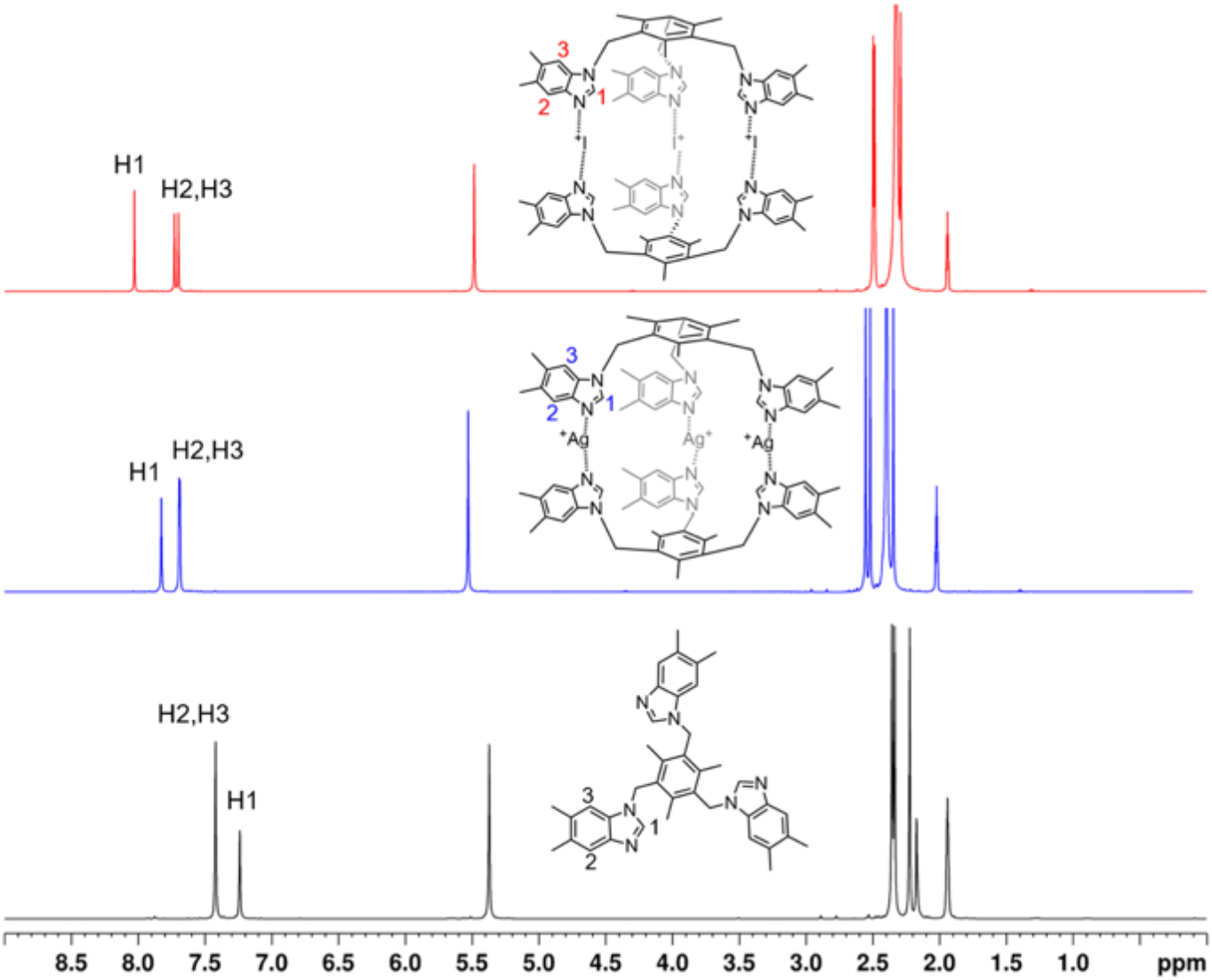

Figure S56. ^{1}H NMR spectra of **5**, **[PF$_6$−⊂5−Ag−5][PF$_6$]$_2$** and **[PF$_6$−⊂5−I−5][PF$_6$]$_2$** in CD_3CN (303 K, 500 MHz).

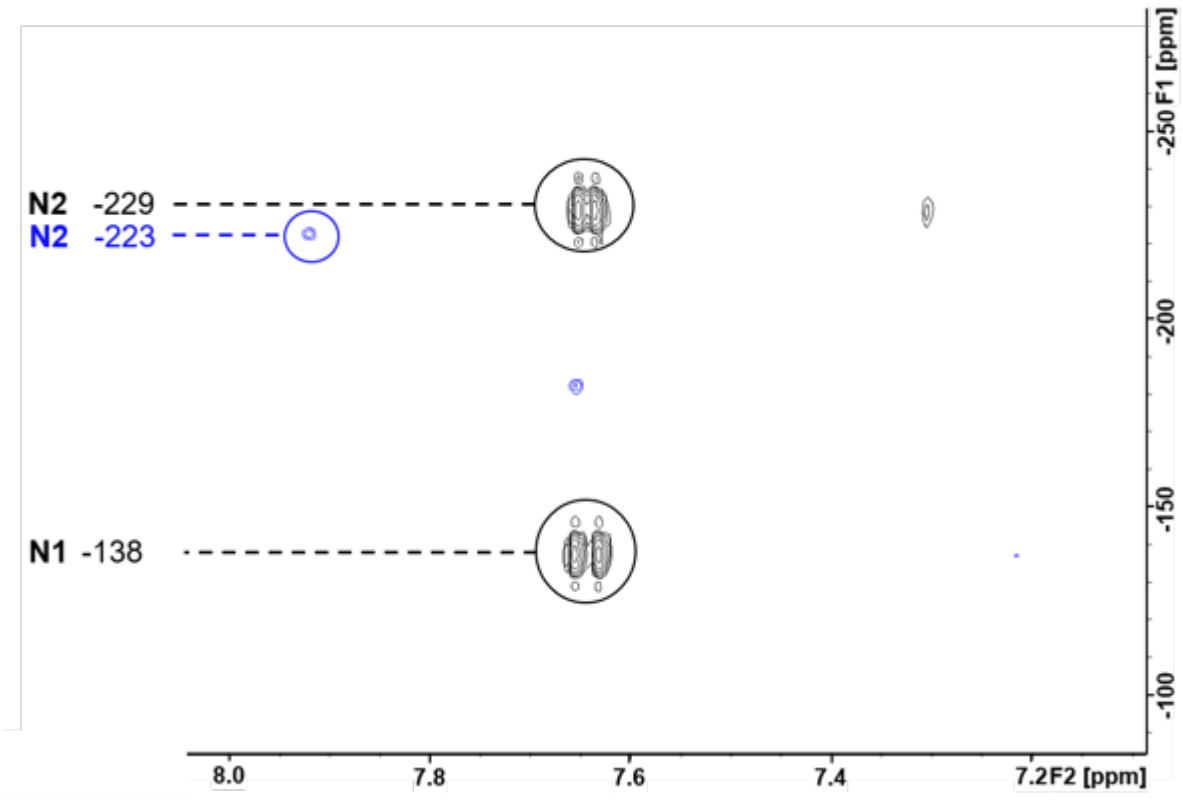

Figure S57. ^{1}H-^{15}N HMBC correlation spectra of the uncomplexed **5** (black) and the silver complex **$[PF_6{-}\subset{\mathbf{5}}{-}Ag{-}\mathbf{5}][PF_6]_2$** (blue) in CD_3CN (303 K, 500 MHz).

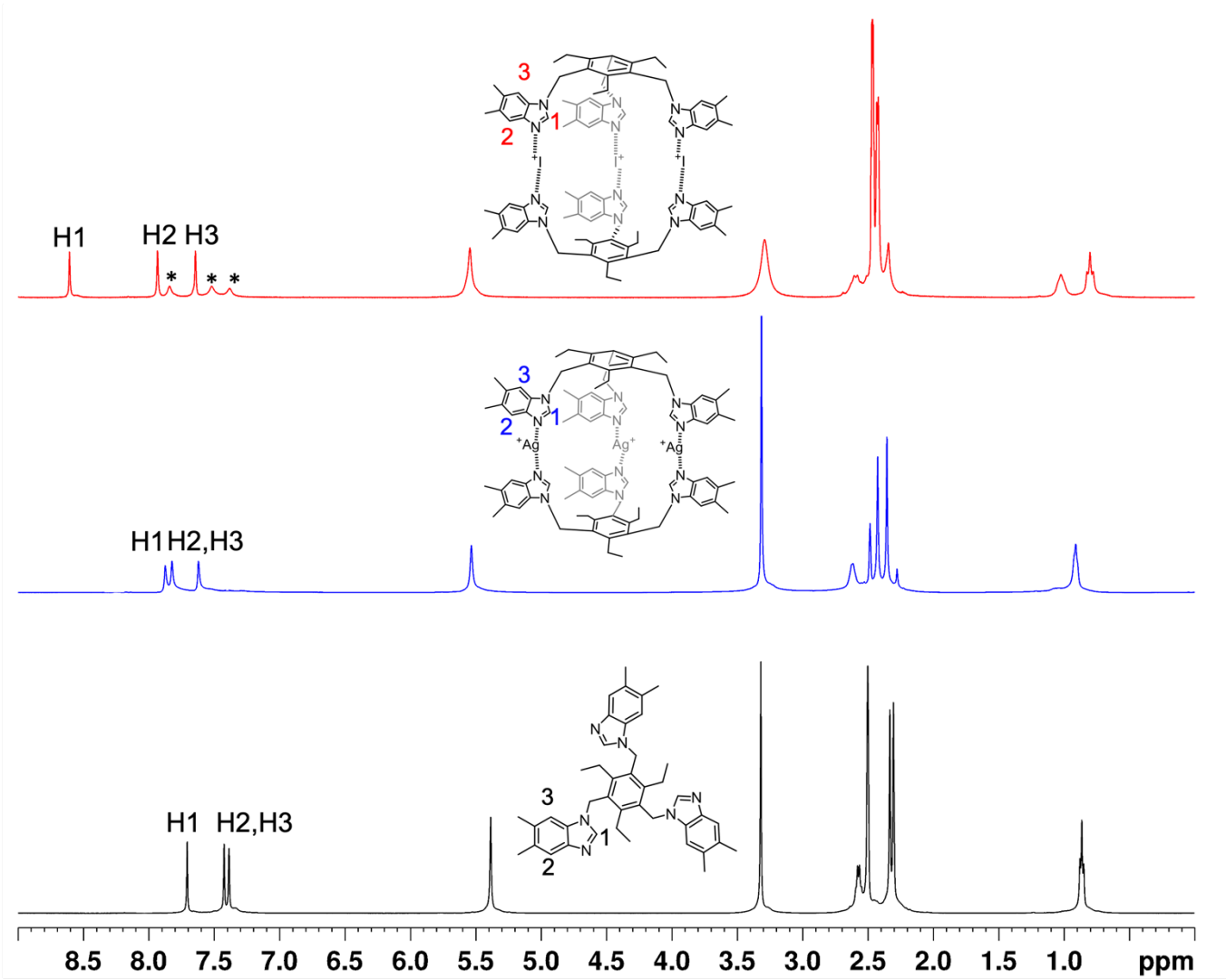

Figure S58. ^{1}H NMR spectra of **6**, **[PF$_6$−⊂6−Ag−6][PF$_6$]$_2$** and **[PF$_6$−⊂6−I−6][PF$_6$]$_2$** in DMSO-d_6 (303 K, 500 MHz) with minor incompletely exchanged intermediates or cage dissociation due to interactions with DMSO (*) in the iodine(I) complex.

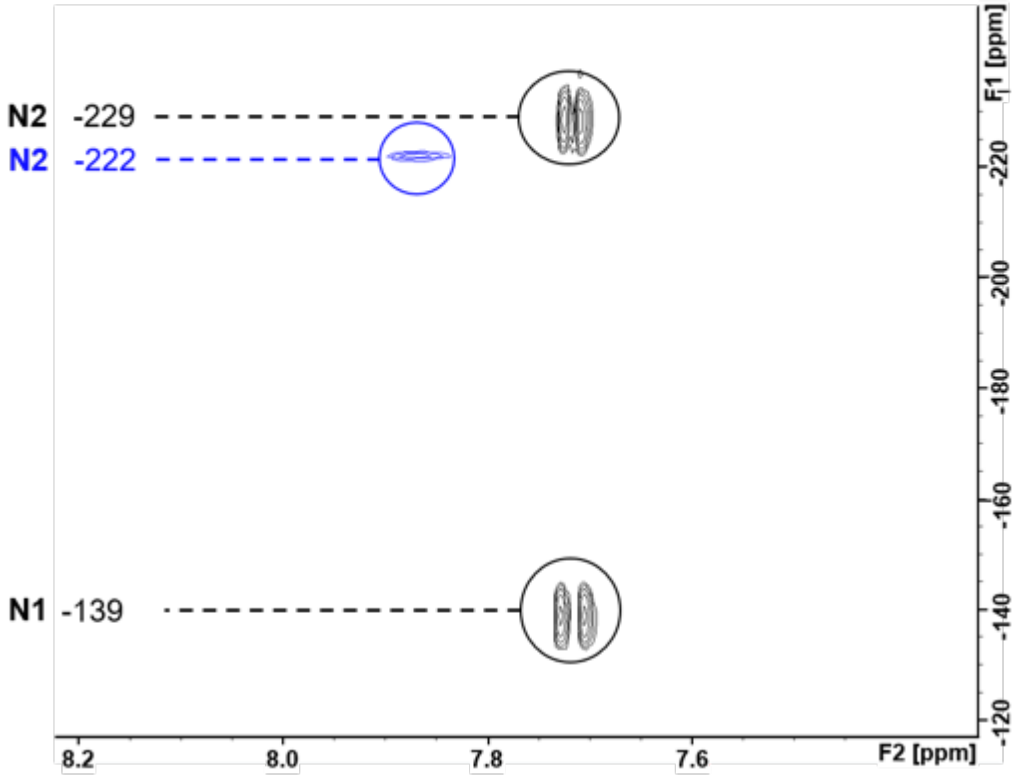

Figure S59. ^{1}H-^{15}N HMBC correlation spectra of the uncomplexed **6** (black) and the silver complex **[PF_6⁻⊂6−Ag−6][PF_6]$_2$** (blue) in DMSO-d_6 (303 K, 500 MHz).

^{19}F NMR Spectra of Selected Compounds

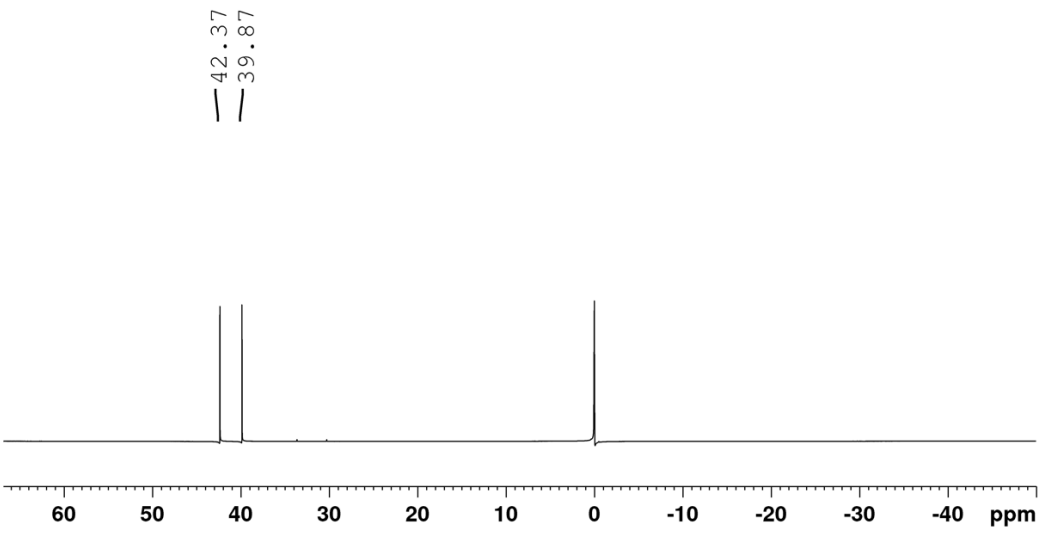

Figure S60. The ^{19}F NMR spectrum of AgPF6 in CD_3CN. All values are in ppm and referenced to an internal standard of C_6H_5F (303K, 282.39 MHz).

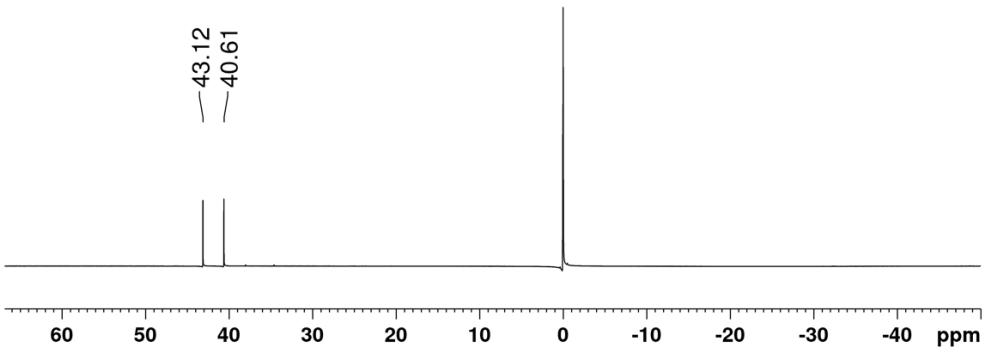

Figure S61. The ^{19}F NMR spectrum of **$[PF_6{-}\subset 5{-}Ag{-}5[PF_6]_2$** in CD_3CN. All values are in ppm and referenced to an internal standard of C_6H_5F (303 K, 282.39 MHz).

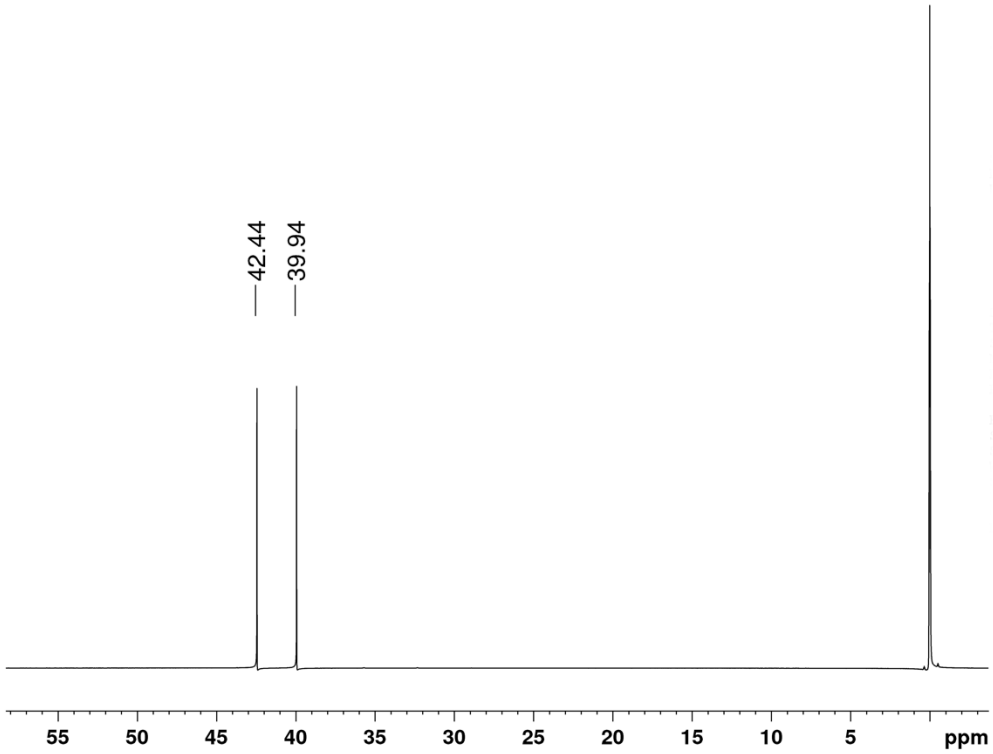

Figure S62. The ^{19}F NMR spectrum of **$[PF_6{-}\subset{\mathbf{5}}{-}I{-}5][PF_6]_2$** in CD_3CN. All values are in ppm and referenced to an internal standard of C_6H_5F (303 K, 282.39 MHz).

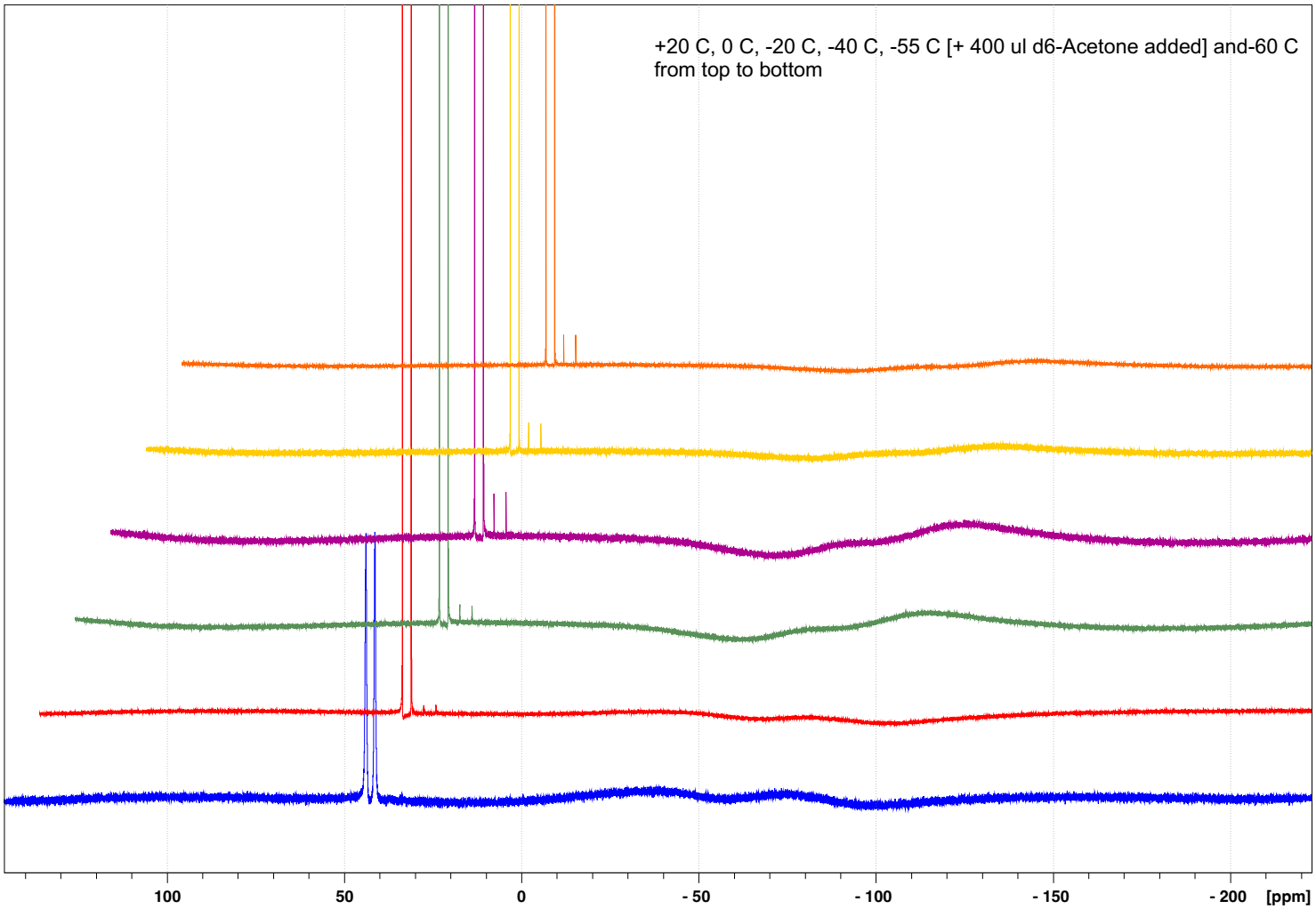

Figure S63. The ^{19}F NMR spectra of **$[PF_6{-}\subset{5-}I{-}5][PF_6]_2$** in CD_3CN with variable temperature. All values are in ppm and referenced to an internal standard of C_6H_5F (282.39 MHz).

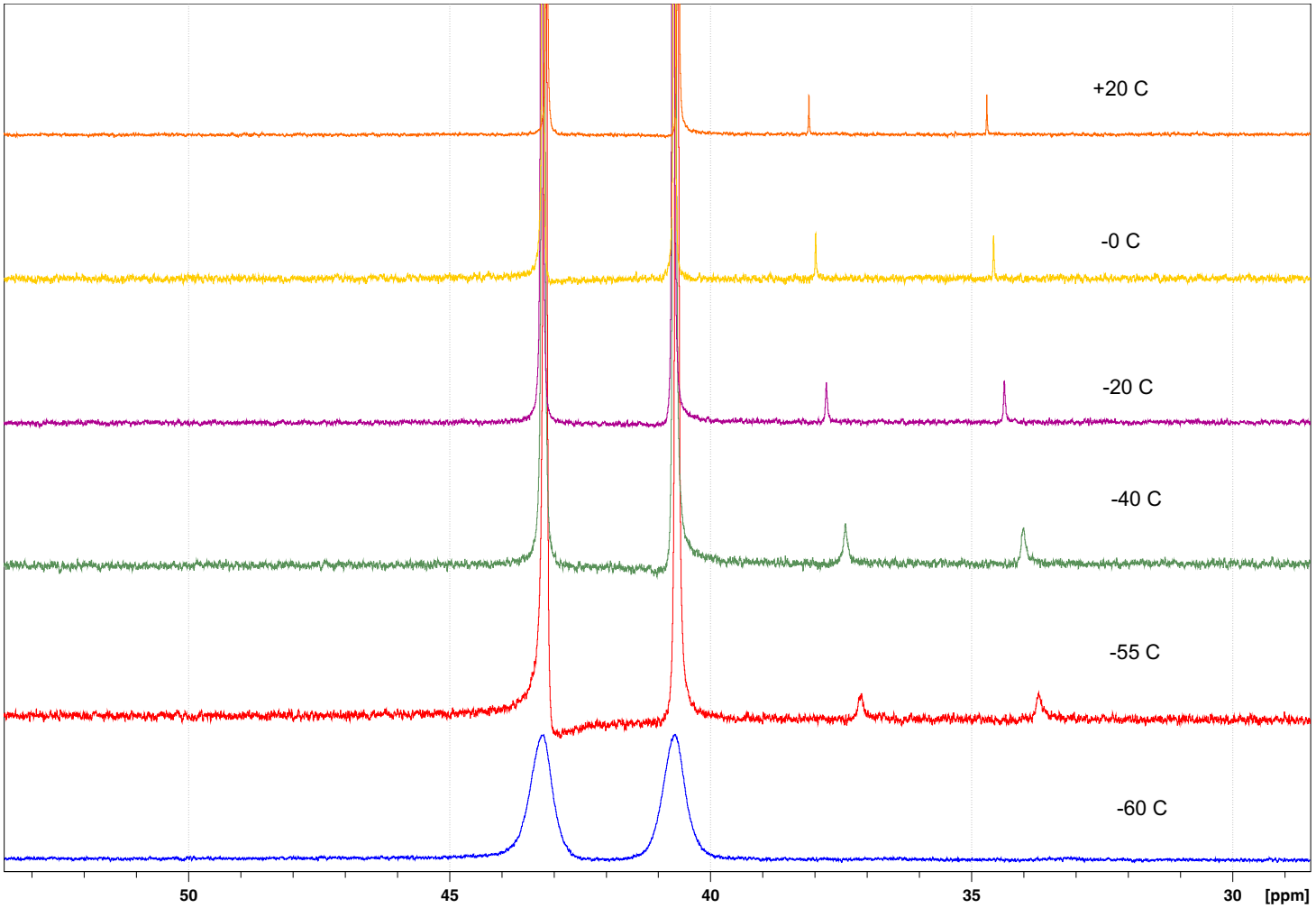

Figure S64. The ^{19}F NMR spectra of **$[PF_6{-}\subset 5{-}I{-}5][PF_6]_2$** in CD_3CN with variable temperature (and added acetone-d_6). All values are in ppm and referenced to an internal standard of C_6H_5F (282.39 MHz). The larger peaks are overlayed to show the change of the relative position of the smRealler peaks.

References

[1] Y. Yuan, Z.-L. Jiang, J.-M. Yan, G. Gao, A. S. C. Chan, R.-G. Xie, *Synth. Commun.* 2000, **30**(24), 4555.

[2] W.-Y. Sun, J. Fan, T.-A. Okamura, J. Xie, K.-B. Yu, N. Ueyama, *Chem. Eur. J.,* 2001, **7**, 2557.

[3] H.-K. Liu, X. Huang, T. Lu, X. Wang, W.-Y. Sun, B.-S. Kang, *Dalton Trans.,* 2008, 3178.

[4] *CrysAlisPro,* 2014, v 1.171.36.35; Agilent Technologies, Ltd, Yarton, UK.

[5] G. M. Sheldrick, *Acta Crystallogr. Sect. A*, 2015, **71**, 3.

[6] O. V Dolomanov, L. J. Bourhis, R. J. Gildea, J. A. K. Howard and H. Puschmann, *J. Appl. Crystallogr.*, 2009, **42**, 339.

[7] G. M. Sheldrick, *Acta Crystallogr. Sect. C*, 2015, **71**, 3.

[8] M. A. Spackman, D. Jayatilaka, *CrystEngComm*, 2009, **11**, 19.

[9] P. R. Spackman, M. J. Turner, J. J. McKinnon, S. K. Wolff, D. J. Grimwood, D. Jayatilaka, M. A. Spackman, *J. Appl. Cryst*., 2021, **54**, 1006.

[10] SPARTAN'18, Wavefunction Inc, Irvine, Ca 92612, USA, 2018.